THESIS

DETERMINING THE INFLUENCE OF WETLAND DRAINAGE ON BASEFLOW IN A HIGH-ELEVATION, SNOWMELT-DOMINATED, HEADWATER WATERSHED, SENATOR BECK BASIN, SAN JUAN MOUNTAINS, SW COLORADO

Submitted by

Nicholas Patrick Chohan

Department of Geosciences

In partial fulfillment of the requirements

For the Degree of Master of Science

Colorado State University

Fort Collins, Colorado

Spring 2025

Master's Committee:

Advisor: William E. Sanford

Steven R. Fassnacht
Jeremy C. Rugenstein

ABSTRACT

DETERMINING THE INFLUENCE OF WETLAND DRAINAGE ON BASEFLOW IN A HIGH-ELEVATION, SNOWMELT-DOMINATED, HEADWATER WATERSHED, SENATOR BECK BASIN, SAN JUAN MOUNTAINS, SW COLORADO

Mountain wetlands may be important for modulating groundwater discharge to streams in high-elevation, snowmelt-dominated, headwater watersheds, particularly in the dry season after snowmelt, when streamflow is at an annual low. While the basic mechanisms of water release from wetlands to streams (hereafter, termed as wetland drainage) are understood, the regional importance of wetland drainage in snowmelt-dominated mountain watersheds and its response to potential changes in climate are unknown. Decreases to winter snowpacks and changes to snowmelt regimes may reduce the volume of water stored in the subsurface available for supporting wetlands and baseflow, diminishing the influence of wetland drainage on streamflow.

The goal of this study was to investigate the role and relative importance of wetland drainage on streamflow in the Senator Beck Basin (SBB), a small, high-elevation, snowmelt-dominated, headwater watershed, located in the San Juan Mountains of southwestern Colorado. The SBB has a single groundwater-supported wetland adjacent to the stream near the watershed outlet, making it an ideal place to study the effects of wetland drainage on streamflow. Wetland drainage, conceptualized as a component of baseflow, has been observed during several summers in the SBB, providing an important component of streamflow when other sources could not.

Data from the SBB were used to estimate baseflow discharge using the Conductivity Mass Balance method. The ratio of baseflow discharge to total discharge was used to track the

timing of when wetland drainage became a substantial component of baseflow. The timing of substantial baseflow was then related to the timing and magnitude of different hydroclimatic processes (precipitation, snowpack, snowmelt, and streamflow) to determine which processes have the greatest influence on wetland drainage. Four hydrologically distinct years were examined: 2018 (dry), 2019 (wet), 2020 (average), and 2021 (dry).

Results show that the timing of substantial baseflow in the wet year (2019) occurred between 40 – 60 days later than the timing of substantial baseflow in the dry years (2018 and 2021), suggesting that wetland drainage plays a relatively larger role in maintaining streamflow in dry years. While wetland drainage plays an important role in maintaining streamflow in every year, the relative importance of wetland drainage varies each year due to variability in hydroclimate processes. Dry years, which rely on wetland drainage to maintain streamflow earlier in the year, will have a greater reliance on groundwater, because groundwater provides a constant source of water year-round and buffers streamflow.

Mountain wetlands that are supported by groundwater may be potentially more resilient to the effects of hydroclimatic variability if the groundwater supply that they are connected to is sufficiently large enough to support them. Given that wetland drainage is important in the SBB, it may also be important for maintaining streamflow in other high-elevation, snowmelt-dominated, headwater watersheds.

ACKNOWLEDGEMENTS

I am profoundly grateful to my advisor, Dr. Bill Sanford, for his mentorship and patience throughout this degree. Thanks, Dude. A great thanks to Dr. Steven Fassnacht and Dr. Jeremy Rugenstein for their knowledge and insight when writing this paper and for their flexibility. I would also like to extend gratitude to Jeff and Kim Derry for their help in answering questions about Senator Beck Basin in the field and elsewhere.

I must also express my sincere gratitude to the donors of the scholarships I received throughout this degree: the Colorado Groundwater Association's Harlan Erker Memorial Scholarship, the Warner College of Natural Resources' Robert L. Stollar Scholarship in Hydrogeology, and the American Water Resources Association's Richard A. Herbert Memorial Scholarship. The generous financial support from these organizations helped make this project and my studies possible.

I would like to extend my deepest thanks to Max Miller, Brian Steen, and Katie Chohan for helping me over the finish line. My acknowledgements would not be complete without a big shout out to my parents, Rob and Brenda, for their love and support. I could never have done it without you guys!

TABLE OF CONTENTS

ABSTRACT ii
ACKNOWLEDGEMENTS iv
LIST OF TABLES vii
LIST OF FIGURES ix
LIST OF EQUATIONS xii
1. INTRODUCTION 1
1.1. Wetland Drainage 2
1.2. Mountain Hydrogeology 3
1.3. Goals and Objectives 5
2. BACKGROUND 8
2.1. Site Description 8
2.1.1. Precipitation and Snow 10
2.1.2. Streamflow 11
2.1.3. Geology 12
2.1.4. Hydrogeology 12
2.1.5. Vegetation 14
2.2. Hydrologic Features of the SBB 14
2.3. Conductivity Mass Balance Model 18
2.3.1. Chemical Hydrograph Separations 19
2.3.2. Streamflow Conceptual Model 21
2.3.3. Derivation of Conductivity Mass Balance Model 22
2.3.4. Baseflow Index 23
3. METHODS 24
3.1. Hydroclimate 25
3.2. Data Sources 25
3.3. Dataset Description 28
3.3.1. Data Pre-Processing 30
3.3.2. SWE Classification 30
3.4. Estimating Baseflow Discharge 31
3.4.1. Endmember Selection 32
3.4.2. Applying the CMB Method to the SBB 33
3.4.3. Baseflow Index 34
3.5. Cumulative Flow and Snowmelt 36
3.6. Estimating the Role of Wetland Drainage 36
3.7. Statistical Analysis 38
4. RESULTS 39
4.1. Precipitation 39
4.2. Snowpack 40
4.3. Snowmelt Period 42
4.4. Stream and Baseflow Discharge 43
4.5. Cumulative Flow 46
4.6. Baseflow Index 48

4.7. Timing of Substantial Baseflow 52
4.8. Statistical Analysis 54
5. DISCUSSION 57
5.1. Hydrological Processes Governing Wetland Drainage 58
5.1.1. Snowpack 59
5.1.2. Precipitation 60
5.1.3. Discharge 61
5.1.4. Snowmelt Timing 62
5.1.5. Snowmelt Rate 63
5.2. Conductivity Mass Balance Model 65
5.2.1. Endmember Sensitivity Analysis 66
5.2.2. Reliability of Model Assumptions 67
5.2.3. Temporal Variability in Endmembers 69
5.2.4. Baseflow Index 71
5.2.5. CMB Model Uncertainty 73
5.2.6. Limitations of BFI for Investigating Wetland Drainage 73
5.3 Statistical Evaluation 74
5.4. The Influence of Groundwater on Wetland Drainage 75
5.5. Conceptual Understanding 76
6. CONCLUSION 79
7. RECOMMENDATIONS 82
7.1. Exploring SBB Groundwater 82
7.2. Characterizing the Swamp Angel Wetland 83
7.3. Wetland Drainage in Other Mountain Watersheds 84
REFERENCES 85
APPENDIX A. Hydrologic Data 100
APPENDIX B. Data Management 108
APPENDIX C. Summer 2021 Data 111
GLOSSARY 114
LIST OF ABBREVIATIONS 117

LIST OF TABLES

Table 3.1. Summary of variables used to characterize hydroclimate variability and the timing of substantial baseflow in the SBB. Each variable has an associated variable type (what the variable represents), a process (the physical process being described), units, and a brief description. 35

Table 4.1. Summary of precipitation and snowpack characteristics for the period of record. A description of variables is in Table 3.1. 40

Table 4.2. Summary of snowmelt timing and peak stream discharge variables for the period of record. A description of variables is in Table 3.1. 43

Table 4.3. Summary of daily and long-term BFI characteristics for the period of record. A description of variables is in Table 3.1. 49

Table 5.1. A comparison of the proportion of groundwater in streams from snowmelt-dominated mountainous watersheds in the southern Rocky Mountains. The Upper Colorado River Basin extends into parts of Colorado, Utah, Wyoming, New Mexico, and Arizona while the Upper Rio Grande River Basin straddles Colorado and New Mexico. 72

Table A.1. Summary of precipitation, snowpack accumulation, and ablation characteristics in the period of record. A description of variables is in Table 3.1. Column 4 represents the date of first snow accumulation which was used to define the winter and summer precipitation groups. 100

Table A.2. Summary of specific conductance characteristics from the period of record. A description of variables is in Table 3.1. 103

Table A.3. Summary of cumulative stream discharge, cumulative baseflow discharge, and BFI values for the period of record. A description of variables is in Table 3.1..... 105

Table A.4. Summary of the timing of substantial baseflow variables for the period of record. A description of variables is in Table 3.1. 106

Table B.1. Summary of sensor metadata used in this study. Metadata for the data collection stations in the SBB (SASP and SBSG) were available from Landry et al., (2014), Center for Snow and Avalanche Studies (2012), and Center for Snow and Avalanche Studies (2020), while metadata for the SNOTEL station was available from the NRCS website. 108

Table B.2. Summary of measurement period characteristics in the period of record. A description of variables is in Table 3.1. Nineteen days of missing data in 2019 were estimated using regression between stream discharge and SC (Figure B.1). 109

Table C.1. Summary of sensor metadata from wells in the SAW and from stream monitoring stations. 113

LIST OF FIGURES

Figure 1.1. Hillshade elevation map of the Senator Beck Basin (SBB; black boundary), showing the stream (blue line) and data collection stations in the watershed (red triangles): Swamp Angel Study Plot (SASP), Senator Beck Stream Gauge (SBSG), and Senator Beck Study Plot (SBSP; not referenced in this research). The flow direction of the stream is towards the SBSG (from left to right). The SNOTEL station (not shown) is located 1.8 km south of the SBB. The yellow star in the inset map denotes the location of the SBB within Colorado and the western United States. 7

Figure 2.1. Map of the lower Senator Beck Basin (SBB; solid black line) showing the Swamp Angel Wetland (SAW; dashed black line), the stream (blue line), the Senator Beck Stream Gauge (SBSG) and Swamp Angel Study Plot meteorological station (SASP; red triangles), the Upper and Lower Stream Monitoring Stations (USMS and LSMS; orange squares), and the Upper Swamp Angel well and Lower Swamp Angel well (USA and LSA; purple circles). The boundary of the SAW is dashed because the true boundary was difficult to determine in the field. The flow direction of the stream is towards the SBSG (from left to right). The yellow arrows denote the general flow direction of surface water and likely flow direction of groundwater in the SAW. 9

Figure 2.2. Photos of the hydrologic features in the Senator Beck Basin (SBB): **(a)** surface flow in the Swamp Angel Wetland (SAW) in the summer (looking east towards watershed outlet); **(b)** surface flow in the SAW during snowmelt (looking east toward watershed outlet); **(c)** wetland drainage from seepage faces (red ovals) and from small channels (red arrow) in the SAW to the stream (looking north; stream flows from left to right). 17

Figure 2.3. A generalized conceptual model of streamflow path in snowmelt-dominated watersheds, showing the relative strengths of stream discharge (Q) and specific conductance (SC) during snowmelt and low flow conditions. During snowmelt, stream discharge is relatively high and SC is relatively low, while during low flow, stream discharge is relatively low and SC is relatively high, reflecting the difference in water paths to the stream. Modified from Miller et al., (2014). 21

Figure 3.1. Daily SWE in mm **(a)** and daily stream discharge in m^3/s **(b)** for 2006 – 2017 (grey lines) and 2018 – 2021 (colored lines). Daily SWE data were available for the water year (1 October to 30 September), while stream discharge data were available for the measurement period (annually variable). For comparison, the 40-yr median daily SWE and 16-yr median daily SWE are in black. 28

Figure 4.1. Daily precipitation (black vertical bars), daily SWE (black line), 40-yr median daily SWE (grey line), daily stream discharge (solid, colored lines), daily baseflow discharge (dashed, colored lines), and 16-yr median daily stream discharge (purple line) for 2018 – 2021 **(a-d)**. Median daily SWE and median daily stream discharge are included to provide context to the annual SWE and discharge curves. The duration of snowmelt (grey window) is approximated using tQ20 to tQ80. 45

Figure 4.2. Cumulative area-normalized stream discharge **(a)** and baseflow discharge **(b)** as volume of flow (mm) for 2018 – 2021. Vertical black bars denote the start and end dates of the standard period (6 April to 28 September). Numbers at the end of each curve represent the total cumulative flow volumes at the end of each year's measurement period. 47

Figure 4.3. Daily precipitation (black vertical bars), daily stream discharge (solid, colored lines), daily baseflow discharge (dashed, colored lines), daily BFI (dashed, black lines), the timing of peak SWE (black vertical bar), and timing of SAG (yellow vertical bar) for 2018 – 2021 **(a-d)**. t_{sub} variables are represented by diamonds on the BFI curves: t_{30} (red), t_{35} (dark green), t_{40} (magenta), and t_{45} (cerulean). The duration of snowmelt (grey window) is approximated using tQ20 to tQ80. BFI increases as baseflow becomes a greater proportion of total stream discharge within the stream. 51

Figure 4.4. Annual dates (points) and mean dates (horizontal lines) for each t_{sub} variable in the period of record: t_{30} (dark blue diamonds); t_{35} (orange triangles); t_{40} (dark green squares); and t_{45} (cerulean plus signs). 53

Figure 4.5. Correlation bar plots displaying the correlation coefficients between hydroclimate variables and t_{sub} variables: **(a)** t_{30}; **(b)** t_{35}; **(c)** t_{40}; **(d)** t_{45}. Variables in grey have no correlation to t_{sub}, while variables in blue (positive) or red (negative) were correlated with t_{sub} at three levels of confidence: dotted borders represent variables correlated at p-values < 0.10; dashed borders represent variables correlated at p-values < 0.05; and solid borders represent variables correlated at p-values < 0.01. 55

Figure A.1. Hydrologic classification of study years based upon value of peak SWE (mm). Study years were either classified as "Dry", "Average", or "Wet" based upon mean peak SWE ± the standard deviation multiplied by 0.5. Mean peak SWE was 634 mm with a standard deviation of ±147 mm (0.5SD = 74 mm), creating a lower limit of 560 mm and an upper limit of 708 mm. "Dry" years were considered as those with peak SWE values < 560 mm; "Average" years were considered as those with peak SWE values between 560 mm and 708 mm; and, "Wet" years were considered as those with peak SWE values > 708 mm. 101

Figure A.2. Hydrograph of 2020 showing the naturally inverse relationship between stream discharge in m^3/s (green) and specific conductance in mS/cm (black). This year was selected as it shows the inverse relationship during snowmelt (May to late June) as well as during large precipitation events (late July to early August). 102

Figure A.3. Correlation matrix (Pearson's r) between various hydroclimate and timing of substantial baseflow variables. Shades of red and blue indicate negative and positive correlations, respectively. The asterisks indicate significant correlations with p-values (p) less than α values of 0.10 (*), 0.05 (**), and 0.01 (***). A description of the variables used in the correlation matrix is in Table 3.1. Because the correlation matrix is symmetric, only the upper half is displayed. 104

Figure A.4. Daily BFI (%) timeseries for each year in the period of record. Study years outside the study period (2006 – 2017) are in grey while years in the study period (2018 – 2021) are colored: 2018 is blue; 2019 is red; 2020 is green; and 2021 is orange. 107

Figure B.1. Daily discontinuous stream discharge and continuous SC for 2019. Increasing bubble size indicates increasing day of year, where smaller bubbles represent values from the beginning of the measurement period and larger bubbles represent values from the end of the measurement period. Data were fitted with a power law equation ($R^2 = 0.71$) to estimate stream discharge during the period of missing data (21 April to 10 May). 110

Figure C.1. Water level in meters (relative to local ground surface) for the Upper Swamp Angel well (USA, red) and Lower Swamp Angel well (LSA, blue). Positive values (above 0 m) indicate that the water table was above the surface while negative values (below 0 m) indicate that the water table was below the surface. The solid segments of the water level curves (any period outside of 23 July to 25 August) were corrected using measured barometric pressure data while the dashed segments were corrected using interpolated barometric pressure data (Figure C.2). The horizontal dashed lines represent the sensor depth (depth at which pressure was measured) in each well (USA: -38 cm (red) and LSA: -67 cm (blue)). Precipitation in mm (black bars) and stream discharge in m^3/s (orange) were included to provide context to fluctuations in water level. Water level data were recorded every 4 hours while precipitation and stream discharge data were recorded every hour. 111

Figure C.2. Linear model used for interpolating barometric pressure data in Pa at SASP. Discontinuous barometric pressure data from SASP were plotted over continuous barometric pressure data from Telluride Regional Airport (KTEX) and produced a linear relationship ($R^2 = 0.85$). The regression equation was used to reconstruct the missing barometric pressure data at SASP. 112

LIST OF EQUATIONS

Equation 2.1. Stream components 22

Equation 2.2. Mass flux of stream components 22

Equation 2.3. Two-endmember CMB model 22

Equation 2.4. Baseflow Index (BFI) 23

CHAPTER 1 – INTRODUCTION

Groundwater discharge from high-elevation, snowmelt-dominated, headwater watersheds maintains mountain streamflow, a phenomenon that is crucial for downstream water supplies, especially during the low flow period after snowmelt (Bales et al., 2006; Hayashi, 2020; Miller et al., 2020). Mountain watersheds can be conceptualized as "water towers" for their ability to store precipitation in the form of snow during the winter and then contribute large portions of discharge to downstream flow in the spring (Messerli et al., 2004; Cooper et al., 2012; Li et al., 2017; Miller et al., 2020; Somers and McKenzie, 2020). Mountain watersheds are often the headwaters of major rivers and have a disproportionate effect on water resources despite making up only about 20% of the global land surface (Messerli et al., 2004; Somers and McKenzie, 2020). Mountainous watersheds are especially important in dry climates and account for larger proportions of total discharge compared to mountainous watersheds in humid regions (Messerli et al., 2004; Meyer et al., 2007; Miller et al., 2020).

Mountain fens (a type of groundwater-fed wetland) are common in high-elevation, headwater watersheds and play an important role in the hydrologic function of watersheds by linking groundwater and surface water to streamflow (Bedford and Godwin, 2003; Meyer et al., 2007; Cohen et al., 2016; Hayashi, 2020). In dry regions, fens are found where groundwater discharges to the surface and maintains saturation year-round (Cooper and McDonald, 2000; Bedford and Godwin, 2003; Meyer et al., 2007; Cooper et al., 2012; Drexler et al., 2013; Kitlasten and Fogg, 2015; Harbert and Cooper, 2017). Fens rely heavily on snowmelt to recharge the groundwater systems that support their function (Winograd et al., 1998; Serreze et al., 1999; Bales et al., 2006; Blanken, 2014; Hathaway et al., 2022). Thus, changes in the timing and

amount of groundwater inflows may greatly affect fens, but they may be resilient to impacts from climate-driven hydrological changes if the groundwater network they are connected to is large enough to buffer changes (Tague and Grant, 2009; Drexler et al., 2013; Austin and Cooper, 2015; Somers et al., 2019).

1.1. Wetland Drainage

Mountain fens are productive ecosystems that are important to watersheds because of the various ecological and hydrological functions and services they provide, including stabilizing water supplies, mitigating flood and drought, improving water quality, recharging groundwater systems, providing habitats, promoting biodiversity, functioning as carbon sinks, and acting as places of sociocultural value (Cooper, 1996; Meyer et al., 2007; Mitsch and Gosselink, 2007; Nielson, 2008; Mitsch et al., 2015; Cohen et al., 2016). One of the most important functions of wetlands is to provide a slow, steady supply of water to downstream areas year-round (Bedford and Godwin, 2003; Meyer et al., 2007; McLaughlin et al., 2014; Cohen et al., 2016; Hathaway et al., 2022). Wetlands in mountainous watersheds have been found to release internally stored water as baseflow to streams, maintaining streamflow when other sources cannot (Hayashi, 2020; Streich and Westbrook, 2020; Hathaway et al., 2022). The provisioning of water from wetlands to downstream areas is key for supporting groundwater recharge and sustaining baseflow in high-elevation, headwater watersheds, which is particularly important during the dry season after snowmelt when streams reach their lowest flows (Meyer et al., 2007; Drexler et al., 2013; Glas et al., 2018; Hayashi, 2020; Miller et al., 2020; Somers and McKenzie, 2020; Wu et al., 2020; Hathaway et al., 2022). In this study, the supply of water to streams from wetlands is termed “wetland drainage” and can be conceptualized as a component of baseflow. Wetland

drainage to streams in high-elevation, snowmelt-dominated watersheds may be regionally important, yet the sensitivity of wetland drainage to hydroclimatic variability (e.g., variability in the timing and magnitude of hydrologic and climatic processes) remains understudied.

1.2. Mountain Hydrogeology

Historically, mountain watersheds were not considered suitable reservoirs of groundwater due to the presence of steep slopes, impermeable bedrock, and a lack of developed soils; all of which were perceived to limit groundwater flow and storage (Clow et al., 2003; Somers and McKenzie, 2020). However, recent research suggests that mountain watersheds may serve as important reservoirs of groundwater as they have high relief topography which can create steep hydraulic gradients, which in turn drive groundwater circulation and discharge rates (Clow et al., 2003; Hayashi, 2020; Somers and McKenzie, 2020). Mountain watersheds with sufficiently large groundwater storages may be less susceptible to climate-driven hydrological changes as they are able to temporarily store water and release it over a long period of time, thus buffering watersheds against the effects of climate change (Winter, 2000; Hayashi, 2020; Somers and McKenzie, 2020).

The presence of groundwater in mountain watersheds suggests that baseflow plays an important role in streamflow generation and in water budgets. In high-elevation watersheds, snow is the primary form of precipitation and snowmelt is often the largest source of recharge, because melting snow is usually slow enough to allow for high infiltration (Winograd et al., 1998; Serreze et al., 1999; Earman et al., 2006; Barnhart et al., 2016; Miller et al., 2020; Somers and McKenzie, 2020). Groundwater stored during snowmelt allows watersheds to supply baseflow during the low flow period, which is the dominant component of streamflow during the

dry season (Winograd et al., 1998; Serreze et al., 1999; Bales et al., 2006; Hathaway et al., 2022). The relative contribution of baseflow to stream discharge to high-elevation streams in the southern Rocky Mountains can be large, with the annual ratios of baseflow discharge to stream discharge on the order of 18 – 89% (Caine, 1989; Liu et al., 2004; Nielson, 2008; Miller et al., 2014; Rumsey et al., 2015), illuminating the importance of groundwater in mountain regions.

The health of mountain watersheds is critical to ensure watershed function and the transmission of water downstream. In the western United States, more than 60 million people rely on water supplies from mountain river basins, where mountain-derived water is used for municipal, industrial, and agricultural purposes (Barnett et al., 2005; Stewart et al., 2005; Bales et al., 2006; Cooper et al., 2012). The number of mountain-derived water users is only expected to increase in the future, thus increasing the importance of mountain watersheds for streamflow generation (Viviroli et al., 2020). In the western United States, projected changes to climate in the future may alter precipitation regimes, decrease winter snow storage, lead to earlier snowmelt, and lower snowmelt contributions to runoff; this will likely reduce dry season baseflow as streams become more reliant on groundwater in the absence of snow storage (Clow, 2010; Harpold et al., 2012; Li et al., 2017; Jenicek and Ledvinka, 2020). Because baseflow is the dominant component of streamflow during the low flow period, decreases to recharge of mountain groundwater will likely result in decreases of baseflow discharge during the low flow period (Godsey et al., 2014; Barnhart et al., 2016; Li et al., 2017).

While the basic mechanisms and controls on wetland drainage are known, the role and relative importance of wetland drainage in high-elevation, headwater watersheds remain poorly understood. There is a growing body of research on wetland drainage in snowmelt-dominated mountain watersheds, but the regional importance of wetland drainage and its response to

potential changes in climate are unknown. Future climate variability is expected to alter temperature regimes and affect the timing, amount, and phase of precipitation, thus modifying the water budgets of high-elevation watersheds. These changes may influence wetland drainage, particularly during the post-snowmelt low flow period when water resources are most stressed. High-elevation, snowmelt-dominated mountain watersheds are important hydrologic settings to study the influence of climate-driven hydrological changes on wetland drainage because snowpack is a critical water resource for ecological functions and for downstream water supply.

1.3. Goals and Objectives

The primary goal of this study was to investigate the role and relative importance of wetland drainage on streamflow in the Senator Beck Basin (SBB), a high-elevation, snowmelt-dominated, headwater watershed in the San Juan Mountains in southwestern Colorado (Figure 1.1). This study seeks to provide a better understanding of the connection between snowmelt, baseflow, and wetland drainage in high-elevation watersheds. The SBB is a small watershed (2.9 km^2) and has a single fen adjacent to the stream near the outlet of the watershed, making it an ideal place to study wetland drainage, hydroclimate variability, and streamflow.

At some point during the post-snowmelt low flow period, stream reaches upstream of the wetland in the SBB dry completely, yet stream reaches adjacent to and downstream of the wetland maintain flow, providing enough discharge to be measured at the stream gauge. Seepage from wetland faces adjacent to the stream has been observed after snowmelt and appears to be the main source of streamflow during the post-snowmelt low flow period, suggesting that wetland drainage is an important component of baseflow to the stream during low flow. Baseflow is assumed to be entirely wetland drainage when the upper reaches of stream are

known to dry. The simple structure of the SBB (a small area with a single fen and stream) allows this study to isolate the effects of wetland drainage on streamflow because unlike larger watersheds, there are no other sources of baseflow to the stream.

This paper also sought to explore how wetland drainage is influenced by hydroclimate variability, represented by the timing and magnitude of precipitation, snowpack, and stream discharge processes. To investigate the role and relative importance of wetland drainage in the SBB, the ratio of baseflow discharge to total stream discharge was evaluated and compared to characteristics of precipitation, snowpack, and streamflow. Emphasis was placed on the post-snowmelt period, when total streamflow is lowest and wetland drainage has the largest influence on streamflow. Wetland drainage in the SBB is a substantial contributor to baseflow but it is hypothesized that it plays a relatively larger role in maintaining baseflow in dry years than in wet years. The objectives of the study were to: (1) estimate daily baseflow discharge for multiple years; (2) determine the relative timing of when wetland drainage becomes a substantial component of streamflow; (3) correlate the timing of when wetland drainage becomes a substantial component of streamflow to variability (timing and magnitude) in precipitation, snowpack, snowmelt, and streamflow characteristics; and (4) develop a conceptual understanding of wetland drainage and baseflow in the SBB.

This study showed that the relative effects of hydroclimate processes on wetland drainage were more complex than previously hypothesized. Data were used to address the following research questions: (1) does wetland drainage play a considerably larger role in dry years than in wet years?; (2) how do variations in the timing and magnitude of different hydroclimate variables affect when wetland drainage becomes substantial?; and (3) do hydrological processes

that occur during the high flow (snowmelt) period or low flow period have the greatest influence on wetland drainage?

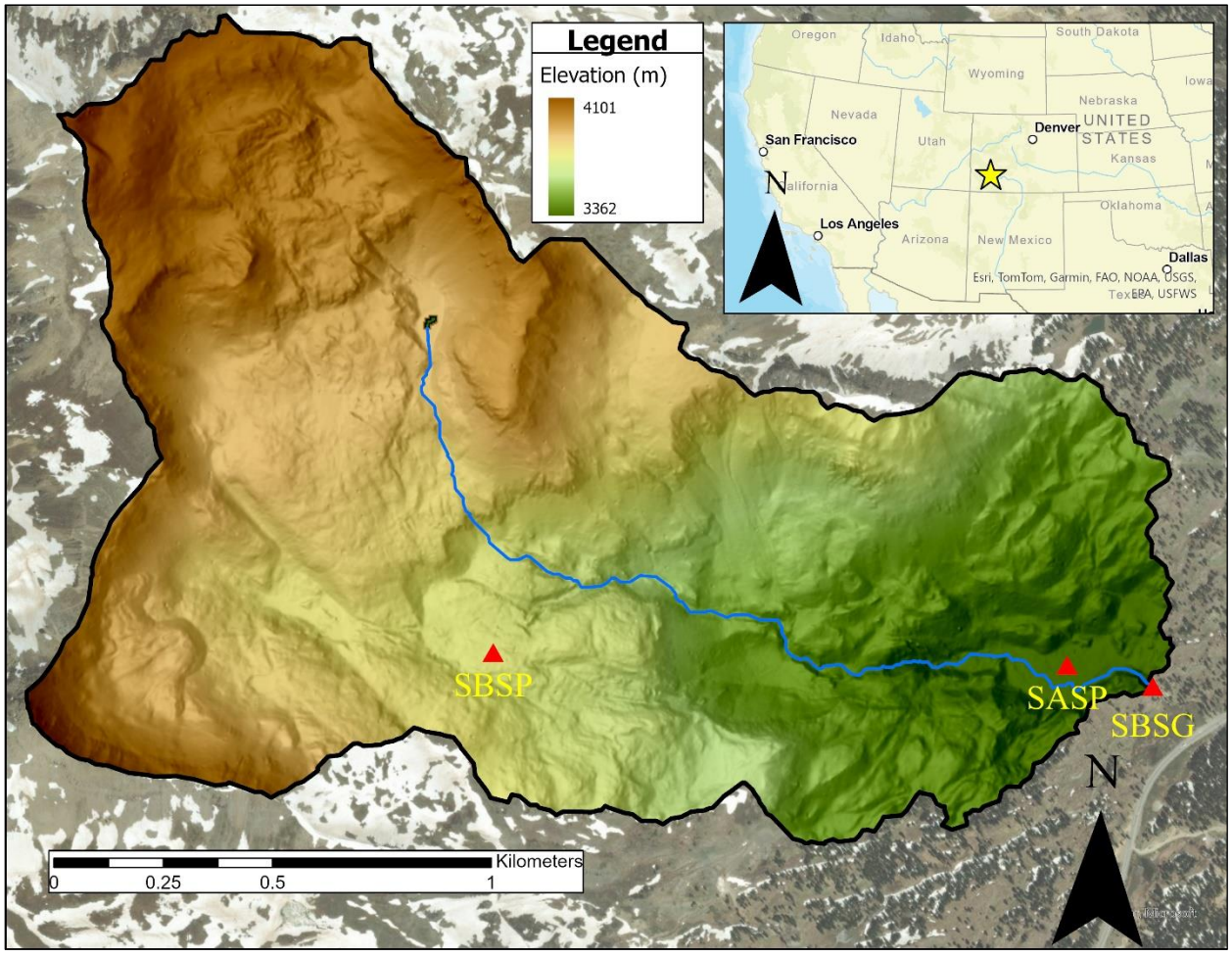

Figure 1.1. Hillshade elevation map of the Senator Beck Basin (SBB; black boundary), showing the stream (blue line) and data collection stations in the watershed (red triangles): Swamp Angel Study Plot (SASP), Senator Beck Stream Gauge (SBSG), and Senator Beck Study Plot (SBSP; not referenced in this research). The flow direction of the stream is towards the SBSG (from left to right). The SNOTEL station (not shown) is located 1.8 km south of the SBB. The yellow star in the inset map denotes the location of the SBB within Colorado and the western United States.

CHAPTER 2 – BACKGROUND

This section introduces the study site, the Senator Beck Basin, and provides a description of the climatic and geologic setting. This section also gives a basic characterization of the wetland under study and introduces the methodology used to estimate baseflow discharge.

2.1. Site Description

This study investigates the hydrology of the Swamp Angel Wetland (SAW), a subalpine fen located in the Senator Beck Basin (SBB) in the San Juan Mountains in southwestern Colorado (Figure 1.1 and Figure 2.1). The San Juan Mountains are a roughly circular uplift, composed of several distinct mountain ranges, that lie at the intersection of the Colorado Plateau and the Southern Rocky Mountains physiographic provinces (Baars, 1992; Blair, 1996). The SBB lies in the western San Juan Mountains and was named after the Senator Beck Mine (located in the upper section of the watershed) as a nod to the area's mining history. The SBB has an area of 2.9 km^2 and ranges in elevation from 3360 m at the outlet to 4100 m at the summit (Figure 1.1). The SBB primarily has a southerly or easterly aspect. The SBB is a dedicated research watershed (operated by the Center for Snow and Avalanche Studies (CSAS) in Silverton, Colorado) with long-term hydrological and meteorological monitoring for over 15 years and represents conditions unique to high-elevation headwater watersheds (Landry et al., 2014). Because of its status as a research watershed, the SBB has minimal human impact and remains relatively pristine compared to other San Juan Mountains watersheds (Landry et al., 2014). The lower section of the SBB (<3400 m) is bowl-shaped with hills surrounding a

relatively flat bottom and contains the SAW, the stream that drains the SBB, a stream gauging station (SBSG), and a meteorological station (SASP; Figure 1.1 and Figure 2.1).

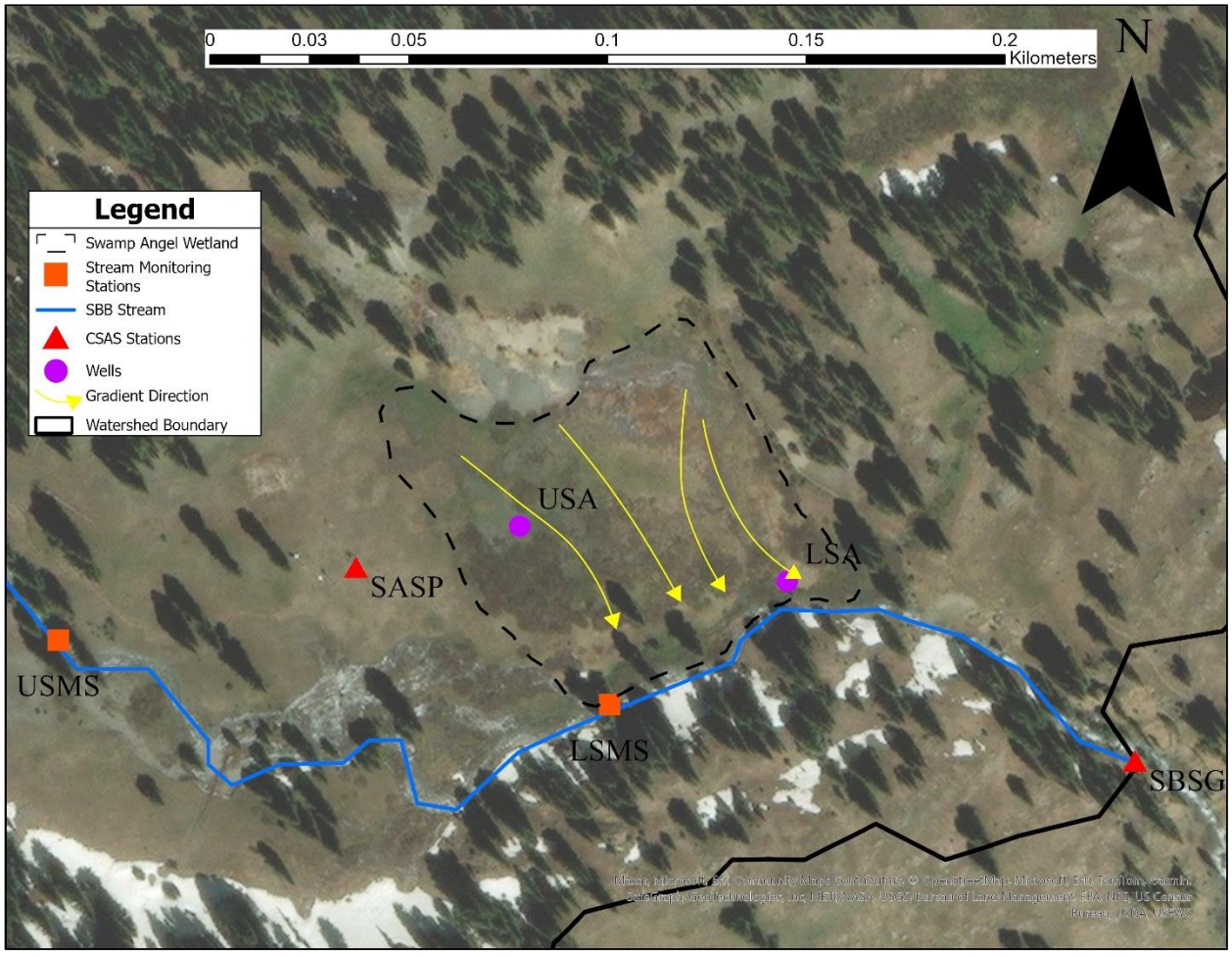

Figure 2.1. Map of the lower Senator Beck Basin (SBB; solid black line) showing the Swamp Angel Wetland (SAW; dashed black line), the stream (blue line), the Senator Beck Stream Gauge (SBSG) and Swamp Angel Study Plot meteorological station (SASP; red triangles), the Upper and Lower Stream Monitoring Stations (USMS and LSMS; orange squares), and the Upper Swamp Angel well and Lower Swamp Angel well (USA and LSA; purple circles). The boundary of the SAW is dashed because the true boundary was difficult to determine in the field. The flow direction of the stream is towards the SBSG (from left to right). The yellow arrows denote the general flow direction of surface water and likely flow direction of groundwater in the SAW.

2.1.1. Precipitation and Snow

Like most of the southern Rocky Mountains, the SBB has a continental, semi-arid, radiation-driven climate, characterized by longer snow accumulation periods, lower snow depths, later snowmelt onset, and lower rates of snowmelt compared to maritime mountains (Keen, 1996; Landry et al., 2014; Trujillo and Molotch, 2014). Storms in these regions are usually low intensity and occur with cold temperatures, which drives the long snow accumulation periods (Serreze et al., 1999). Between water years 2004 and 2012, mean air temperature in the SBB ranged between -0.1 to 1.2°C (Landry et al., 2014). Precipitation in the San Juan Mountains can be described as "biseasonal" and is primarily dominated by snowfall in winter and by rainfall in summer (Toney and Anderson, 2006). Snowfall generally occurs between October and May while rainfall generally occurs between May and October, but the phase of precipitation is governed by local atmospheric and surface conditions as well as regional and global climate effects (Fassnacht et al., 2013; Fassnacht et al., 2022).

In the SBB, snowpack accumulation usually begins in October of the previous year, peak snowpack extent occurs between April and May, followed by full snowpack ablation (complete disappearance of snowpack) by June or July. From July to September, the precipitation regime is dominated by the North American Monsoon, which brings moisture from the Pacific Ocean to the southwest and accounts for about 30% of annual precipitation (Carrara et al., 2011; Landry et al., 2014). This study found that from water years 2006 through 2021, mean annual precipitation in the SBB was 1118 mm, with a range of 724 – 1397 mm (Table A.1). Between water years 2005 and 2012, 74% of annual precipitation fell as snow (Landry et al., 2014) and is consistent with the proportion of precipitation that falls as snow in other areas of the western United States (Serreze et al., 1999; Woods et al., 2006).

2.1.2. Streamflow

Snowmelt-dominated watersheds are defined as those that have an identifiable snowmelt pulse or watersheds where peak stream discharge is at least an order of magnitude greater than low flow discharge (Cayan et al., 2001; Miller et al., 2014). Snowmelt is a major contributor to streamflow in high-elevation headwater watersheds (Li et al., 2017; Hathaway et al., 2022), and snowmelt rate determines the quantity of water held within snowpack that becomes streamflow (Barnhart et al., 2016; Duncan et al., 2020). Snow precipitation is more efficient than rain precipitation at generating streamflow because snowmelt allows for a concentrated period of infiltration and occurs at a time when potential evapotranspiration is low (Barnhart et al., 2016; Li et al., 2017; Jenicek and Ledvinka, 2020; Somers and McKenzie, 2020). In these watersheds, streamflow is conceptualized as being composed of two components: surface water runoff, which comprises waters that travel across the land surface as overland flow, and baseflow, which comprises waters that comes from groundwater storage or delayed sources and may follow shallow subsurface or deeper subsurface paths to reach the stream (Hall, 1968; Price, 2011; Miller et al., 2014; Rumsey et al., 2015).

The hydrographs of the SBB exhibit two periods each year: (1) high streamflow, often occurring between May and July, representing snowmelt or freshet ("the snowmelt period"), and (2) low streamflow, often occurring between July and extending into late autumn or winter ("the post-snowmelt low flow period"). During freshet, some meltwater follows surface or shallow subsurface flow paths that produce large discharges, while some meltwater follows deeper groundwater paths and enters subsurface storage (Hammond et al., 2019; Somers and McKenzie, 2020). Surface water runoff primarily contributes to streamflow during the snowmelt period but also contributes during precipitation events. Baseflow discharge is constant source of stream

water year-round, yet the magnitude of subsurface contributions to streamflow is highest during snowmelt. As snowmelt progresses and lessens, baseflow begins to become the dominant source of streamflow and eventually may become the only source. The presence of a post-snowmelt low flow period consisting of steady, low magnitude discharge, indicates the presence of groundwater storage in high-elevation watersheds (Hayashi, 2020).

2.1.3. Geology

The SBB is primarily underlain by the Oligocene Burns Formation, which is composed of intermediate rhyodacite and quartz latite lava flows (Burbank and Luedke, 1964; Lipman et al., 1973; Steven and Lipman, 1976; Yager and Bove, 2002). The lower section of the SBB, where this study was primarily conducted, is composed of the Burns Formation, with patches of Quaternary alluvium near the stream and wetland (Burbank and Luedke, 1964). Soil thickness in SBB varies between 0 m (bare rock) and >2 m (wetland soils). At the highest elevations, the SBB is capped by sequences of welded ash-flow tuffs, which were deposited after explosive caldera-forming eruptions that formed the nested San Juan and Silverton calderas, located just east of the SBB (Burbank and Luedke, 1964; Lipman et al., 1973; Steven and Lipman, 1976; Yager and Bove, 2002).

2.1.4. Hydrogeology

Mountain watersheds are often considered recharge zones while low elevation areas are often considered discharge zones (Meyer et al., 2007; Hayashi, 2020; Somers and McKenzie, 2020). While it is known that there are volcanic and volcaniclastic aquifers present in the San Juan Mountains, due to the lack of hydrogeologic data and highly spatially variable geologic

environments, there is little constraint on the pervasiveness of aquifer storage, groundwater flow, and surface water-groundwater interactions in the San Juan Mountains (Caine, 2003; Caine and Wilson, 2011). However, there is evidence of a regional-scale groundwater flow system in the San Juan Mountains, even at high elevations, as shown by the existence of groundwater surface features (zones of discharge) such as hot springs, seeps, and wetlands (Caine and Wilson, 2011; Drexler et al., 2013; Rondeau et al., 2020).

Caldera eruptions formed ring fractures that strike roughly North-South within the SBB which may act as groundwater flow paths (Burbank and Luedke, 1964; Lipman et al., 1973; Fetchenhier, 1996; Bove et al., 2001; Yager and Bove, 2002). Ring fracturing, glaciation, and weathering of rocks create geological discontinuities which may act as groundwater circulation pathways (Caine and Wilson, 2011), but it is unknown exactly what role they play in providing preferential flow paths for groundwater in the SBB.

Snowmelt is the primary form of recharge to mountain groundwater (Winograd et al., 1998; Serreze et al., 1999; Bales et al., 2006; Earman et al., 2006) but can be spatially variable (Somers and McKenzie, 2020). In the SBB, snowmelt is probably the only source of recharge, because the proportion of precipitation that falls as snow is large (74%; Landry et al., 2014), because recharge and infiltration from summer rainfall is likely negligible due to the relatively short duration and high intensity of monsoon storm events, and because rainfall probably cannot overcome potential evapotranspiration or overwhelm soil storage capacity as well as snowmelt can (Flint et al., 2004; Earman et al., 2006).

2.1.5. Vegetation

There are three distinct vegetation zones within the SBB: subalpine forests, consisting of Engelmann spruce (*Picea engelmannii*), sub-alpine fir (*Abies lasiocarpa*), and lodgepole pine (*Pinus contorta*) from the watershed outlet until timberline, below 3600 m; bands of krummholz between 3600 – 3700 m; and alpine tundra, consisting of bare rock and low-growing plants, above 3700 m (Toney and Anderson, 2006; Johnson et al., 2013; Landry et al., 2014). The SBB can be divided into the relatively steep upper section (>3400 m) with slopes >10% and the relatively flat lower section (<3400 m) with slopes ≤10% (Figure 1.1). The lower section of the SBB, which contains the SAW, slopes gently towards the watershed outlet. The adjacent hillslopes are primarily covered with evergreen forest and exposed rock outcrops. Vegetation in the SAW consists of sedges (*Carex spp.*), grasses, large patches of willows (*Salix spp.*), and other flowering plants (Figure 2.2).

2.2. Hydrologic Features of the SBB

The stream that drains the SBB is a headwater tributary of the Uncompahgre River, which is a tributary of the Gunnison River, which is itself one of the largest tributaries of the Colorado River, the major river in the southwestern United States. The stream begins in the higher elevation section of the watershed and flows eastward towards the watershed outlet (Figure 1.1). Reaches of stream in the lower section of the SBB (<3400 m) are relatively gentle, while reaches of stream in the middle and upper sections (>3400 m) are relatively steep. Streamflow is sourced primarily from overland flow during snowmelt, and from baseflow during the low flow period. Discharge is greatest during snowmelt, decreasing in magnitude as the

snowpack dissipates. Much of the stream dries during the post-snowmelt low flow period but reaches of stream adjacent to and downstream of the SAW still flow.

The SAW is classified as a mountain fen, distinguished from other wetland types by the presence of saturation conditions in the dry season; the presence of peat, a high organic matter soil that forms in saturated conditions, low growing plants; and a lack of trees (Cooper and Andrus, 1994; Chimner et al. 2010; Crockett et al., 2015; Kitlasten and Fogg, 2015; Malone and Lemly, 2019; Gonzales et al., 2020). The SAW has an area of 0.006 km^2 (0.6 ha), which constitutes 0.2% of the total SBB area, and slopes gently (≤6%) southeastward towards the watershed outlet (Figure 2.1 and Figure 2.2a–b). Measurements taken in the northern part of the SAW show that peat thickness varies between 0.1 m to >1.5 m, which is similar to measurements from other fens in the San Juan Mountains (Chimner et al., 2010). The southern side of the SAW is adjacent to the stream for about 60 m and is hydraulically connected to the stream through surface flow on top of the SAW and seepage from wetland faces adjacent to the stream (Figure 2.1 and Figure 2.2c).

Inflow to the SAW comes as overland flow originating from the adjacent hillslopes and from *in situ* melting snow on the wetland during snowmelt, while inflowing groundwater discharge occurs year-round (Cooper and Andrus, 1994; Cooper et al., 1998; Reeve et al., 2000; Woods et al., 2006; Chimner et al., 2010; Crockett et al., 2015; Mitsch et al., 2015). Outflow from the SAW varies by time of year: seepage from wetland faces is a year-round source of water to the stream while surface flow from the SAW to the stream dominates during snowmelt and periods of high precipitation (Figure 2.2c). There are several surface water drainages in the SAW; most flow strongest during snowmelt.

Observations of seepage from faces in the SAW during the dry season in consecutive summers indicate that wetland drainage is the primary driver of streamflow in the post-snowmelt low flow period; a time when the stream has its lowest annual flows. Like other mountain fens in the southern Rocky Mountains, the SAW exists in a zone of groundwater discharge, as evidenced by the presence of peat soils and constant saturation, even in the dry season when precipitation is infrequent and streamflow is variable (Caine and Wilson, 2011; Drexler et al., 2013; Rondeau et al., 2020). In terms of magnitude, wetland drainage is likely greatest during snowmelt and least during the low flow period. However, the relative importance of wetland drainage to streamflow varies seasonally as it is based on the relative proportion of stream water derived from the SAW.

There are two potential sources of water for wetland drainage from the SAW: discharge from storage within the peat soils of the SAW (contribution) and groundwater supplied to the SAW (transmission; Spence, 2007; Spence et al., 2011; Streich and Westbrook, 2020). Wetland storage may be a large component of drainage from the SAW because of the high porosity of peat soil and potential for preferential flow paths, which allows wetlands to act like aquifers (Glenn and Woo, 1997; Letts et al., 2000). Discharge from wetland storage may not always result in a negative change in storage because it may be replenished by incoming groundwater. Wetland drainage sourced from groundwater provides more consistent flow because it comes from a larger flow system (Roulet, 1990; Branfireun and Roulet, 1998). The water drained by the SAW is mostly from transmitted groundwater, rather than water generated from wetland storage because the SAW is too small to continuously support streamflow during the low flow period. Studies have found that groundwater input into wetlands can be highly spatially variable (Branfireun and Roulet, 1998), but because the SAW is relatively small (0.006 km^2), it can be conceptualized as a point source of groundwater discharge.


(a)


(b)

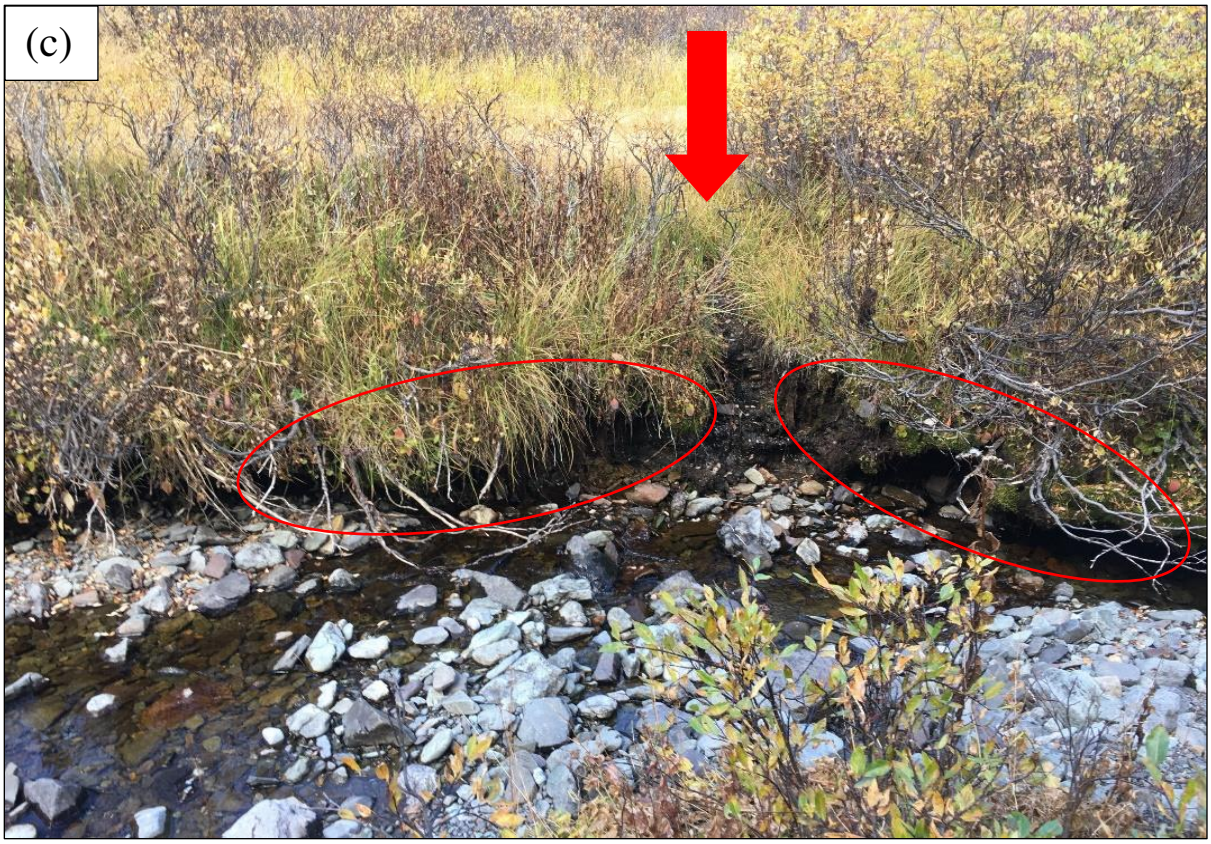

Figure 2.2. Photos of the hydrologic features in the Senator Beck Basin (SBB): **(a)** surface flow in the Swamp Angel Wetland (SAW) in the summer (looking east towards watershed outlet); **(b)** surface flow in the SAW during snowmelt (looking east toward watershed outlet); **(c)** wetland drainage from seepage faces (red ovals) and from small channels (red arrow) in the SAW to the stream (looking north; stream flows from left to right).

2.3. Conductivity Mass Balance Model

Baseflow discharge is often estimated by using hydrograph separation techniques, which seek to estimate the relative proportions of different components of streamflow. Hydrograph separations are often applied to streams when there is a large change in streamflow over a short period, such as flood peaks during snowmelt or during storm events (Pinder and Jones, 1969; Wels et al., 1991; Caissie et al., 1996). When using these techniques, hydrographs are often separated into two components: surface water runoff and baseflow (Pinder and Jones, 1969; Stewart et al., 2007; Miller et al., 2014).

2.3.1. Chemical Hydrograph Separations

While many hydrograph separation techniques exist, a common form used in mountain watersheds are chemical hydrograph separation methods, which utilize hydrochemical tracers to estimate the proportion of different stream components (Pinder and Jones, 1969, Stewart et al., 2007, Miller et al., 2014; Rumsey et al., 2015; Miller et al., 2020). Each stream component has its own source and follows certain paths to reach the stream, which allows them to come into contact with geologic materials of the watershed (e.g., soils or bedrock) (Pilgrim et al., 1979; Matsubayashi et al., 1993; Winter et al., 1998). Depending on the material encountered and the duration that water is in contact with geologic materials, the stream waters will pick up solutes from these materials, altering their chemical signature (Pilgrim et al., 1979; Matsubayashi et al., 1993; Winter et al., 1998; Zhang et al., 2013). Compared to stream waters that come from overland flow, stream waters that come from baseflow move slower and are in contact with subsurface geologic materials for longer, which often gives them greater concentrations of dissolved constituents (Winter et al., 1998). Thus, each component of streamflow is a function of the hydrological and geochemical characteristics of the watershed.

Chemical hydrograph separation methods are advantageous over other methods because they incorporate geochemical information about the watershed, which reflect the characteristics and physical processes that occur within the watershed (Stewart et al., 2007; Miller et al. 2014). Knowledge of the physiographic characteristics of the watershed enhances interpretation of baseflow discharge estimated using chemical hydrograph separation methods (Uhlenbrook et al., 2002; Miller et al., 2014). Therefore, hydrograph separation techniques that use chemical data are deemed more objective than other techniques and may be viewed as more accurate, depending upon the quality of the data used (Hooper and Shoemaker, 1986; Zhang et al. 2013).

A common type of hydrochemical tracer is specific conductance (SC), which is a measure of the ability of water to conduct an electrical current; this, in turn, is a function of the total amount of dissolved ions within the water as well as the type, charge, and mobility of those ions (Miller et al., 1988; Matsubayashi et al., 1993; Laudon and Slaymaker, 1997; Zhang et al., 2013). SC has been used as an indicator of total solute concentrations in stream waters and has also been cited as a robust predictor of other solute concentrations, suggesting that it can be used alone in chemical hydrograph separation methods (Pilgrim et al., 1979; Matsubayashi et al., 1993; Caissie et al., 1996; Covino and McGlynn, 2007). SC is easy to measure and readily accessible long-term datasets can easily be produced for large-scale hydrograph separation applications (Caissie et al., 1996).

The Conductivity Mass Balance (CMB) method is a type of chemical hydrograph separation method that separates out the baseflow component of the hydrograph by using stream discharge and SC of the stream waters (Pinder and Jones, 1969; Stewart et al., 2007; Miller et al., 2014; Miller et al., 2020). The CMB is an effective method for estimating baseflow discharge in mountainous watersheds because stream discharge and SC are relatively easy to measure continuously, both at short time intervals and for long durations (Miller et al., 2014). Continuous discharge and hydrochemical data are tantamount to understanding the inherent heterogeneity in groundwater flow paths and travel times (Stewart et al., 2007). The CMB method is also advantageous to other baseflow estimation methods that involve collecting samples and conducting laboratory analysis because of the associated financial and time requirements (Matsubayashi et al., 1993; Miller et al., 2014).

2.3.2. Streamflow Conceptual Model

During snowmelt, streamflow is dominated by overland flow and shallow subsurface flow (relatively low SC), with minor contributions from baseflow (relatively high SC) (Figure 2.3). The SC of pure snow is generally lower than the SC of snowmelt waters because snowmelt waters travel across the land surface on their way to the stream, coming into contact with surficial geologic materials and picking up solutes along the way, leading to a "geochemically evolved" chemical signature when compared to the signature of pure snow (Pilgrim et al., 1979; Williams and Melack, 1991; Stottlemyer, 2001; Miller et al. 2014). During the low flow period after snowmelt, streamflow is dominated by baseflow (relatively high SC), with minor inputs from shallow subsurface and overland flow (Figure 2.3; relatively low SC). Stream contributions from overland flow during the low flow period usually only occur during summer precipitation events (e.g., monsoon storms).

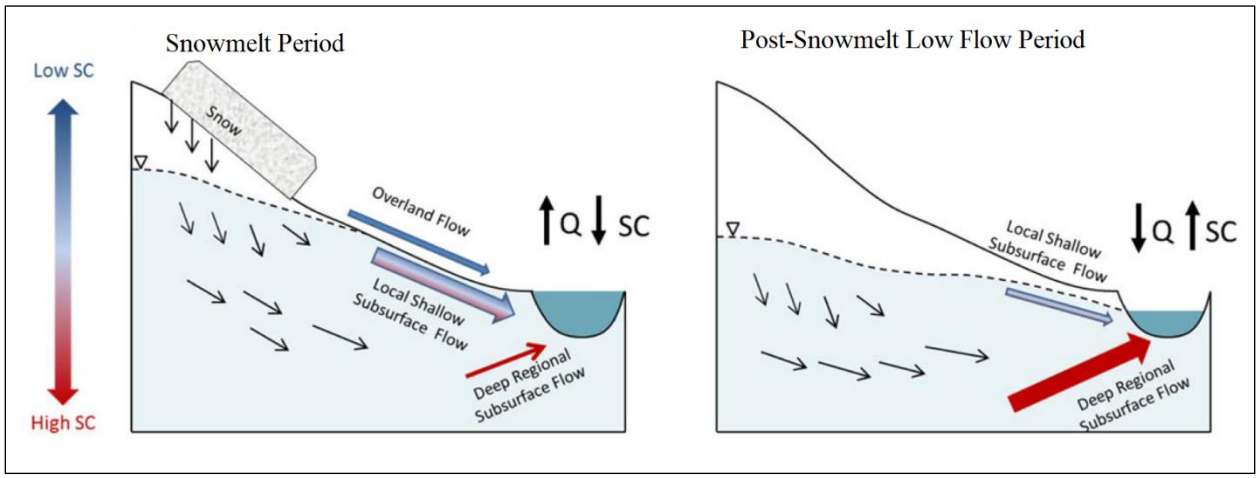

Figure 2.3. A generalized conceptual model of streamflow path in snowmelt-dominated watersheds, showing the relative strengths of stream discharge (Q) and specific conductance (SC) during snowmelt and low flow conditions. During snowmelt, stream discharge is relatively high and SC is relatively low, while during low flow, stream discharge is relatively low and SC is relatively high, reflecting the difference in water paths to the stream. Modified from Miller et al., (2014).

2.3.3. Derivation of Conductivity Mass Balance Model

The mathematics behind the Conductivity Mass Balance method using two components of streamflow results in the following model:

$$Q_S = Q_{RO} + Q_{BF} \quad \text{Eqn. 2.1}$$

Q_S represents total streamflow, Q_{RO} represents the surface water runoff component of streamflow, and Q_{BF} represents the baseflow component of streamflow. The total mass flux (discharge value × tracer value) in the stream is the sum of the mass flux due to runoff and of the mass flux due to baseflow:

$$(Q_S)(SC_S) = (Q_{RO})(SC_{RO}) + (Q_{BF})(SC_{BF}) \quad \text{Eqn. 2.2}$$

SC_S is the specific conductance measured in the stream and SC_{RO} and SC_{BF} are the surface water runoff and baseflow endmembers, respectively. When used in the CMB model, stream components are referred to as "endmembers", which have no physical presence but represent some component of the hydrograph (Uhlenbrook, 2012). The final CMB model is written as follows:

$$Q_{BF} = Q_S \left(\frac{SC_S - SC_{RO}}{SC_{BF} - SC_{RO}}\right) \quad \text{Eqn. 2.3}$$

SC_{RO}, the surface water runoff endmember, is the average conductivity of all runoff waters upstream of the measurement location and best represents waters that are derived from snowmelt (water that enters the stream during snowmelt) and SC_{BF}, the baseflow discharge endmember, is the average conductivity of all subsurface water that discharges to the stream upstream of the measurement location and best represents water that enters the stream during low flow (Stewart et al., 2007; Miller et al., 2014). Endmember values are estimated at different times of the year, when it is easy to distinguish when one component of streamflow dominates over another and when a full record of data is available for endmember selection (Caissie et al.,

1996; Stewart et al., 2007; Miller et al., 2014). SC_{RO} is chosen when discharge is high and SC is low (e.g., during flood peaks induced by snowmelt or stormflow), while SC_{BF} is chosen when discharge is low and SC is high (e.g., during the post-snowmelt low flow period) (Pinder and Jones, 1969; Stewart et al., 2007). SC_{BF} is estimated during low flow because it is impossible to distinguish a single subsurface concentration that represents all baseflow (Miller et al., 2014), but it can be best estimated by examining SC values during low flow.

2.3.4. Baseflow Index

An important metric for quantifying the relative importance of baseflow discharge is the baseflow index (BFI), which is the ratio of baseflow discharge (Q_{BF}) to total stream discharge (Q_S) for a certain time period (Eqn. 2.4; Wahl and Wahl, 1988; Bloomfield et al., 2009). BFI is often calculated on an annual or seasonal basis in order to best represent the long-term proportion of baseflow but can also be calculated on a daily timestep. BFI typically is lowest when stream discharge is highest (i.e., during snowmelt), a characteristic commonly seen in snowmelt-dominated watersheds (Miller et al., 2014; Rumsey et al., 2015; Miller et al., 2020).

$$BFI = \left(\frac{Q_{BF}}{Q_S}\right) \times 100 \qquad \text{Eqn. 2.4}$$

CHAPTER 3 – METHODS

The objectives of the study were to: (1) estimate daily baseflow discharge for multiple years; (2) determine the relative timing of when wetland drainage becomes a substantial component of streamflow; (3) correlate the timing of when wetland drainage becomes a substantial component of streamflow to variability (timing and magnitude) in precipitation, snowpack, snowmelt, and streamflow characteristics; and (4) develop a conceptual understanding of wetland drainage and baseflow in the SBB. To achieve these objectives, this study uses 16 years (2006 – 2021) of meteorological, snowpack, and streamflow data to investigate the role and relative importance of wetland drainage in the SBB.

Baseflow discharge was estimated using the Conductivity Mass Balance method (CMB; Eqn. 2.3). The relative timing of when wetland drainage becomes "substantial" was determined by using threshold BFI values. Several variables that represent precipitation, snowpack, snowmelt, streamflow, and baseflow processes were quantified to relate the influence of hydroclimate variability to wetland drainage (Table 3.1). To emphasize variability in hydroclimate, this study focuses on four recent, consecutive, hydrologically distinct years (2018 – 2021; hereafter, "the study period"). For visualization purposes, each year in the study period has a unique color in tables and figures throughout the document: 2018 is blue, 2019 is red, 2020 is green, and 2021 is orange. Study years 2018 and 2019 are of particular interest because they are the best representative examples of a "dry" (2018) and a "wet" (2019) year.

Field visits to the SBB between June and September 2021 were undertaken to provide further insight into wetland drainage. Two stream monitoring stations (including stream intermittency loggers and time-lapse trail cameras) were installed to observe when and where the

stream dried during the post-snowmelt low flow period while two shallow groundwater wells were installed in the SAW to monitor the water table (Figure 2.1 and Figure C.1; Table C.1). Peat thickness and land surveying data were collected to enhance the analysis and discussion.

3.1. Hydroclimate

The hydroclimate of continental mountains in the western United States is spatiotemporally variable, which can obfuscate significant trends in climate and make determining the impacts of climate-driven hydrological changes on water resources difficult (Clow, 2010; Harpold et al., 2012; Pepin et al., 2015). Because of the complexity of analyzing the influence of climate change on wetland drainage and because of the relatively short length of climate data available at the study site (16 years), this study instead focuses on "hydroclimate variability", which constitutes the relative differences in the timing and amount of precipitation, snowpack, streamflow, and baseflow (Table 3.1). Understanding the complexities of wetland hydrology in high-elevation, snowmelt-dominated watersheds requires a multidisciplinary approach due to the inherent spatial and temporal variability in hydrologic inputs, groundwater recharge, and climate. It is important to understand how variations in the timing and magnitude of hydrologic inputs influence wetland drainage to understand how wetland drainage currently affects streamflow in the SBB and how it may change in the future.

3.2. Data Sources

The SBB is operated as a research watershed by the Center for Snow and Avalanche Studies (CSAS), based in Silverton, Colorado. CSAS maintains two meteorological stations that collect continuous near-surface meteorological and hydrological data (Landry et al., 2014;

Center for Snow and Avalanche Studies, 2020). The lower elevation meteorological station, the Swamp Angel Study Plot (SASP; 3371 m), is located adjacent to the SAW (Figure 1.1 and Figure 2.1), and the higher elevation meteorological station, the Senator Beck Study Plot (SBSP; 3714 m), is located within the alpine tundra zone (Figure 1.1; Landry et al., 2014; Center for Snow and Avalanche Studies, 2020). Data from the SBSP are not referenced in this research. CSAS also operates the Senator Beck Stream Gauge (SBSG; 3362 m), which is located at the watershed outlet in a narrow, incised reach of bedrock (Figure 1.1 and Figure 2.1; Center for Snow and Avalanche Studies, 2012; Landry et al., 2014).

Snowpack data are represented by Snow Water Equivalent (SWE), the liquid amount of water contained within the snowpack, measured in mm (Figure 3.1a). Continuous SWE data were recorded at the nearby Red Mountain Pass Snow Telemetry Station (SNOTEL; Station #713; 3377 m), located about 1.8 km south of the SBB (Table B.1). The SNOTEL network is operated by the Natural Resources Conservation Service (NRCS) and seeks to monitor snowpack conditions; namely, SWE and snow depth. The SNOTEL station sits in a clearing to mitigate wind redistribution of fallen snow. Since the SNOTEL station and the SBB are relatively close to each other and have similar elevations, snowpack characteristics at the SNOTEL station were assumed to be similar to snowpack characteristics in the SBB.

Daily data and station metadata from SASP and SBSG were retrieved from CSAS website <*https://www.snowstudies.org/*>, while SNOTEL data were retrieved from NRCS website <*https://www.nrcs.usda.gov/*>. The SNOTEL station has been in operation since 1980, while SASP and SBSG have both been in operation since at least 2005. Due to incomplete records, data available for analysis were limited to a period of 16 years (2006 – 2021); hereafter, known as “the period of record”. This period was selected because it contained a reasonable

amount of hydrologic variability (i.e., wet and dry years). Data preparation, analysis, and visualization were conducted using Microsoft Excel, ESRI ArcGIS Pro, and with the R statistical package (Environmental Systems Research Institute, 2022; Microsoft, 2025; R Core Team, 2025). Though some of the data used in the preparation of this study were recorded on an hourly timestep, all data presented within this document occur on a daily timestep. To convert hourly measurements to daily values, hourly precipitation data were summed up for a given day, while hourly SC and stream discharge data were averaged across a given day. Sensor specifications and measurement accuracies for the CSAS and SNOTEL stations are in Table B.1.

Both the SNOTEL and SASP stations provide continuous year-round data and can thus be analyzed by water year (1 October – 30 September), but the SBSG does not, and therefore cannot be analyzed by water year (Figure 3.1). The SBSG has a limited measurement period since the pressure transducer and conductivity meter are installed in early spring when the site can be accessed and are removed every autumn before freezing temperatures set in (Center for Snow and Avalanche Studies, 2012; Landry et al., 2014). Therefore, the length of time during which the SBSG instrumentation is installed varies interannually and is hereafter referred to as the "measurement period". All datasets derived from SBSG, such as stream and baseflow discharge, are limited to the measurement period length. Between 2006 – 2021, the mean measurement period length was 241 days with a mean start date of 20 March and a mean end date of 17 November (Table B.2). In every year, the measurement period covers the entire snowmelt period as well as portions of the low flow periods before and after snowmelt (Figure 3.1b). For further comparison, a 175-day period known as the "standard period", ranging from 6 April to 28 September, was used to compare different variables across a standardized timeframe, as this was the longest period in which SBSG data concurrently exists in all 16 years.

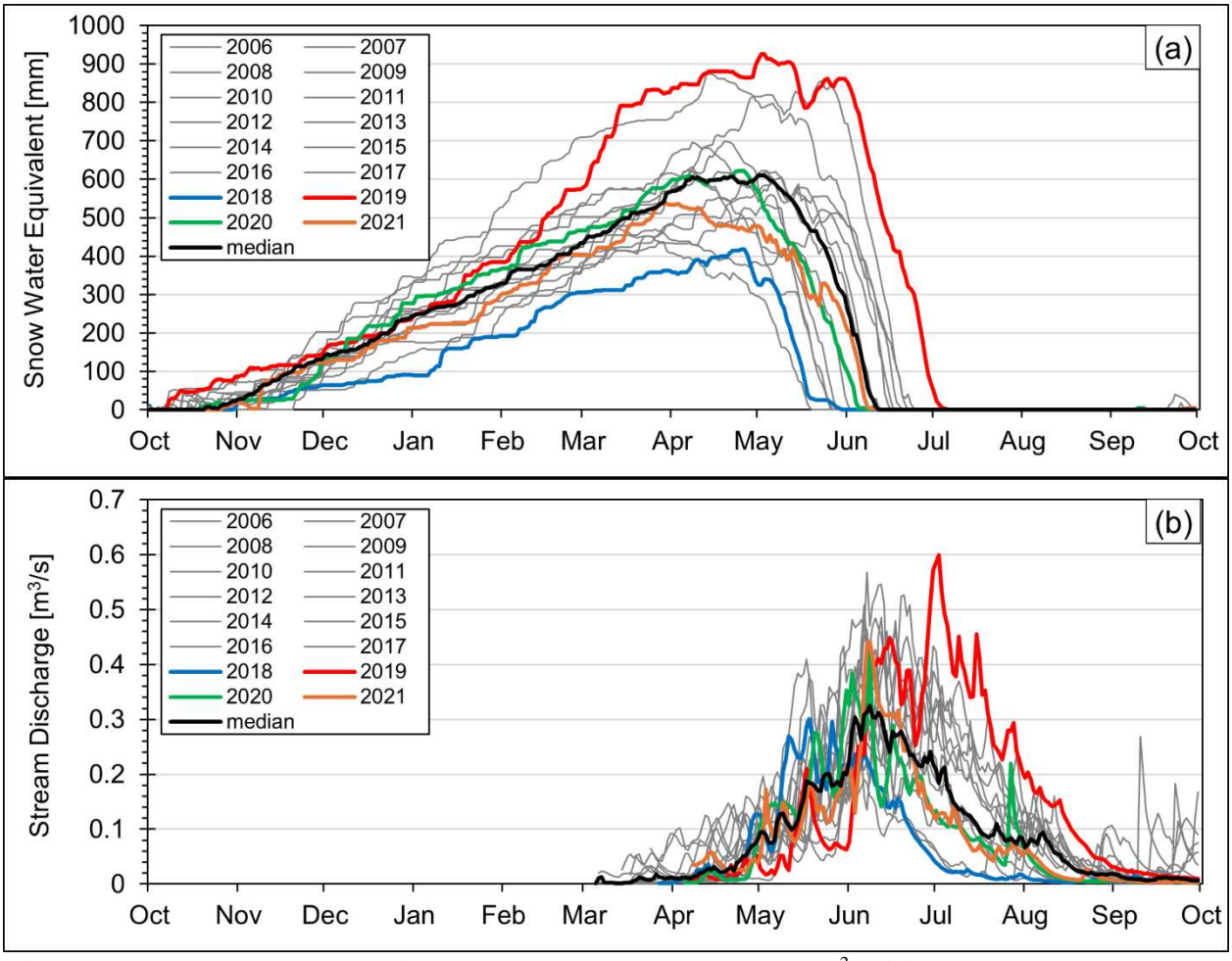

Figure 3.1. Daily SWE in mm **(a)** and daily stream discharge in m^3/s **(b)** for 2006 – 2017 (grey lines) and 2018 – 2021 (colored lines). Daily SWE data were available for the water year (1 October to 30 September), while stream discharge data were available for the measurement period (annually variable). For comparison, the 40-yr median daily SWE and 16-yr median daily SWE are in black.

3.3. Dataset Description

At the SBSG, stream stage was measured using a Druck PDCR Pressure Transducer located 0.61 m upstream of a concrete weir and measurements are calibrated using a rating curve to calculate stream discharge (Center for Snow and Avalanche Studies, 2012; Landry et al., 2014; Table B.1). Stream water temperature (°C) and stream specific conductance (SC; mS/cm corrected to 25°C) were measured at the SBSG using a Campbell Scientific CS547A

Conductivity and Temperature Probe. Streamflow characteristics were represented by the timing (date) and magnitude (m^3/s) of peak stream discharge and by amount of cumulative stream and baseflow discharge (normalized by watershed area, mm; Table 3.1).

Maximum snowpack accumulation was represented by the timing and amount of peak SWE (Table 3.1), which indicates the snowpack size and incorporates the accumulation characteristics as well as precipitation and temperature processes of the snowpack (Fassnacht et al., 2020). Snowmelt characteristics were represented by the date of Snow-All-Gone (SAG), which represents the date of full snowpack ablation (when SWE = 0 mm) and by the timing of the passage of certain percentages of cumulative discharge, which represent the start, center of volume, and end of snowmelt contributions to streamflow (Table 3.1).

Daily precipitation at SASP was measured using an ETI Noah II All-Weather Precipitation Gauge while barometric pressure (Pa) was measured using a Vaisala Barometric Pressure Sensor (Center for Snow and Avalanche Studies, 2020; Table B.1). While a comprehensive analysis of precipitation events was not conducted, daily precipitation was included on some figures and in discussion to provide context to changes in discharge and SWE.

Precipitation characteristics are represented by cumulative water year precipitation (the summation of precipitation between 1 October to 30 September); winter precipitation (the summation of precipitation between the first date of snow accumulation (SWE > 0) and the date of peak SWE); residual precipitation (the summation of precipitation between the day after peak SWE and SAG); and summer precipitation (the summation of precipitation between the day after SAG and the day before the first date of snow accumulation (SWE > 0) of the following winter (Table 3.1). Because winter, summer and residual precipitation are based upon annually variable dates, they do not represent the full water year (Table A.1).

3.3.1. Data Pre-Processing

All data were visually inspected prior to analysis. There were no gaps or obvious errors in the SNOTEL data as those data undergo strict quality control and assurance measures before publication (NRCS, 2014). However, there were a few issues and inconsistencies in the CSAS datasets. In the SBB, instruments can fail, be under maintenance, or other factors such as freezing temperatures or a poor radio transmission signal can interfere with data collection and recording (Jeff Derry, 2020, personal communication). In 2021, the first 6 days of data recorded at the SBSG were omitted due to abnormally high observed SC values.

In 2019, there were 19 days of missing stream discharge data (21 April to 10 May), yet SC and temperature were still recorded. The missing stream discharge data were estimated by plotting continuous SC and discontinuous discharge from the entire 2019 measurement period (n = 189 days; Figure B.1). A power law relationship was determined between the two variables and since the R^2 value was reasonably high ($R^2 = 0.71$) and the curve fit reasonably well, the resulting equation was used to estimate stream discharge during the period of missing data. A power law relationship between stream discharge and SC has been observed in other snowmelt-dominated watersheds (Miller et al., 2014).

3.3.2. SWE Classification

Because there can be high interannual variability in the timing and amount of maximum snowpack accumulation, snowmelt, and the subsequent streamflow (Pepin et al., 2015; Hayashi, 2020), each year was classified into one of three categories based on annual peak SWE magnitude: “wet”, “dry”, and “average” (Figure A.1). Threshold values of mean peak SWE ±0.5SD (one half of the standard deviation) were used to define the upper and lower boundaries

of an “average” hydrologic year. Mean peak SWE was 634 mm while 0.5SD was 74 mm, meaning that dry years were those with peak SWE values <560 mm; average years were those with peak SWE values between 560 mm and 708 mm; and wet years were those with peak SWE values >708 mm. Eight years were classified as average, five years were classified as dry, and three years were classified as wet. In the study period, 2018 and 2021 were dry, 2019 was wet, and 2020 was average.

3.4. Estimating Baseflow Discharge

Since the SBSG had 16 years of readily available, long-term, and continuous stream discharge and SC data, the Conductivity Mass Balance method (CMB) was selected to estimate baseflow discharge in the SBB. The SBB was an ideal place to apply the CMB method because it is a small, pristine, snowmelt-dominated, headwater watershed with little human impact (Landry et al., 2014). The CMB method was selected to estimate baseflow discharge over other approaches because it incorporates physical aspects of the watershed that other approaches cannot (Stewart et al. 2007, Uhlenbrook, 2012, Miller et al. 2014). The CMB method has also been applied effectively to both large and small watersheds across a variety of landscapes and hydrologic regimes, including in snowmelt-dominated, mountainous settings in the western United States (Caine, 1989; Covino and McGlynn, 2007; Miller et al., 2014; Miller et al., 2020).

Following the methods of Pinder and Jones, (1969), Stewart et al., (2007), and Miller et al., (2014), hydrographs were separated into two components: surface water runoff and baseflow discharge (Eqn. 2.1). Surface water runoff represents water that flows to the stream over the land while baseflow represents water that flows to the stream through subsurface flow paths. Here, baseflow is a combination of groundwater from many flow paths and represents water from

various groundwater networks (Hall, 1968; Price, 2011; Miller et al., 2014). A two-endmember mass balance model was selected because the SBB is small and probably has relatively homogenous and impermeable volcanic geology, suggesting that subsurface flow is likely homogenous (i.e., there is likely one baseflow component discernable in stream data). Secondly, during the low flow period, there were no observations of baseflow contributions to the stream other than from the SAW, meaning that the SAW is likely the sole source of streamflow in the post-snowmelt low flow period.

Baseflow discharge characteristics for each year was represented by cumulative baseflow discharge (normalized by area; mm), mean measurement period SC (mean of daily SC values for a given period; mS/cm), minimum SC (the lowest SC value in any year), and SC_{BF} (the value of the baseflow endmember in the CMB model; Table 3.1).

3.4.1. Endmember Selection

Endmember selection was conducted after data collection to ensure that the largest range of stream SC data were observed (Caissie et al., 1996). Based on the work of previous studies, SC_{RO} was estimated as an annually constant SC value and SC_{BF} was estimated as an annually variable SC value (Pinder and Jones, 1969; Stewart al., 2007; Miller et al., 2014). An annually constant SC_{RO} endmember was used because variations in the SC of surface water runoff were expected to be relatively small between years, while an annually variable SC_{BF} endmember was used because variations in the SC of baseflow were expected to be large and to account for potential shifts in climate or from anthropogenic effects on stream water quality (Pinder and Jones, 1969; Stewart et al., 2007; Miller et al., 2014). Different subsurface flow paths may be used at different times during the year and choosing an annually variable SC_{BF} integrates all

possible flow paths that subsurface waters can take before reaching the stream, reflecting their unique travel times and signatures (Stewart et al., 2007; Miller et al., 2014).

3.4.2. Applying the CMB method to the SBB

To apply the CMB method to estimate baseflow discharge in the SBB, four assumptions were made: (1) there is a natural inverse relationship between SC and stream discharge, where SC decreases as discharge increases (Pinder and Jones, 1969, Pilgrim et al., 1979, Stewart et al., 2007, Miller et al., 2014; Rumsey et al., 2015); (2) contributions from other components are negligible (Sklash and Farvolden, 1979; Wels et al., 1991; Miller et al., 2014; Miller et al., 2015; Rumsey et al., 2015); (3) endmembers are significantly different from each other (Uhlenbrook, 2012, Miller et al., 2014, Miller et al., 2015, Rumsey et al., 2015); and (4) endmembers remain constant in time (Pinder and Jones, 1969; Stewart et al., 2007; Miller et al., 2014; Miller et al., 2015; Rumsey et al., 2015). Further examination of these assumptions and model uncertainty is in Chapter 5.

In snowmelt-dominated watersheds, stream discharge and SC have a naturally inverse relationship, where during snowmelt stream discharge is high and SC is low and during low flow stream discharge is low and SC is high (Pinder and Jones, 1969; Pilgrim et al., 1979, Stewart et al., 2007, Miller et al., 2014; Rumsey et al., 2015). In every year in the SBB, stream discharge and SC were inversely related to each other. Figure A.2 shows the inverse relationship between stream discharge and specific conductance in 2020, highlighting that the inverse relationship is present during snowmelt and during the low flow period. While minimum SC occurs during snowmelt, it does not always occur on the day of maximum discharge (e.g., minimum SC only occurred on the same day as peak streamflow in 5 of 16 years).

By using a two-component CMB model (Eqn. 2.3), all possible flow paths to stream are integrated into either the surface water runoff component or the baseflow component, making contributions from other endmembers negligible.

The SC_{RO} and SC_{BF} endmembers are estimated at different times of the year (SC_{RO} was chosen during snowmelt and SC_{BF} was chosen during low flow), when different streamflow regimes dominate, to ensure that endmembers had significantly different values. SC_{RO} was selected as the lowest SC value seen in the entire period of record at the SBSG (0.031 mS/cm), which occurred in May 2012, one of the driest years on record (Table A.2).

For every year, SC_{RO} was held constant at 0.031 mS/cm, while SC_{BF} was estimated annually as the 99th percentile value of all SC values each year (Table A.2). The 99th percentile of annual SC values was selected because it eliminates outliers and because it is impossible to identify a single SC value that represents baseflow (Miller et al., 2014). Once selected, endmember values were held constant for each measurement period.

3.4.3. Baseflow Index

BFI (as a percentage) was calculated on a daily timestep and for the measurement period, standard period, snowmelt period (tQ20 to tQ80), and low flow periods (tQ80 to end of measurement) for every year using Eqn. 2.4. Due to the use of the 99th percentile SC value for SC_{BF}, some BFI values (<1%) exceeded 100%, often during periods of low flow. BFI values for these days were forced to 100% (Table B.2).

Table 3.1. Summary of variables used to characterize hydroclimate variability and the timing of substantial baseflow in the SBB. Each variable has an associated variable type (what the variable represents), a process (the physical process being described), units, and a brief description.

Variable	Type	Process	Units	Description
Cumulative Water Year Precipitation	Amount	Precipitation	mm	Cumulative Precipitation between 1 Oct and 30 Sept
Winter Precipitation	Amount	Precipitation	mm	Cumulative precipitation between the first date of snow accumulation (SWE > 0) and date of peak SWE
Residual Precipitation	Amount	Precipitation	mm	Cumulative precipitation between day after peak SWE and SAG
Summer Precipitation	Amount	Precipitation	mm	Cumulative precipitation between day after SAG and day before first date of snow accumulation of the following year
Peak SWE Magnitude	Magnitude	Snowpack	mm	Magnitude of maximum annual snow accumulation
Peak SWE Date	Timing	Snowpack	date	Date of maximum annual snow accumulation
Peak Stream Discharge	Magnitude	Streamflow	m^3/s	Magnitude of maximum annual stream discharge
Peak Stream Discharge Date	Timing	Streamflow	date	Date of maximum measurement period streamflow
Cumulative Stream Discharge	Amount	Streamflow	mm	Total cumulative stream discharge for the measurement or standard period
SAG	Timing	Snowmelt	date	First date of no snow SWE = 0 mm)
Difference between Peak SWE and SAG	Timing	Snowmelt	days	How long it takes for the snowpack to completely ablate (peak SWE to 0 mm SWE)
tQ20	Timing	Snowmelt	date	Start of snowmelt contribution to streamflow
tQ50	Timing	Snowmelt	date	Center of volume of snowmelt
tQ80	Timing	Snowmelt	date	End of snowmelt contribution to streamflow
Mean Measurement Period SC	Magnitude	Baseflow	mS/cm	Mean of all daily values in the measurement period
Minimum SC	Magnitude	Baseflow	mS/cm	Minimum annual observed SC value
SC_{BF}	Magnitude	Baseflow	mS/cm	Represents the baseflow endmember in the CMB model
Cumulative Baseflow Discharge	Amount	Baseflow	mm	Total cumulative baseflow discharge for the measurement or standard period
Measurement Period BFI	Ratio	Baseflow	%	Ratio of cumulative baseflow discharge to cumulative stream discharge over the measurement period
Standard Period BFI	Ratio	Baseflow	%	Ratio of cumulative baseflow discharge to cumulative stream discharge over the standard period (6 April to 28 September)
Snowmelt Period BFI	Ratio	Baseflow	%	Ratio of cumulative baseflow discharge to cumulative stream discharge over the snowmelt period (tQ20 – tQ80)
Low Flow Period BFI	Ratio	Baseflow	%	Ratio of cumulative baseflow discharge to cumulative stream discharge over the low flow period (tQ80 – end of measurement)
t_{30}	Timing	Wetland Drainage	date	Date of daily BFI of 30% or greater
t_{35}	Timing	Wetland Drainage	date	Date of daily BFI of 35% or greater
t_{40}	Timing	Wetland Drainage	date	Date of daily BFI of 40% or greater
t_{45}	Timing	Wetland Drainage	date	Date of daily BFI of 45% or greater

3.5. Cumulative Flow and Snowmelt

Cumulative stream discharge and baseflow discharge normalized by area (volume per area; mm), also known as cumulative flow volumes, were calculated for the measurement and standard periods to compare flow volumes in different years (Table 3.1). Cumulative flow volumes for the standard period were calculated as if discharge started on 6 April and ended on 28 September.

The date of the start, center of volume, and end of snowmelt contributions to streamflow were approximated by calculating the timing of the passage of certain percentages of cumulative discharge in the standard period for each year, a common metric in snowmelt-dominated watersheds (Stewart et al., 2004; Clow, 2010; Fassnacht et al., 2014; Pfohl, 2016; Fassnacht et al., 2022). The start of snowmelt was approximated by the timing of the passage of 20% of cumulative stream discharge (tQ20); the center of volume of snowmelt or timing of peak snowmelt input into the stream was approximated by the timing of the passage of 50% of cumulative discharge (tQ50); and the end of snowmelt was approximated by the timing of the passage of 80% of cumulative discharge (tQ80) (Stewart et al., 2004; Clow, 2010; Fassnacht et al., 2014; Pfohl, 2016; Fassnacht et al., 2022). The period after tQ80 until the end of measurement period represents the post-snowmelt low flow period.

3.6. Estimating the Role of Wetland Drainage

Observations of seepage from faces in the SAW (Figure 2.2c) during the dry season indicate that wetland drainage is the primary driver of streamflow in the post-snowmelt low flow period. The SAW appears to be a zone of groundwater discharge because it is constantly saturated throughout the year and because of its relatively small size. There is no evidence of

groundwater discharge anywhere in the reach of stream between the SAW and stream gauge and because that reach is underlain by relatively impermeable volcanic bedrock, there are probably no other sources of baseflow to the stream other than the SAW. Because all groundwater that enters the stream comes through the SAW, the SAW integrates all possible subsurface flow paths to the stream. Any other amount of baseflow discharge to the stream outside of wetland drainage from the SAW is considered negligible.

Daily BFI data are used to define the point in time at which baseflow discharge (representing wetland drainage) becomes a "substantial" component of streamflow following snowmelt. At some point during the low flow period, the relative contribution of baseflow begins to become a substantial portion of total streamflow and signifies when wetland drainage dominates in the stream.

To represent the timing of substantial baseflow, a suite of four variables was created based on incremental threshold BFI values. Each variable represents the day on which BFI meets and always exceeds a certain threshold value. The variables used are: t_{30} which represents the day at which BFI equals 30%; t_{35} which represents the day at which BFI equals 35%; t_{40} which represents the day at which BFI equals 40%; and, t_{45} which represents the day at which BFI equals 45%. Collectively, these four variables are referred to as "t_{sub}" variables, meaning "the timing of substantial baseflow". Four t_{sub} variables were selected because: (1) wetland drainage from the SAW was not measured directly in this study; (2) BFI values between 30 – 45% appear to be reasonable values for describing "substantial baseflow" because values of 30 to 45% captures the range of minimum daily BFI values in the period of record; (3) there is uncertainty and error in the estimated baseflow discharge and BFI datasets; and, (4) the importance of

wetland drainage cannot be represented by a single estimative variable, and therefore should be captured by a comprehensive suite of variables.

t_{sub} is expected to vary annually, reflecting interannual variability in hydroclimate. A relatively early t_{sub} signifies that wetland drainage becomes substantial earlier in the year, whereas a relatively late t_{sub} signifies that wetland drainage becomes substantial later in the year. An earlier t_{sub} indicates that the stream is more reliant on wetland drainage, and a later t_{sub} indicates that the stream is less reliant on wetland drainage.

3.7. Statistical Analysis

Because t_{sub} is influenced by many processes, several hydroclimatic variables were identified for statistical analysis. The correlation coefficient, which describes the strength and direction of the linear relationship between two quantitative variables, was employed to help explain the relationships between hydroclimate variables and t_{sub} (Table 3.1). Each variable used has a type (e.g., the timing (day of year), magnitude, cumulative amount, or relative amount (ratio)) and a hydrologic process (e.g., precipitation, snowmelt, streamflow, baseflow, or t_{sub}). Correlation bar plots and a correlation matrix, which display the Pearson's product-moment correlation coefficient (also known as correlation coefficient or Pearson's r), were constructed to explore what factors have the strongest relationship to wetland drainage in the SBB (Figure 4.5 and Figure A.3). The correlation bar plots display the correlation coefficient and significance levels between t_{sub} variables and hydroclimate variables as bars, while the correlation matrix compiles the correlation coefficient and significance levels into a grid. Statistically significant patterns were recognized with three levels of confidence: moderately significant (*) for $p < 0.10$, statistically significant (**) for $p < 0.05$, and highly significant (***) for $p < 0.01$.

CHAPTER 4 – RESULTS

Since this study is concerned with the factors influencing wetland drainage, the results of this paper focus on how variability in hydroclimatic processes influences t_{sub} in the study period: 2018 (dry), 2019 (wet), 2020 (average), 2021 (dry) (Figure A.1). For visualization purposes, each year in the study period has a unique color in tables and figures: 2018 is blue, 2019 is red, 2020 is green, and 2021 is orange. Study years 2018 and 2019 are of particular interest because they are the best representative examples of a "dry" (2018) and a "wet" (2019) year. Throughout the text, mean values refer to averages calculated across the period of record (2006 – 2021), not the averages calculated across the study period (2018 – 2021).

4.1. Precipitation

Mean cumulative water year precipitation was 1118 mm (Table 4.1). In the study period, cumulative precipitation was highest in 2019 (1256 mm), below average in 2020 (943 mm) and 2021 (964 mm) and lowest in 2018 (724 mm). Cumulative precipitation was >1000 mm in 12 of the 16 years on record. Three years with cumulative precipitation <1000 mm occurred during the study period (2018, 2020, and 2021). Most precipitation events were small in magnitude (<10 mm), but about 10% of all precipitation events in the period of record were >10 mm. Precipitation occurred in all months of the year with December through April being the wettest months and June being the driest (Table A.1).

Precipitation amounts were also computed for three groups: mean winter precipitation was 706 mm; mean residual precipitation was 91 mm; and mean summer precipitation was 327 mm (Table 4.1). In the study period, winter precipitation was above average in 2019 and 2020

and below average in 2018 and 2021; residual precipitation was above average in 2019 and 2021 and below average in 2018 and 2020; and summer precipitation was above average in 2018 and 2021 and below average in 2019 and 2020 (Table A.1).

Table 4.1. Summary of precipitation and snowpack characteristics for the period of record. A description of variables is in Table 3.1.

Year	Classif.	Cumulative Precip. (mm)	Winter Precip. (mm)	Resid. Precip. (mm)	Summer Precip. (mm)	Peak SWE (date)	Peak SWE (mm)	SAG (date)	No. Days between Peak SWE and SAG (days)
2006	Avg	1214	691	57	468	8-Apr	620	28-May	50
2007	Avg	1233	785	54	369	9-May	602	12-Jun	34
2008	Wet	1238	848	130	269	14-Apr	874	19-Jun	66
2009	Avg	1220	757	80	344	19-Apr	699	28-May	39
2010	Avg	1127	664	140	338	8-Apr	615	1-Jun	54
2011	Wet	1397	1078	41	310	22-May	856	24-Jun	33
2012	Dry	897	481	94	243	22-Mar	452	18-May	57
2013	Dry	1045	588	37	506	26-Apr	498	24-May	28
2014	Avg	1209	684	90	396	2-May	622	12-Jun	41
2015	Dry	1063	756	57	356	26-May	513	20-Jun	25
2016	Avg	1219	752	96	298	3-May	592	13-Jun	41
2017	Avg	1136	709	152	308	5-Apr	696	14-Jun	70
2018	Dry	724	432	40	339	26-Apr	417	30-May	34
2019	Wet	1256	812	159	154	3-May	925	6-Jul	64
2020	Avg	943	710	76	156	25-Apr	622	11-Jun	47
2021	Dry	964	543	156	380	2-Apr	536	12-Jun	71
Mean:	-	1118	706	91	327	23-Apr	634	9-Jun	47

4.2. Snowpack

Mean peak SWE occurred on 23 April and ranged between late March (2012) and late May (2011 and 2015) (Figure 3.1a; Table 4.1). In the study period, peak SWE occurred near the mean date in 2018 and 2020, later than average in 2019, and earlier than average in 2021. Mean peak SWE magnitude was 634 mm (Table 4.1). Peak SWE in 2018 and 2019 were the lowest and highest peak SWE values in the 16-yr record (2006 – 2021) and some of the lowest and

highest values in the 40-yr SNOTEL record, respectively. Despite each having similar peak SWE values, 2021 was classified as dry while 2020 was classified as average (Figure A.1).

Compared to the median SWE curve (Figure 4.1, black lines), daily SWE in 2018 was consistently lower than and had a lower and earlier peak than median daily SWE; daily SWE in 2019 was consistently higher than and had a higher and later peak than median daily SWE; daily SWE in 2020 tracked similarly to median daily SWE (SWE increases were similar in timing and magnitude); and daily SWE in 2021 tracked similarly to median daily SWE until early April 2021, after which the 2021 daily SWE curve diverged from median daily SWE. Despite peak SWE occurring 21 days earlier than average in 2021, daily SWE remained relatively high (>450 mm) until early May (Figure 4.1d).

The mean date of SAG was 9 June and occurred earlier than average in 2018, later than average in 2019, and close to average in 2020 and 2021 (Table 4.1). SAG in 2019 was the latest on record. The length of time between peak SWE date and SAG represents the time it takes for snowpack to fully ablate (maximum SWE to 0 mm SWE) and was shorter than average in 2018, average in 2020, and longer than average in 2019 and 2021.

The relative rate of snowmelt can be estimated from the steepness of daily SWE curves and from dates of peak SWE and SAG (Figure 4.1; Table 4.1). The steepness of daily SWE curves generally increases with distance in time from peak SWE. The 2018 snowpack melted out quickly as evidenced by the shorter period between peak SWE and SAG, whereas the 2019 snowpack took a long time to melt out because of its large size and longer period between peak SWE and SAG. The 2020 daily SWE curve had similar values compared to the median daily SWE curve (increased, decreased, and peaked at similar times), showing a snowmelt period similar to the median in terms of duration and rate. In 2021, peak SWE occurred 21 days earlier

than average, yet SAG occurred near the average date, creating a longer period between peak SWE and SAG. Despite the early peak SWE date in 2021, the snowpack did not begin to decline rapidly until early May (Figure 4.1d). The 2021 stream discharge hydrograph during snowmelt was similar in shape to the median and 2020 hydrographs.

4.3. Snowmelt Period

Snowmelt contributions to streamflow were represented by tQ20 (snowmelt start; mean date: 21 May), tQ50 (snowmelt center of volume; mean date: 12 June), and tQ80 (snowmelt end; mean date: 15 July) (Table 4.2). Mean tQ80 occurred about 1 month after mean tQ50 and about 2 months after mean tQ20, while mean tQ50 occurred about 1 month after mean tQ20. SAG and tQ50 were temporally very close in the SBB, as also observed by previous researchers (Doskocil et al., 2021; Fassnacht et al., 2022). Both 2020 and 2021 had the same tQ80 and peak stream discharge date, with a 1-day and a 4-day difference in tQ20 and tQ50, respectively (Table 4.2).

The mean snowmelt period (tQ20 to tQ80) was 56 days long and in the study period was longest in 2019 (44 days) and shortest in 2018 (37 days) (Figure 4.1 (grey area); Table 4.2). Relative to 2018, 2020, and 2021, the snowmelt period in 2019 was shifted later by about 3 weeks (Figure 4.1). The mean post-snowmelt low flow period length (tQ80 to end of measurement period) was 121 days and in the study period was longest in 2018 (155 days) and shortest in 2019 (79 days) (Table 4.2). Snowmelt period lengths in the study period were about 15 days shorter than average. However, the length of the post-snowmelt low flow period is heavily influenced by the measurement period end date, which varied between late September and late December due to removal of the stream gauge (Table B.2).

Table 4.2. Summary of snowmelt timing and peak stream discharge variables for the period of record. A description of variables is in Table 3.1.

Year	Classif.	tQ20 (date)	tQ50 (date)	tQ80 (date)	Peak Stream Discharge (date)	Peak Stream Discharge (m^3/s)	Snow-melt Period (days)	Low Flow Period (days)
2006	Avg	17-May	9-Jun	2-Aug	25-May	0.346	77	89
2007	Avg	19-May	16-Jun	1-Aug	2-Jun	0.332	74	108
2008	Wet	31-May	23-Jun	20-Jul	16-Jun	0.432	50	126
2009	Avg	11-May	1-Jun	1-Jul	15-May	0.410	51	142
2010	Avg	23-May	10-Jun	15-Jul	4-Jun	0.509	53	133
2011	Wet	7-Jun	27-Jun	19-Jul	15-Jun	0.479	42	118
2012	Dry	27-Apr	22-May	14-Jun	22-May	0.293	48	147
2013	Dry	17-May	8-Jun	30-Aug	16-May	0.381	105	117
2014	Avg	28-May	20-Jun	7-Aug	31-May	0.481	71	113
2015	Dry	24-May	18-Jun	14-Jul	10-Jun	0.485	51	137
2016	Avg	24-May	16-Jun	17-Jul	5-Jun	0.568	54	147
2017	Avg	21-May	15-Jun	9-Jul	18-Jun	0.526	49	130
2018	Dry	11-May	28-May	17-Jun	17-May	0.301	37	155
2019	Wet	10-Jun	1-Jul	24-Jul	1-Jul	0.599	44	79
2020	Avg	18-May	5-Jun	30-Jun	6-Jun	0.419	43	90
2021	Dry	19-May	9-Jun	30-Jun	6-Jun	0.442	42	112
Mean:	-	21-May	12-Jun	15-Jul	3-Jun	0.438	56	121

The snowmelt period was notably longer in 2013 because tQ80 in 2013 occurred in late August (about 45 days later than average). If 2013 were removed, mean tQ80 would decrease by 3 days from 15 to 12 July and mean snowmelt period length would decrease from 56 to 52 days.

4.4. Stream and Baseflow Discharge

Stream discharge hydrographs in the SBB are typical of snowmelt-dominated watersheds and show three distinct periods: a low flow period in early spring (March to April), a high flow (snowmelt) period in late spring to early summer (April to June), and a post-snowmelt low flow period beginning in summer continuing into autumn (July to November) (Figure 4.1). Mean peak stream discharge occurred on 3 June and in the study period, peak stream discharge occurred earliest and was lowest in 2018, occurred latest and was highest in 2019, and was approximately average in timing and magnitude in 2020 and 2021 (Figure 4.1; Table 4.2). In most years, peak stream discharge date and tQ50 were similar in timing, with a mean difference of 9 days (Table

4.2). Peak stream discharge and tQ50 differed by 11 days in 2018 and by 1 – 3 days for 2019 – 2021. In 2018, which had a double peak in streamflow during snowmelt, tQ50 (28 May) occurred 11 days later than peak stream discharge (17 May, 0.30 m^3/s), but was only 3 days later than the second discharge peak (25 May, 0.29 m^3/s) (Figure 4.1a; Table 4.2). During the low flow period, stream discharge generally remained low, except after large precipitation events, such as in late July 2020 (Figure 4.1c).

Baseflow discharge was generally highest during snowmelt and lowest during the post-snowmelt low flow period (Figure 4.1). Despite baseflow discharge fluctuations being reflective of total stream discharge, baseflow discharge curves were not a mirror image of stream discharge, lagging behind stream discharge peaks on the scale of hours to days (Figure 4.1). Peak baseflow discharge usually occurred on the rising limb of the hydrograph during snowmelt but could also occur during the low flow period during large precipitation events (e.g., late July 2020; Figure 4.1c; Table A.2). Peak baseflow discharge occurred within the snowmelt period in 10 of 16 years. Baseflow discharge was usually higher on the rising limb of the hydrograph than on the falling limb (Figure 4.1), showing that subsurface flow is an important component of streamflow during snowmelt (Pinder and Jones, 1969; Miller et al., 2014). Like stream discharge, baseflow discharge often reached its lowest values during autumn. Consistent stream discharge values during the low flow period (<0.01 m^3/s) suggest constant baseflow inputs to the stream.

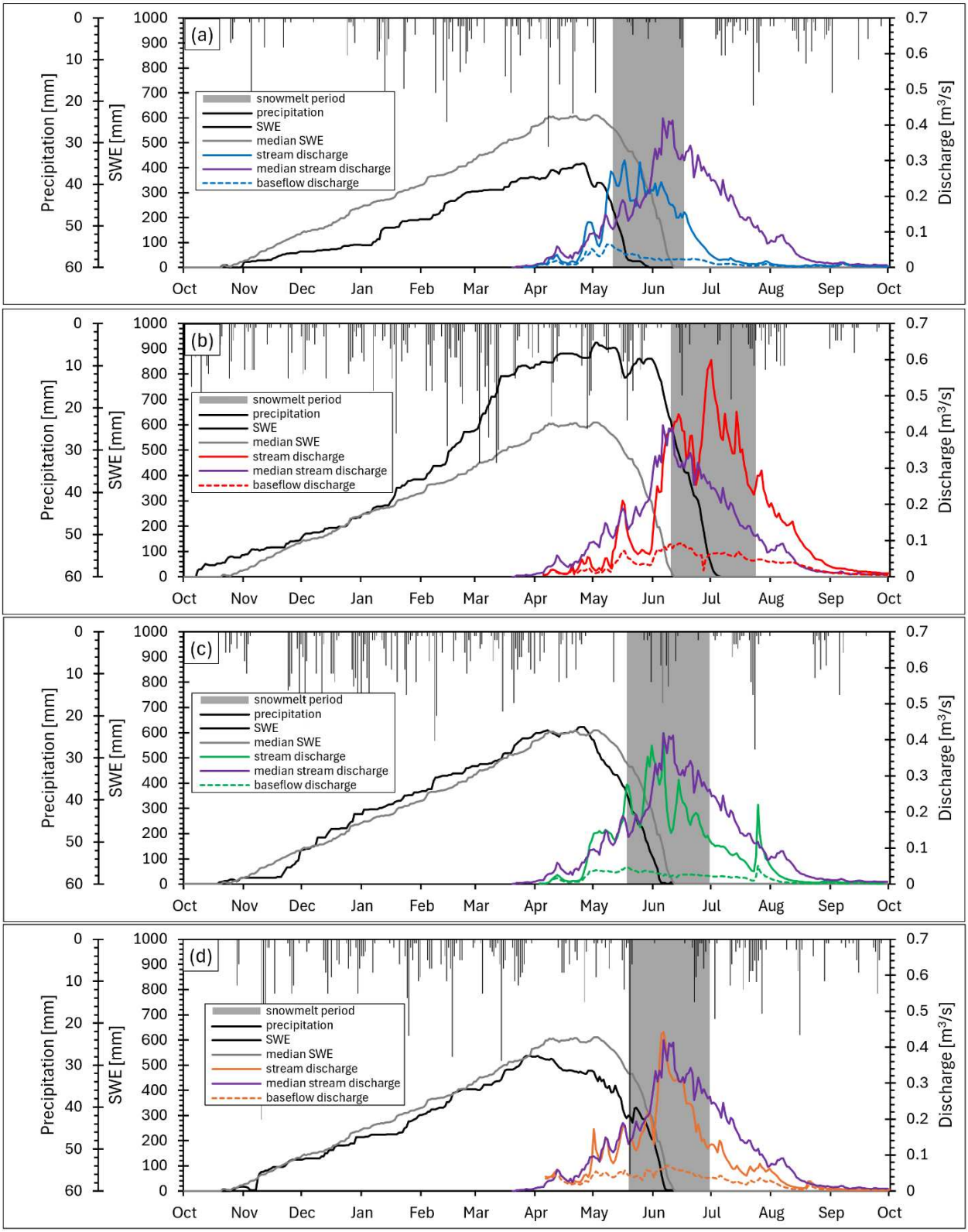
(a)
(b)
(c)
(d)
Precipitation [mm]
SWE [mm]
Discharge [m³/s]
snowmelt period
precipitation
SWE
median SWE
stream discharge
median stream discharge
baseflow discharge
Oct
Nov
Dec
Jan
Feb
Mar
Apr
May
Jun
Jul
Aug
Sep
Oct

Figure 4.1. Daily precipitation (black vertical bars), daily SWE (black line), 40-yr median daily SWE (grey line), daily stream discharge (solid, colored lines), daily baseflow discharge (dashed, colored lines), and 16-yr median daily stream discharge (purple line) for 2018 – 2021 **(a-d)**. Median daily SWE and median daily stream discharge are included to provide context to the annual SWE and discharge curves. The duration of snowmelt (grey window) is approximated using tQ20 to tQ80.

4.5. Cumulative Flow

During the measurement period, mean cumulative discharge was 647 mm and mean cumulative baseflow discharge was 244 mm (Figure 4.2; Table A.3). During the standard period, mean cumulative discharge was 611 mm and mean cumulative baseflow discharge was 215 mm (Table A.3). Most years had some period of time, either before or after the standard period (6 April to 28 September), during which additional flow accumulated. Since the standard period was always shorter than the measurement period, cumulative flow volumes in the standard period were always lower than cumulative flow volumes in the measurement period. Cumulative flow volumes in 2018, 2020, and 2021 were some of the lowest values on record. In terms of cumulative precipitation, these three years were also some of the driest on record (Table 4.1).

The rate of increase in both cumulative stream discharge and baseflow discharge can provide insight into how water moves throughout the SBB. The highest rates of increase (steepest slopes) occurred during snowmelt, while the lowest rates of increase (shallowest slopes) occurred outside of snowmelt, reflecting changes in water inputs throughout the year (Figure 4.2). In the beginning of each year, increases in cumulative discharge were low, but accelerated over time, coinciding with the start of snowmelt. In 2019, cumulative flow volumes began increasing sharply in late May, while cumulative flow volumes in the other three years increased more gently (Figure 4.2). Near the end of snowmelt, the rate of increase in cumulative

flow volumes began to slow in all years, appearing to reach an asymptote (flatter slopes), coinciding with a decrease in water inputs from snowmelt and a change towards low flow conditions. There were also noticeable 'jumps' in cumulative flow volumes, representing large increases in flow over short periods of time. For example, there were large increases in cumulative flow volumes in late July 2019 and late July 2020, corresponding to precipitation events (Figure 4.1a–b and Figure 4.2a–b).

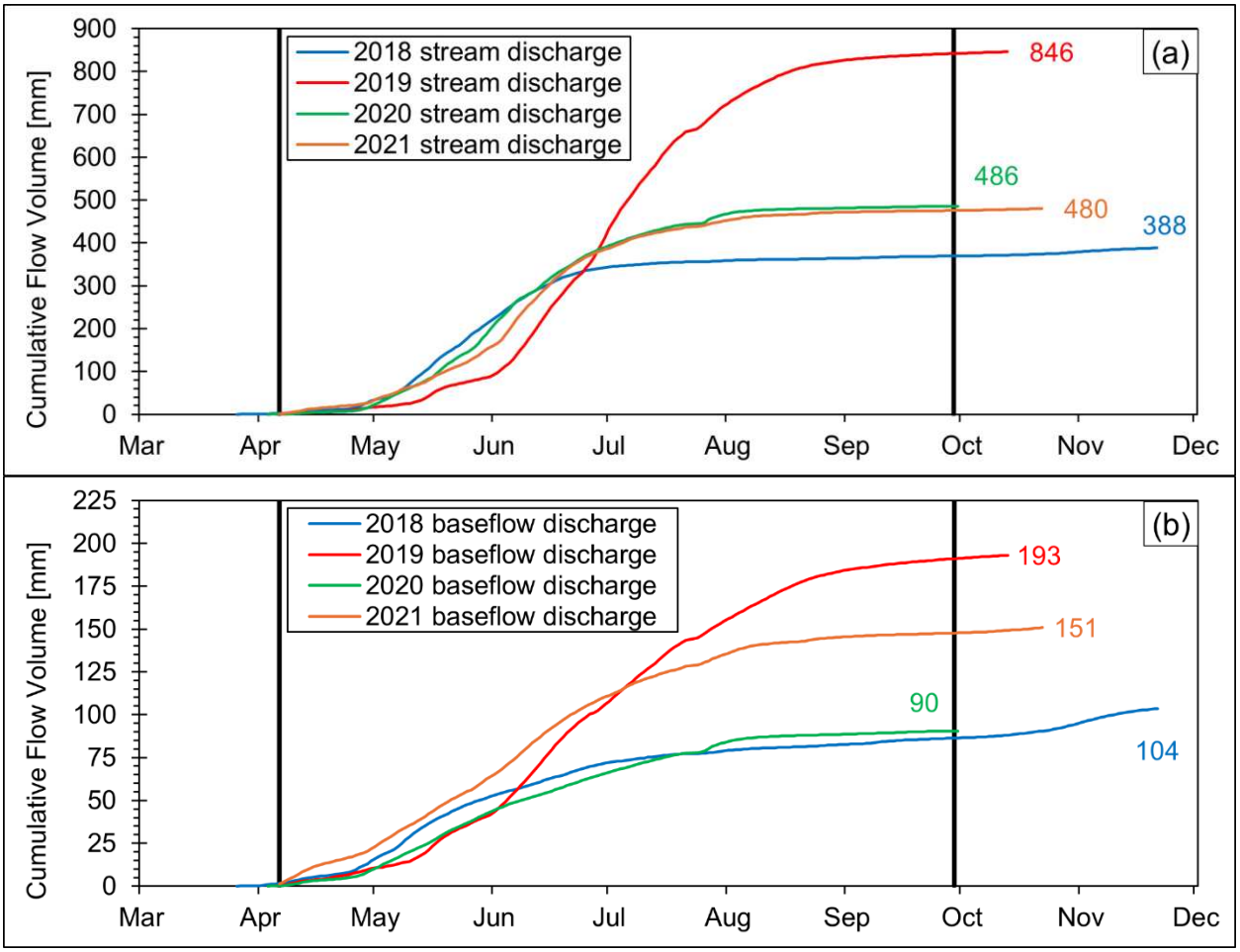

Figure 4.2. Cumulative area-normalized stream discharge **(a)** and baseflow discharge **(b)** as volume of flow (mm) for 2018 – 2021. Vertical black bars denote the start and end dates of the standard period (6 April to 28 September). Numbers at the end of each curve represent the total cumulative flow volumes at the end of each year's measurement period.

4.6. Baseflow Index

In most years, the highest daily BFIs occurred outside of snowmelt (between late March and early April or autumn), while the lowest daily BFIs always occurred on or within a few days of peak stream discharge or during flood peaks (Figure 4.3). Maximum daily BFI values sometimes occurred both before and after snowmelt (Figure A.4). Minimum daily BFIs in each measurement period ranged from 0% (2012) to 28% (2007 and 2016; Table 4.3).

BFI values in the SBB were inversely related to stream discharge (Figure 4.3), a phenomenon that is also seen in other snowmelt-dominated watersheds (Miller et al., 2014; Miller et al., 2020). However, the relationship between stream discharge and BFI is not always perfectly inverse as maximum BFIs did not always occur in both periods before and after snowmelt in each year. After peak flow, BFIs continuously increased, decreasing only temporarily when precipitation events corresponded to increases in stream discharge, resulting in decreased BFI (Figure 4.3). For example, after a cluster of precipitation events in late July 2020, stream discharge and baseflow discharge both rose and fell quickly, yet BFI fell because stream discharge rose higher than baseflow discharge did (Figure 4.3c). The continuously increasing daily BFIs after snowmelt suggest that wetland drainage is driving the high ratio of baseflow discharge in the stream.

Often, BFI did not necessarily reach its highest value during the post-snowmelt low flow period but did so before snowmelt (e.g., 2019 – 2021; Figure 4.3b – d). Daily BFIs at the end of the measurement period were greater than daily BFIs at the start of the measurement period in 9 of 16 years (Table 4.3). While the start day BFI values in the study period were generally high (>70%), end day BFI was only high in 2018 while the end day BFIs in 2019 – 2021 were much lower than average (45 – 63%).

Table 4.3. Summary of daily and long-term BFI characteristics for the period of record. A description of variables is in Table 3.1.

Year	Classif.	Min. Daily BFI (%)	Meas. Period Start BFI (%)	Meas. Period End BFI (%)	Meas. Period BFI (%)	Std. Period BFI (%)	Snowmelt Period BFI (%)	Low Flow Period BFI (%)
2006	Avg	17	79	85	42	38	29	79
2007	Avg	28	79	87	50	47	40	79
2008	Wet	22	72	98	41	33	30	53
2009	Avg	22	90	93	42	41	35	59
2010	Avg	16	65	60	43	42	42	57
2011	Wet	20	96	85	40	39	31	55
2012	Dry	0	77	98	24	21	11	45
2013	Dry	6	71	74	34	30	27	64
2014	Avg	23	84	81	48	45	38	76
2015	Dry	14	79	94	43	40	32	57
2016	Avg	28	80	98	50	48	37	76
2017	Avg	3	83	99	31	29	20	34
2018	Dry	8	74	90	27	23	14	52
2019	Wet	4	99	53	23	23	17	27
2020	Avg	6	87	45	19	19	13	26
2021	Dry	14	100	68	31	31	22	42
Mean:	-	14	82	82	37	34	27	55

Long-term baseflow indices were calculated for the measurement period, standard period, snowmelt period (tQ20 to tQ80), and low flow periods (tQ80 to end of measurement) in each year (Table 4.3). Mean measurement period BFI was 37%, while the mean standard period BFI was 34%. The highest measurement period BFI was 50% (2007 and 2016), while the highest standard period BFI was 48% (2016) and the lowest BFI in the measurement and standard periods was 19% (2020). Measurement period and standard period BFIs between 2018 and 2021 (19 – 31%) were lower than the mean values of 37% and 34%, respectively.

The standard period BFIs were always equal to or smaller than the measurement period BFIs and may suggest that baseflow generation after the end of the standard period (28 September) may be important for streamflow. For example, in 2018, the measurement period BFI was 27% while the standard period BFI was 23%, meaning that about 4% of the cumulative

baseflow occurred outside of the 2018 standard period (in 2018, 52 days of data were recorded after 28 September (Figure 4.3a; Table 4.3 and Table B.2).

Mean snowmelt period BFI was 27% while mean low flow period BFI was 55% (Table 4.3). The highest snowmelt period BFI was 42% (2010), while the highest low flow period BFI was 79% (2006 and 2007). Both snowmelt period and low flow period BFIs in the study period (13 – 22% and 27% – 52%, respectively) were lower than average.

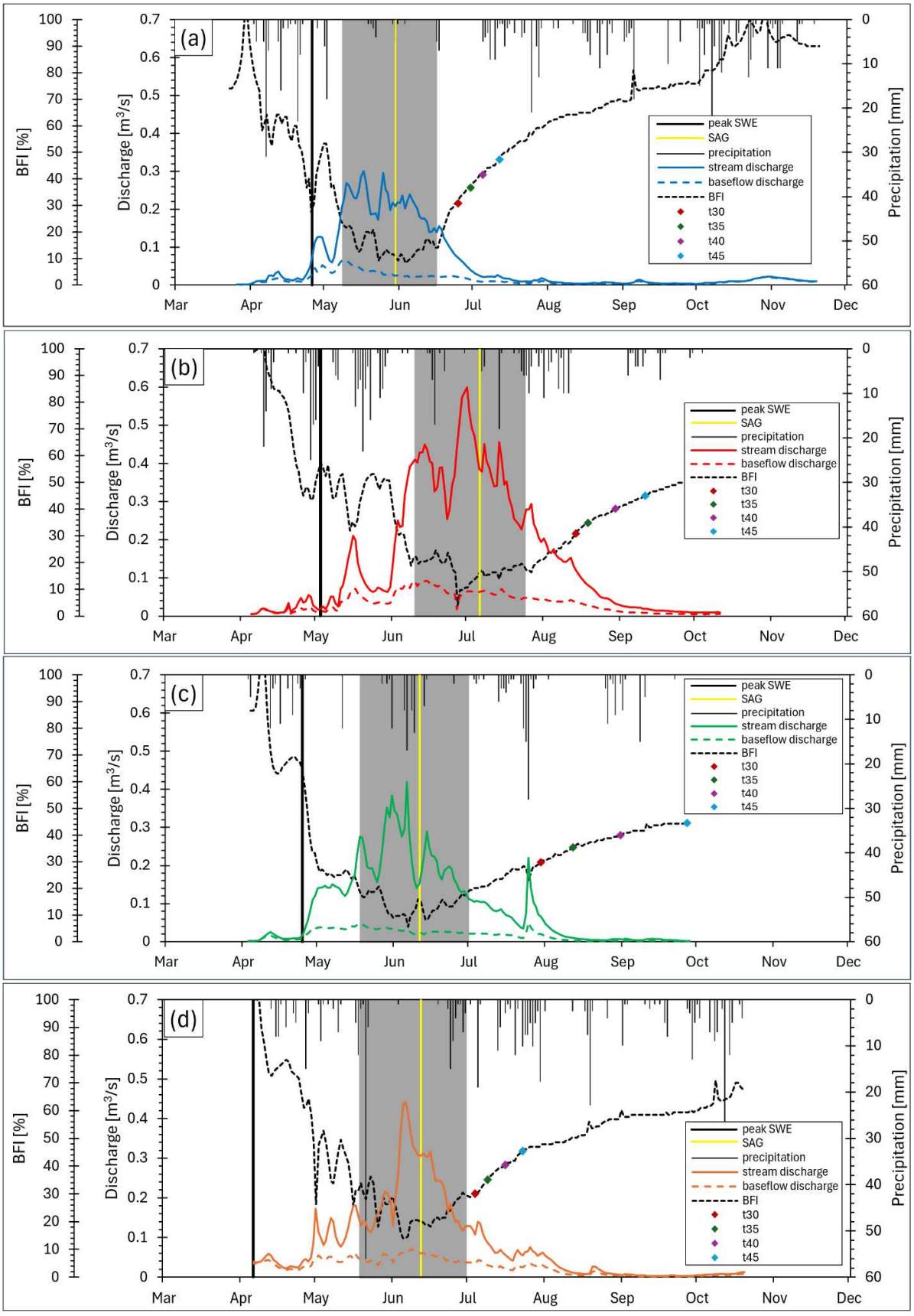
(a)
(b)
(c)
(d)
BFI [%]
Discharge [m³/s]
Precipitation [mm]
Mar
Apr
May
Jun
Jul
Aug
Sep
Oct
Nov
Dec
peak SWE
SAG
precipitation
stream discharge
baseflow discharge
BFI
t30
t35
t40
t45

Figure 4.3. Daily precipitation (black vertical bars), daily stream discharge (solid, colored lines), daily baseflow discharge (dashed, colored lines), daily BFI (dashed, black lines), the timing of peak SWE (black vertical bar), and timing of SAG (yellow vertical bar) for 2018 – 2021 **(a-d)**. t_{sub} variables are represented by diamonds on the BFI curves: t_{30} (red), t_{35} (dark green), t_{40} (magenta), and t_{45} (cerulean). The duration of snowmelt (grey window) is approximated using tQ20 to tQ80. BFI increases as baseflow becomes a greater proportion of total stream discharge within the stream.

4.7. Timing of Substantial Baseflow

The mean dates of the four t_{sub} variables (t_{30}, t_{35}, t_{40}, t_{45}) occurred between late June and late July, with each t_{sub} variable corresponding with later and later dates (the larger the BFI threshold for a given t_{sub} variable, the later that variable occurred) (Figure 4.4 and Table A.4). Mean t_{30} occurred on 29 June, ranging between May and August; mean t_{35} occurred on 12 July, ranging between June and August; mean t_{40} occurred on 18 July, ranging between June and August; and mean t_{45} occurred on 25 July, ranging between July and September.

t_{sub} in 2018 (except for t_{30}) occurred about 2 weeks earlier than average; >1 month later than average for 2019; between about 1 – 2 months later than average in 2020; and nearly average (±5 days) in 2021 (Figure 4.4 and Table A.4). t_{30} in the wet year (2019) occurred 50 days later than t_{30} in the dry year (2018) and 41 days later than t_{30} in dry year (2021); t_{35} in the wet year (2019) occurred 50 days later than t_{35} in the dry year (2018) and 41 days later than t_{35} in another dry year (2021); t_{40} in the wet year (2019) occurred 56 days later than t_{40} in the dry year (2018) and 45 days later than t_{40} in another dry year (2021); t_{45} in the wet year (2019) occurred 61 days later than t_{45} in the dry year (2018) and 50 days later than t_{45} in another dry year (2021).

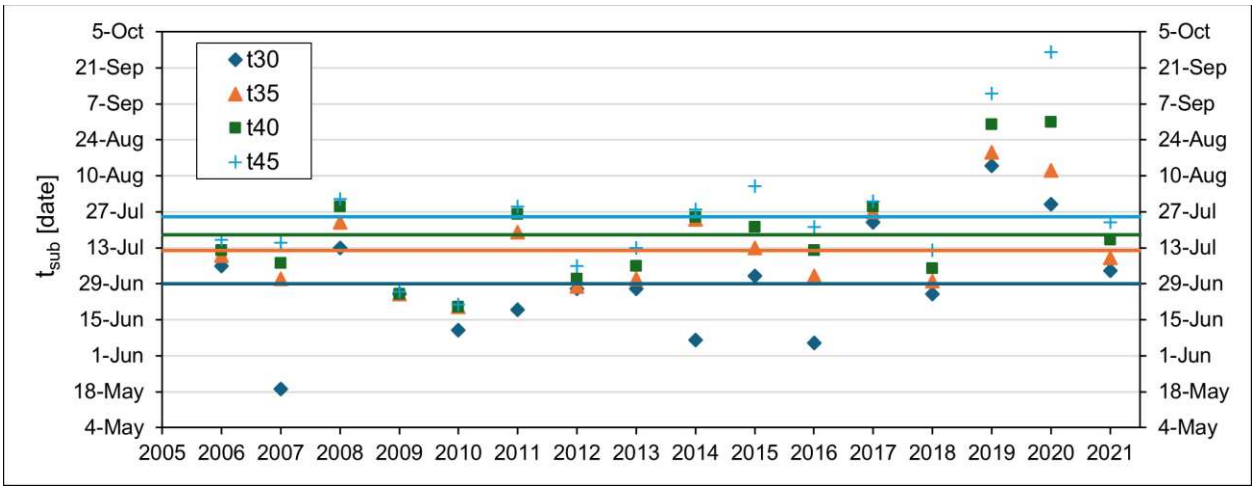

Figure 4.4. Annual dates (points) and mean dates (horizontal lines) for each t_{sub} variable in the period of record: t_{30} (dark blue diamonds); t_{35} (orange triangles); t_{40} (dark green squares); and t_{45} (cerulean plus signs).

Results suggest that t_{sub} occurs earlier in dry years, while t_{sub} occurs later in wet years. t_{sub} in 2019 occurred approximately 50 – 60 days later than t_{sub} in 2018 and approximately 40 – 50 days later than t_{sub} in 2021; regardless of the t_{sub} variable used. Each t_{sub} variable occurs noticeably later in the wet year than in the dry year, highlighting the importance of wetland drainage on streamflow in the post-snowmelt low flow period. Despite being classified as average, all four variables in 2020 occurred later than average and t_{40} and t_{45} occurred the latest on record. Regardless of the t_{sub} variable used, t_{sub} was much later in the wet year (2019) than in the dry years (2018 and 2021) and shows that it doesn't matter what variable is selected when using BFI to determine t_{sub} because the response is identical. However, the t_{sub} variables are based solely on BFI and therefore require scrutiny before conclusive results can be drawn.

4.8. Statistical Analysis

The correlation coefficient and significance levels between t_{sub} variables and hydroclimate variables are displayed in correlation bar plots (Figure 4.5) and a correlation matrix (Figure A.3); both figures display the same data, but correlation bar plots were constructed for better visualization of statistical data from the correlation matrix. For precipitation and snowpack data, cumulative water year precipitation, winter precipitation, residual precipitation, and peak SWE date had no correlation to t_{sub} variables (t_{30}, t_{35}, t_{40}, t_{45}), while cumulative amount of summer precipitation had a negative statistically significant relationship with all t_{sub} variables ($p < 0.05$) and peak SWE magnitude had a positive statistically significant relationship with t_{35} and t_{40} ($p < 0.05$). For snowmelt data, SAG was strongly positively correlated with t_{35}, t_{40}, and t_{45} ($p < 0.01$), snowmelt start (tQ20) and center of volume of snowmelt (tQ50) were moderately positively correlated with t_{35}, t_{40}, and t_{45} ($p < 0.10$), and snowmelt end (tQ80) was not correlated with any t_{sub} variable. For streamflow data, peak stream discharge magnitude was moderately positively correlated with t_{35} and t_{40} ($p < 0.10$), cumulative stream discharge was not correlated with t_{sub}, and peak stream discharge date was strongly positively correlated with t_{35}, t_{40}, and t_{45} ($p < 0.01$) and moderately positively correlated with t_{30} ($p < 0.10$). For baseflow data, mean measurement period SC was strongly negatively correlated with all t_{sub} variables ($p < 0.01$), minimum SC and cumulative baseflow discharge had a negative statistically significant relationship with t_{30} ($p < 0.05$), SC_{BF} (baseflow endmember in CMB model) was not correlated with any t_{sub} variable, while measurement period and low flow period BFIs were moderately negatively correlated with all t_{sub} variables ($p < 0.10$) and snowmelt period BFI was strongly negatively correlated with t_{30} ($p < 0.01$) and moderately negatively correlated with t_{40} and t_{45} ($p < 0.10$).

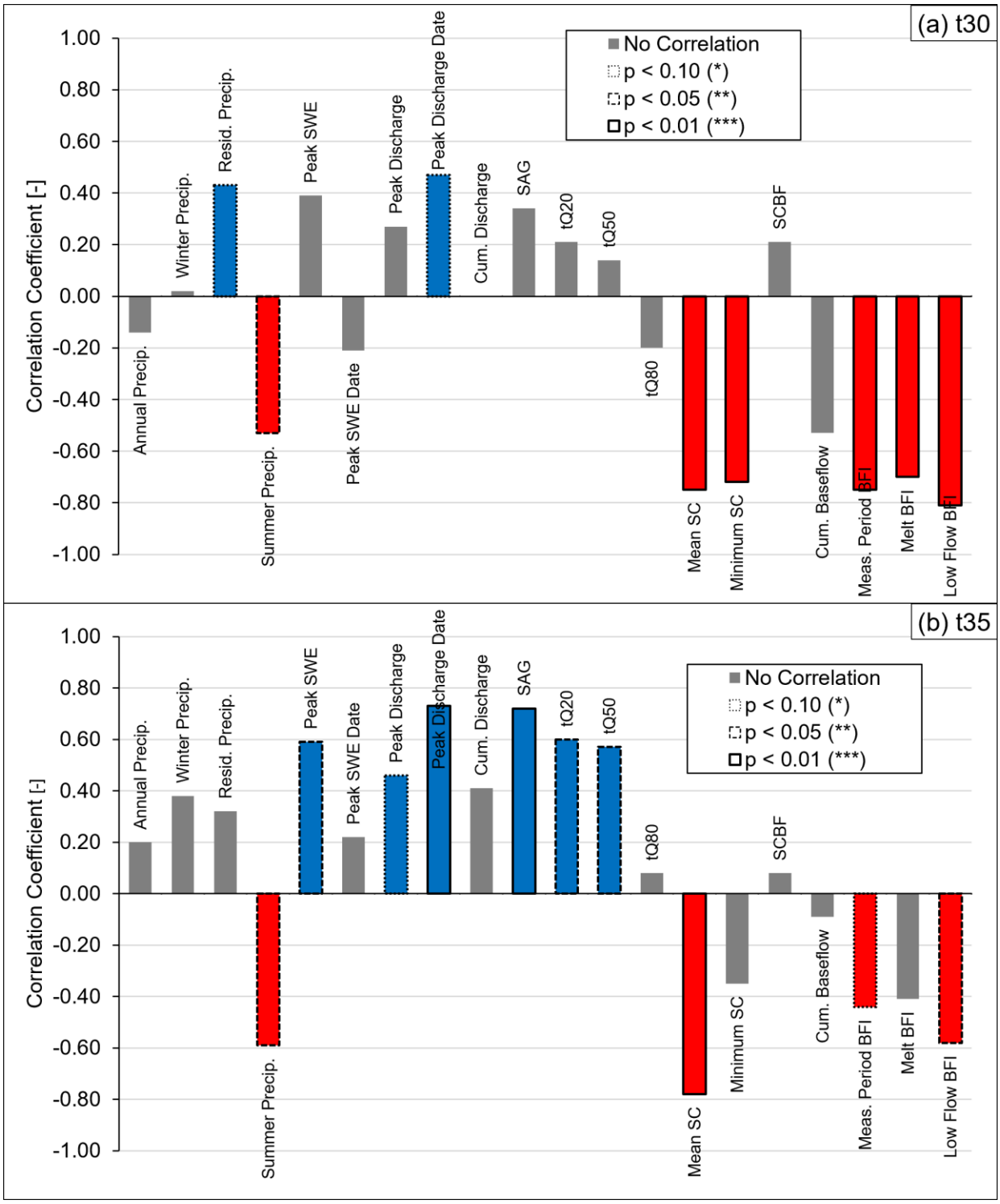
(a) t30
Correlation Coefficient [-]
1.00
0.80
0.60
0.40
0.20
0.00
-0.20
-0.40
-0.60
-0.80
-1.00
No Correlation
p < 0.10 (*)
p < 0.05 (**)
p < 0.01 (***)
Annual Precip.
Winter Precip.
Resid. Precip.
Summer Precip.
Peak SWE
Peak SWE Date
Peak Discharge
Peak Discharge Date
Cum. Discharge
SAG
tQ20
tQ50
tQ80
Mean SC
Minimum SC
SCBF
Cum. Baseflow
Meas. Period BFI
Melt BFI
Low Flow BFI
(b) t35
Correlation Coefficient [-]
1.00
0.80
0.60
0.40
0.20
0.00
-0.20
-0.40
-0.60
-0.80
-1.00
No Correlation
p < 0.10 (*)
p < 0.05 (**)
p < 0.01 (***)
Annual Precip.
Winter Precip.
Resid. Precip.
Summer Precip.
Peak SWE
Peak SWE Date
Peak Discharge
Peak Discharge Date
Cum. Discharge
SAG
tQ20
tQ50
tQ80
Mean SC
Minimum SC
SCBF
Cum. Baseflow
Meas. Period BFI
Melt BFI
Low Flow BFI

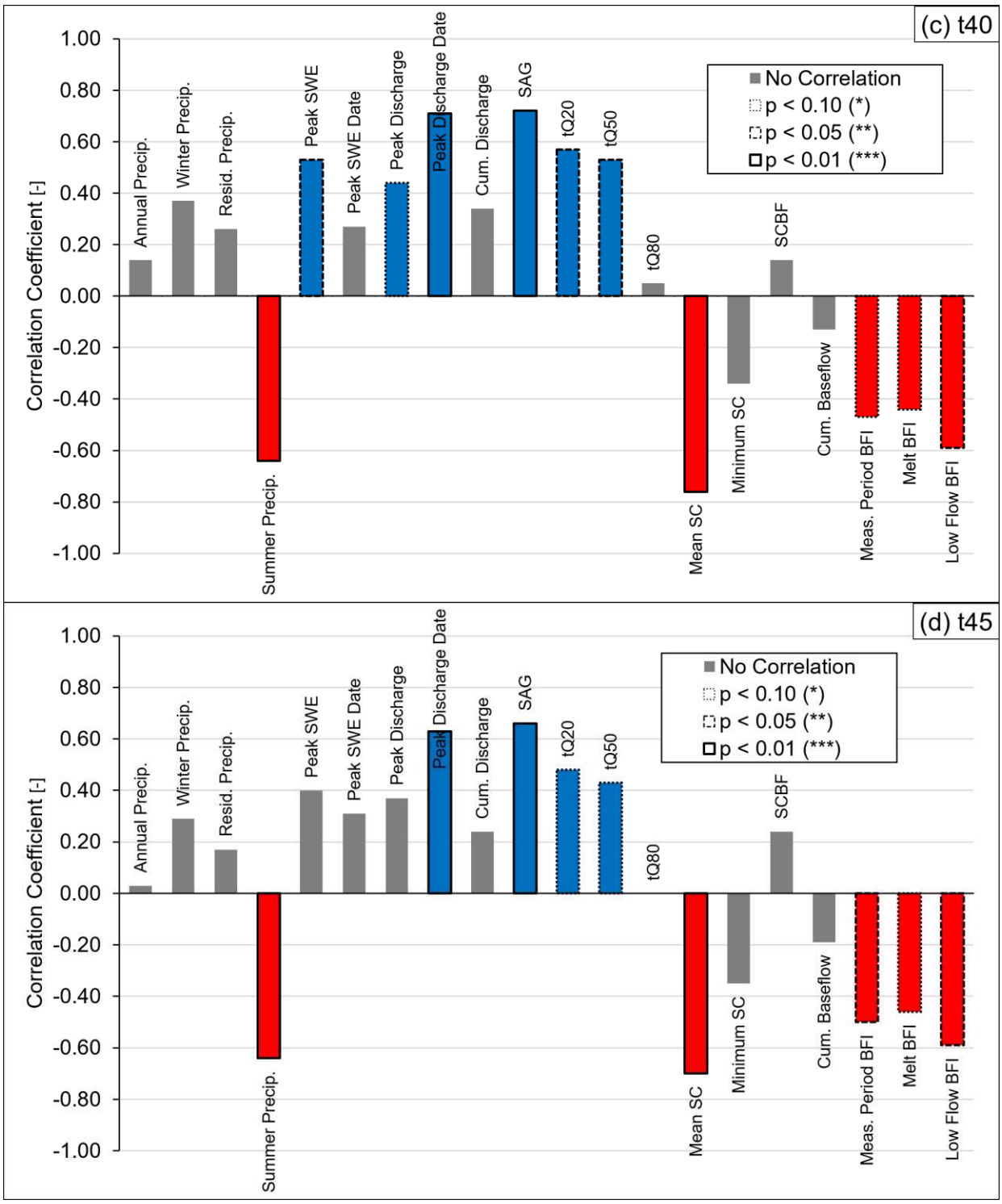

Figure 4.5. Correlation bar plots displaying the correlation coefficients between hydroclimate variables and t_{sub} variables: **(a)** t_{30}; **(b)** t_{35}; **(c)** t_{40}; **(d)** t_{45}. A description of variables is in Table 3.1. Variables in grey have no correlation to t_{sub}, while variables in blue (positive) or red (negative) were correlated with t_{sub} at three levels of confidence: dotted borders represent variables correlated at p-values < 0.10; dashed borders represent variables correlated at p-values < 0.05; and solid borders represent variables correlated at p-values < 0.01.

CHAPTER 5 – DISCUSSION

This study investigated the influence of wetland drainage on streamflow in the Senator Beck Basin (SBB), a high-elevation, headwater watershed in the San Juan Mountains in southwestern Colorado. It was hypothesized that wetland drainage plays a relatively larger role in maintaining baseflow in dry years than in wet years. Results from the study period show that t_{sub} is later in wet years than in dry years, suggesting that wetland drainage plays a relatively smaller role in maintaining streamflow in wet years than in dry years. However, because the SAW contributes to streamflow year-round, wetland drainage is still important in wet years. Wetland drainage may play a relatively larger role in wet years than in dry years, but the role of wetland drainage in a given year is highly dependent upon the timing and magnitude of different hydrologic processes. Results and insights discovered here may be used to better understand wetland drainage processes in other high-elevation, snowmelt-dominated, headwater watersheds and how those processes may be affected by changes to hydrology and climate.

In the study period, 2018 was a dry year with low cumulative precipitation, below average winter precipitation, yet above average summer precipitation, a small and early maximum snowpack accumulation, early and short snowmelt, low cumulative flow volumes, and low measurement period BFI, with wetland drainage playing a relatively large role in streamflow maintenance; 2019 was a wet year with high cumulative precipitation, above average winter precipitation, yet below average summer precipitation, a large and late maximum snowpack accumulation, late and long snowmelt, high cumulative flow volumes, with wetland drainage playing a relatively small role in streamflow maintenance; 2020 was an average year with low cumulative precipitation, average winter precipitation, yet below average summer precipitation, a

maximum snowpack accumulation, snowmelt, and cumulative flow volumes similar in timing and amount to their respective mean values, with wetland drainage playing a relatively small role in streamflow maintenance; and 2021 was a dry year with low cumulative precipitation, below average winter precipitation, yet above average summer precipitation, a small and early maximum snowpack accumulation, early and long snowmelt, and low cumulative flow volumes, with wetland drainage playing a relatively moderate role in streamflow maintenance (Figure 3.1 and Figure 4.1; Table 4.1, Table 4.2, and Table 4.3). Despite 2018 and 2021 both being classified as dry, wetland drainage played a larger role in maintaining streamflow in 2018 because t_{sub} occurred earlier than in 2021. Similarly, wetland drainage played a relatively small role in both 2019 and 2020, despite each year having considerably different hydroclimatic characteristics.

5.1. Hydrological Processes Governing Wetland Drainage

Relationships between hydroclimate variables and t_{sub} variables (t_{30}, t_{35}, t_{40}, t_{45}) were mixed (Figure 4.5). t_{sub} was best correlated (positively) with peak stream discharge date and SAG, and (negatively) with amount of summer precipitation and mean measurement period SC, suggesting that study years with later snowmelt timings (later SAG and peak stream discharge), lower mean measurement period SC values, and lower amounts of summer precipitation are associated with later occurrences of t_{sub}, and thus a decreased role of wetland drainage (Figure 4.5; Table A.3).

Not every t_{sub} variable was correlated to the same hydroclimate variable (nor at the same significance level) and shows that the processes governing t_{sub} in the SBB are highly spatiotemporally variable. Even though baseflow was always an ever-increasing proportion of streamflow during the low flow period and t_{sub} variables occurred in succession, they did not

always occur in a linear fashion indicating that the processes that govern t_{sub} are non-linear. Only cumulative amount of summer precipitation, peak stream discharge date, mean measurement period SC, and measurement period and low flow period BFIs were significantly correlated to all four t_{sub} variables (Figure 4.5). t_{30} is a more sensitive measure of the t_{sub} than the other three t_{sub} variables because of the generally lower correlation coefficient values and lack of significant correlations between t_{30} and variables that were correlated to t_{35}, t_{40}, or t_{45} (Table A.3).

5.1.1. Snowpack

t_{sub} had a positive statistically significant relationship with peak SWE magnitude (t_{35} and t_{40}: Pearson's $r = 0.53$ to 0.59, $p < 0.05$) and was strongly positively correlated with SAG (t_{35}, t_{40}, and t_{45}: Pearson's $r = 0.66$ to 0.72, $p < 0.01$), suggesting that study years with higher peak SWE and later dates of SAG were associated with later occurrences of t_{sub}, regardless of when peak SWE occurs (Figure 4.5b–d). Peak SWE is not a perfect measure of snow accumulation because it is a point measurement and because SWE can vary significantly in space and time (Fassnacht et al., 2020). SAG represents the end of snow in the SBB, but it does not imply the end of snowmelt contributions to streamflow (tQ80) as snowmelt infiltrates and recharges groundwater and discharges as baseflow during the low flow period (Winograd et al., 1998; Li et al., 2017; Miller et al., 2020). The lack of correlation between peak SWE date and t_{sub} compared to the strong correlation between t_{sub} and SAG implies that the timing of snowmelt is more important for determining t_{sub} than the timing of the snowpack peak. In 2021, peak SWE occurred about 1 month earlier than average while peak stream discharge, snowmelt (tQ20 to tQ80), and t_{sub} still occurred near their mean dates (Figure 4.3d and Figure 4.4), providing some evidence that peak SWE date has minimal influence over t_{sub} in the SBB.

5.1.2. Precipitation

Cumulative water year precipitation, winter precipitation, and residual precipitation were not correlated with t_{sub} (except between t_{30} and residual precipitation; Pearson's $r = 0.43$, $p < 0.10$) and appear to have no bearing on wetland drainage in the SBB, suggesting that the effect of precipitation on wetland drainage may be more nuanced than the total amount of precipitation received in a given period (Figure 4.5). The response of streamflow to precipitation events appears to be greater during the low flow period than during snowmelt (Figure 4.1). Summer precipitation had a negative statistically significant relationship with all four t_{sub} variables (Figure 4.5; Pearson's $r = -0.53$ to -0.64, $p < 0.05$), highlighting that study years with higher summer precipitation amounts were associated with earlier occurrences of t_{sub}. In the study period, summer precipitation was relatively larger and t_{sub} occurred relatively earlier in 2018 and 2021 than in 2019 and 2020 (Table 4.1). The weak relationships between t_{sub} and precipitation variables suggests that wetland drainage is not influenced by how much water enters the watershed in a given period, but perhaps more by the timing of input, how the water travels through the watershed (either surface or subsurface), and how long it takes to reach the stream. The influence of summer precipitation on baseflow discharge is also difficult to discern because the proportion of precipitation that is transformed into streamflow varies based on the amount of precipitation received, rainfall intensity, and antecedent conditions (Sklash and Farvolden, 1979; Matsubayashi et al., 1993; Branfireun and Roulet, 1998).

An example of the influence of summer precipitation on t_{sub} was a cluster of events in late July 2020, where 57 mm of rain precipitation fell between 22 and 25 July, culminating in a 28 mm event which corresponded to a large flood peak on 25 July (peak discharge: 0.22 m^3/s; Figure 4.3c). The 2020 hydrograph shows that discharge was receding before late July, and it

appears that the large quantity of precipitation received delayed t_{sub} by about 1 – 2 months (Figure 4.3c; Table A.4). t_{sub} in 2020 may have occurred earlier had the flood event not occurred. It seems that t_{sub} was unaffected by the below average peak SWE and cumulative precipitation and more influenced by the late July flood peak as the t_{sub} dates were some of the latest on record (Figure 4.1c; Table A.4). This suggests that t_{sub} and BFI can be sensitive to precipitation during the low flow period. Precipitation events during the winter or residual periods (peak SWE date to SAG) may also delay t_{sub}, but the impact of these events on baseflow response are difficult to disentangle from the effects of snowmelt.

5.1.3. Discharge

Despite only a moderately significant positive correlation between peak stream discharge magnitude and t_{35} and t_{40} (Figure 4.5b–c; Pearson's $r = 0.44$ to 0.46, $p < 0.10$), there was a highly significant positive correlation detected between t_{35}, t_{40}, and t_{45} and peak stream discharge date (Pearson's $r = 0.63$ to 0.73, $p < 0.01$) and a moderately significant positive correlation between t_{35} and peak stream discharge date (Pearson's $r = 0.47$, $p < 0.10$), suggesting that study years with later peak stream discharge dates tended to have later occurrences of t_{sub}. The strong positive correlation between t_{sub} and peak stream discharge date was expected as study years with later peak stream discharge dates have shorter low flow periods and therefore do not rely on wetland drainage as early in the year. This relationship was observed in the study period where peak stream discharge occurred earlier than average in 2018 and later than average in 2019 (Figure 4.1a–b). In 2019, the late occurrences of t_{sub} (38 – 48 days later than average) were at least partially due to higher water inputs from a larger snowpack, which prolonged snowmelt and kept stream discharge relatively high well into September (Figure 4.1b).

Cumulative streamflow or baseflow were not correlated with t_{sub} (except for a statistically significant relationship between cumulative baseflow and t_{30}; Figure 4.5a; Pearson's = -0.53, $p < 0.05$), suggesting that cumulative flow volumes have no association with t_{sub}. This appears to be similar to the relationship between precipitation and t_{sub}, where total precipitation has little effect on t_{sub}, suggesting that the timing of water inputs exerts a greater influence on t_{sub}.

5.1.4. Snowmelt Timing

The start (tQ20) and center of volume of snowmelt (tQ50) had a positive moderately significant correlation with t_{35}, t_{40}, and t_{45} (Figure 4.5b–d; Pearson's r = 0.43 to 0.60, $p < 0.10$), providing more evidence of a positive association between the timing of the annual snowmelt pulse and t_{sub}. Later snowmelt results in a shorter low flow period and a shorter period of time during which wetland drainage plays an important role in maintaining streamflow. t_{sub} was not correlated to the end of snowmelt (tQ80) and suggests that the conclusion of snowmelt effects on streamflow is not an important control on t_{sub}.

Measurement period length affects the timing of the passage of certain percentages of cumulative discharge (tQ20, tQ50, and tQ80) as shorter measurement periods could cause tQ20, tQ50, and tQ80 variables to occur earlier than if the dataset length was longer, thus affecting snowmelt contributions to streamflow and estimates of the snowmelt period length. Despite being widely used in snowmelt-dominated watersheds, tQ20, tQ50, and tQ80 are imperfect metrics for determining the timing of snowmelt contributions to streamflow as they are fixed values and do not account for variability in the timing and amount of inputs to streamflow (Fassnacht, 2006; Whitfield, 2013; Pfohl and Fassnacht, 2023). Instead of using fixed values, the timing of snowmelt contributions to streamflow could be estimated by manually extracting the

start and end dates of snowmelt contributions (Pfohl and Fassnacht, 2023) or by using the "melt year" (Flynn et al., 2021; Flynn et al., 2024), which defines a hydrological year that begins with the first deviation from low flow conditions (snowmelt onset) and concludes the day before snowmelt onset of the following year. Using a melt year is advantageous over using the water year because it contains a single snowmelt and baseflow period and only focuses on water inputs from that year (Flynn et al., 2021).

5.1.5. Snowmelt Rate

Snowmelt rate controls the relative partitioning of snowmelt water between recharge, evapotranspiration, and streamflow and lower snowmelt rates have been linked to lower streamflow volumes (Barnhart et al., 2016). In 2021, despite peak SWE occurring about 1 month earlier than average, the timing of SAG, timing and magnitude of peak stream discharge, and t_{sub} were similar to their respective mean values (Figure 4.3d and Figure 4.4). It appears that there were two distinct phases of snowmelt in 2021 that can be observed from daily SWE data: (1) a period of relatively low snowmelt (primarily in April), and (2) a subsequent period of relatively high snowmelt (primarily in May; Figure 4.1d). During the first phase (April), the shallow slope in the daily SWE curve suggests that the rate of snowmelt was relatively low (Figure 4.1d). During this time, the meteorological and snowpack energy conditions were probably not conducive to high rates of snowmelt; namely, the snowpack was probably not fully ripened (Colbeck, 1976). During the second phase (May), the steeper slope in the daily SWE curve suggests that the rate of snowmelt was relatively higher (Figure 4.1d), likely spurred by meteorological conditions that were more conducive for snowmelt; namely, higher air temperature and higher shortwave radiation (Bales et al., 2006).

It is hypothesized that the relatively early and apparently low rate of snowmelt observed in April 2021 lead to saturation and recharge of the subsurface and the apparently high rate of snowmelt observed in May 2021 lead to more runoff, producing a stream discharge peak that was similar in shape and size to the 2020 and median hydrographs (Figure 4.1c–d). The relatively lower rate of snowmelt in April 2021 likely allowed for more water to be partitioned to recharge, leading to concentrated infiltration occurring at a time when potential evapotranspiration was relatively low and soil storage capacity was easily overwhelmed (Flint et al., 2004; Barnhart et al., 2016; Miller et al., 2020; Somers and McKenzie, 2020). The steep rate of increase in cumulative baseflow discharge in April 2021 indicates that cumulative baseflow discharge was the highest of the four study years until early July and provides some support for slower snowmelt and increased recharge in April 2021 (Figure 4.2b).

Previous investigators have found that larger snowpacks and higher rates of snowmelt drive greater percolation and recharge, which lead to higher streamflow and baseflow (Barnhart et al., 2016; Miller et al., 2020). Higher snowmelt rates, which often coincide with later snowmelt onset, increase subsurface flow by bringing soils above their field capacity, inducing percolation and driving shallow subsurface flow and drainage (Trujillo and Molotch, 2014; Barnhart et al., 2016; Miller et al., 2020). This interpretation is consistent with the results from Miller et al., (2020) who found that watersheds with lower snowmelt rates and earlier snowmelt onsets (those with higher proportions of south-facing areas and shorter snow cover durations) had greater proportions of baseflow than watersheds with later snowmelt onsets (those with higher proportions of north-facing areas and longer snow cover durations). It appears that t_{sub} was unaffected by the variable rates in snowmelt because even though peak SWE and snowmelt

onset occurred earlier than average, t_{sub} did not; suggesting that t_{sub} may be insensitive to variable snowmelt rates or earlier snowmelt timings because groundwater can buffer streamflow.

5.2. Conductivity Mass Balance Model

Estimations of t_{sub} rely heavily on the way baseflow discharge and BFI were computed with the CMB model, meaning that the accuracy of SC data used is crucial for determining t_{sub} and the influence of wetland drainage. Factors such as snowmelt rates and precipitation inputs influence the proportion of baseflow in the stream, but CMB endmember values play a very important role in determining baseflow discharge and BFI. Though the determination of endmember values is somewhat arbitrary and adds some amount of uncertainty to the baseflow discharge and BFI datasets, it likely does not affect the main conclusions of t_{sub} nor long-term (measurement period, standard period, snowmelt period, or low flow period) BFIs.

Mean measurement period SC was strongly significantly negatively correlated with t_{sub} (Figure 4.5; Pearson's r = -0.70 to -0.78, $p < 0.01$), suggesting that study years with higher mean measurement period SC values tended to have earlier occurrences of t_{sub}. This was expected because of the naturally inverse relationship between SC and stream discharge (Figure A.2), where higher SC is associated with lower stream discharge and probably higher BFI, and thus an earlier t_{sub}. t_{sub} was not correlated to SC_{BF} nor minimum SC (except between t_{30} and minimum SC; Figure 4.5a; Pearson's r = -0.72, $p < 0.01$), suggesting that the endmember values do not have any association with t_{sub}. However, endmember values must exert some influence on t_{sub} because they are used in the CMB model (Eqn. 2.3) to estimate baseflow discharge and BFI.

5.2.1. Endmember Sensitivity Analysis

A sensitivity analysis was conducted modeling scenarios using different endmember values in the CMB model to determine the influence of changing SC endmembers on BFI and t_{sub}. The smallest differences in BFI occurred when SC_{BF} was held constant, even if SC_{RO} was increased. The largest differences in BFI occurred when both SC_{RO} and SC_{BF} were increased. Analysis shows that endmembers are inversely related to BFI but changing SC_{BF} results in larger differences in BFI than changing SC_{RO} does; suggesting that adjusting SC_{RO} has a limited impact on BFI, a phenomenon also found by Miller et al., (2014). This may suggest that the endmember methodology followed in this study (annually constant SC_{RO} and annually variable SC_{BF}) was appropriate. Lastly, differences in modeled BFIs were greater during snowmelt than during low flow, further limiting the impact of adjusting SC endmembers on t_{sub}, since wetland drainage only becomes substantial after snowmelt.

In the last three years of the study period (2019 – 2021), cumulative baseflow and long-term BFIs were lower than average (Figure 4.2; Table 4.3), likely due to the way in which baseflow discharge was estimated. In these three years, daily BFI never exceeded 75% (Figure 4.3b–c) and daily BFI values after snowmelt in 2019 and 2020 were the two lowest on record (Figure A.4). One possible reason for low BFI values was because the SC_{BF} endmembers were higher than average (Table A.2), resulting in lower estimations of baseflow discharge and later occurrences of t_{sub}. While both SC_{RO} and SC_{BF} have an inverse relationship with BFI, changing SC_{BF} has a much stronger effect on BFI than changing SC_{RO} does, meaning that study years with higher SC_{BF} values will likely have lower BFIs and later occurrences of t_{sub}.

It is possible that BFI increased after the measurement periods in 2019 – 2021, but these changes were not recorded. The temporal ranges of the datasets used in this study are important

for interannual comparisons and for calculating the CMB. While using the water year is important for comparing precipitation and snowpack data, for best estimation of baseflow discharge using the CMB, consistency in date ranges is important when selecting SC endmembers, as it allows the full range of SC values and baseflow conditions to be observed (Caissie et al., 1996; Stewart et al., 2007; Miller et al., 2014). Despite the importance of having consistent date ranges, the general t_{sub} results from this study are not expected to be affected.

5.2.2. Reliability of Model Assumptions

The assumptions used when applying the CMB model must be verified because chemical mass balance methods may overestimate baseflow discharge if the assumptions used are violated (Pilgrim et al., 1979). There were four assumptions that were made when employing the CMB model to estimate baseflow discharge: (1) there is a natural inverse relationship between SC and stream discharge, where SC decreases as discharge increases (Pinder and Jones, 1969, Pilgrim et al., 1979, Stewart et al., 2007, Miller et al., 2014; Rumsey et al., 2015); (2) contributions from other components are negligible (Sklash and Farvolden, 1979; Wels et al., 1991; Miller et al., 2014; Miller et al., 2015; Rumsey et al., 2015); (3) endmembers are significantly different from each other (Uhlenbrook, 2012, Miller et al., 2014, Miller et al., 2015, Rumsey et al., 2015); and (4) endmembers remain constant in time (Pinder and Jones, 1969; Stewart et al., 2007; Miller et al., 2014; Miller et al., 2015; Rumsey et al., 2015).

The first assumption was met as a naturally inverse relationship between SC and stream discharge was observed in all years on record, indicating that the CMB method was an appropriate method to use to estimate baseflow discharge in the SBB (Miller et al., 2014). An example of the inverse relationship between SC and stream discharge in 2020 is shown in Figure

A.2, displaying the relationship in both the snowmelt and low flow periods. The naturally inverse relationship between SC and stream discharge displayed in all years shows one that does not appear to be affected by external (anthropogenic) forces (Miller et al., 2014). The effect of anthropogenic forces on baseflow in the SBB are expected to be small because of the SBB's elevation, distance from urban areas, and because anthropogenic effects are more pronounced in larger watersheds (Uhlenbrook et al., 2002; Landry et al., 2014; Miller et al., 2014).

For the purposes of this study, the second assumption was met as only two components were used in the CMB model and all other potential components of streamflow were lumped into either surface water runoff or baseflow discharge. It is possible that there are more than two components of streamflow in the SBB, where additional components would likely follow additional subsurface pathways (e.g., intermediate subsurface component; Miller et al., 2020), but they could not be differentiated for this study. For example, overland flow and shallow subsurface flow waters may have similar conductivities (Figure 2.3), but it would be too difficult to distinguish additional components from the SC record without additional measurements.

The third assumption that the endmembers in the model are significantly different from each other was met because surface water runoff and baseflow endmember values were selected at different points on the hydrograph. SC_{RO} was selected during high flow when SC was low and SC_{BF} was selected during low flow when SC was high (Figure 2.3), ensuring that endmember values would be significantly different. Each year, the value of SC_{BF} was at least four times as great as the value of SC_{RO} (Table A.2).

For the purposes of this study, the fourth assumption was met because once endmembers were selected, they were held constant for every year. However, this assumption may be invalid because endmember values may shift across the year, reflecting changes in flow paths (e.g.,

snowmelt to wetland drainage) and because of the potential mixing of components in the stream. The mixing of stream components affects the chemical signature measured at the gauge if the tracer being used to estimate stream components is non-conservative (i.e., the tracer reacts with other materials) (Hooper and Shoemaker, 1986; Caine, 1989; Wels et al., 1991). If the tracer is non-conservative, then the SC of stream components may mix or react, leading to dilution, and to a potential overestimation of the proportion of baseflow in the stream (Pilgrim et al., 1979; Hooper and Shoemaker, 1986). It is unknown if SC is a conservative tracer. Future hydrograph separations using SBB data should use known conservative tracers to avoid inaccuracies in estimation of the proportions of stream water components.

5.2.3. Temporal Variability in Endmembers

The concentrations of solutes dissolved within stream water components may also vary due to the length of contact time with subsurface materials, chemistry of subsurface material, rate of flow, and storm intensity; and this should be accounted for when using the CMB model (Pilgrim et al., 1979; Hooper and Shoemaker, 1986; Wels et al., 1991; Bishop et al., 2004; Stewart et al., 2007). In the early phases of storm events, increases in concentration are greatest but slow over time as concentrations approach equilibrium; after which further contact results in no change in concentration (Pilgrim et al., 1979; Wels et al., 1991; Matsubayashi et al., 1993). Longer contact times between stream components and subsurface materials provide a longer period of time for chemical reactions to occur, potentially increasing solute concentrations and SC (Wels et al., 1991; Matsubayashi et al., 1993; Laudon and Slaymaker, 1997).

Provided that solutes have had enough time to accumulate, new inputs of water (e.g., snowmelt) can flush large amounts of solutes out of the shallow subsurface in the early phases of

storms, raising the water table and mobilizing pre-event water stored in the unsaturated zone (Pilgrim et al., 1979; Laudon and Slaymaker, 1997). As the water table rises, it encounters near-surface soil layers with higher hydraulic conductivities, contributing large amounts of water and solutes to runoff (Sklash and Farvolden, 1979; Kirchner, 2003; Bishop et al., 2004). The higher concentrations of solutes in the beginning of snowmelt may be due to piston flow replacing water in soil with new waters, resulting in some waters discharging with higher concentrations of solutes, followed by waters discharging with lower concentrations of solutes (Pilgrim et al., 1979; Caine, 1989; Sueker et al., 2000; Miller et al., 2020).

This phenomenon has been observed in snowmelt-dominated watersheds where delayed subsurface flow reaches the stream on the rising limb of the daily hydrograph while daily snowmelt reaches the stream on the falling limb of the daily hydrograph (Miller et al., 2020). During snowmelt, there are more flow paths on the rising limb of the annual hydrograph, due to higher connectivity between the snowpack and the stream (Miller et al., 2020); probably explaining the high proportions of baseflow on the rising limbs of the snowmelt hydrograph observed in this study (Figure 4.1) and others (Sklash and Farvolden, 1979).

While the results from previous researchers suggest that endmember concentrations are time-dependent and that the SC values recorded in the early phases of storms or annual snowmelt may not be representative of the true surface water runoff endmember, caution must be used when considering these results as they were derived experimentally and may not be easily extrapolated to other sites due to differences in watershed and storm characteristics (Pilgrim et al., 1979; Wels et al., 1991; Matsubayashi et al., 1993). Temporally variable endmembers were likely not an issue in this study because SC_{RO} was selected during peak flow, not the early phases of snowmelt, which may have allowed the SC_{RO} endmember to reach its 'true' value (i.e., reach

an equilibrium value). However, additional measurement would be required to verify the true value of SC_{RO}. Direct measurement of the SC of stream components in the field (measuring SC_{RO} during peak flow and measuring SC_{BF} during low flow or from shallow wells) would alleviate this issue and provide better estimates of endmember values for the CMB model (Caine, 1989; Covino and McGlynn, 2007; Stewart et al., 2007).

5.2.4. Baseflow Index

Regardless of endmember values, daily SC also influences BFI and t_{sub} as it is reflective of stream conditions at the time. SC and BFI have a direct relationship with each other, and both have an inverse relationship with stream discharge. The highest daily BFIs often occur after the monsoon season ends in September when streamflow, precipitation, and evapotranspiration are at seasonal lows (Figure A.4; Wigley and Jones, 1985; Carrara et al., 2011; Miller et al., 2014). It is during this time that the stream is most dependent upon groundwater to maintain streamflow.

Measurement period BFI was highly significantly negatively correlated with all t_{sub} variables (Figure 4.5; Pearson's $r = -0.44$ to -0.75, $p < 0.10$), highlighting that study years with higher measurement period BFIs were associated with earlier t_{sub}. This was expected because higher measurement period BFIs represent an overall greater presence of groundwater in streamflow and coincide with higher daily BFIs and earlier t_{sub}. The high measurement period BFIs observed in this study (19 – 50%) are consistent with findings from other studies of baseflow elsewhere in the southern Rocky Mountains, which estimate long-term BFI values between 18 – 89% (Table 5.1). Some estimates of the groundwater proportion in Table 5.1 were from watersheds that exist at different elevations and are different sizes than the SBB or may have been estimated with different hydrograph separation methods (e.g., isotope hydrograph

separations; Sueker et al., 2000; Liu et al., 2004) which may affect comparisons of groundwater proportions between this study and others. The high measurement period BFIs observed in this study show limited evidence for the presence of groundwater in the highest elevations of the San Juan Mountains (Caine and Wilson, 2011; Rondeau et al., 2020).

Table 5.1. A comparison of the proportion of groundwater in streams from snowmelt-dominated mountainous watersheds in the southern Rocky Mountains. The Upper Colorado River Basin extends into parts of Colorado, Utah, Wyoming, New Mexico, and Arizona while the Upper Rio Grande River Basin straddles Colorado and New Mexico.

Study	**Region**	**Elevation (m)**	**Watershed Area (km^2)**	**Groundwater (%)**
Caine (1989)	Front Range, Colorado	3380 – 4000	0.08	24 – 51
Sueker et al., (2000)	Front Range, Colorado	2490 – 3260	7.8 - 104	37 – 89
Clow et al., (2003)	Front Range, Colorado	3097 – 4009	6.9	75
Liu et al., (2004)	Front Range, Colorado	3380 – 4000	0.08 – 2.25	18 – 64
Miller et al., (2014)	Upper Colorado River Basin	940 – >4000	1,160 – 62419	21 – 58
Miller et al., (2020)	Upper Colorado River Basin	2570 – 3620	0.53 - 63	22 – 46
Rumsey et al., (2020)	Upper Rio Grande River Basin	1509 – 2578	94 – 45169	49
Present Study	San Juan Mountains, Colorado	3360 – 4100	2.9	19 – 50

Snowmelt period and post-snowmelt low flow period BFIs were moderately negatively correlated with t_{sub} (Figure 4.5; Pearson's r = -0.44 to -0.81, $p < 0.10$), highlighting that study years with higher snowmelt or low flow period BFIs tended to have earlier t_{sub}. This relationship was expected because higher BFIs during snowmelt or low flow represent an overall greater presence of groundwater in streamflow and coincide with higher daily BFIs and earlier t_{sub}. The

snowmelt period BFIs (11 – 42%) and low flow period BFIs (26 – 79%) determined in this study are also comparable to estimates of snowmelt period BFIs (13 – 45%) and low flow period BFIs (40 – 86%) from large watersheds (>1000 km^2) in the Upper Colorado River Basin (Miller et al., 2014). While the BFI values between these two studies are generally similar, caution must be used when generalizing results taken at different scales (e.g., small watersheds versus large watersheds), as different processes can affect baseflow generation at different scales.

5.2.5. CMB Model Uncertainty

The CMB method was assumed to be the most robust method to estimate baseflow discharge because using measured SC incorporates the influence of watershed geology on stream waters (Stewart et al., 2007; Miller et al., 2014). However, the accuracy of the baseflow dataset estimated with the CMB method in this study has not been evaluated. Results from the CMB model used in this study could be corroborated by estimating the amount of model uncertainty (Genereux, 1998) or by comparing estimations of baseflow discharge from the CMB to estimations of baseflow discharge from other tracer-based hydrograph separation methods (Caine, 1989; Laudon and Slaymaker, 1997; Covino and McGlynn, 2007; Stewart et al., 2007). Uncertainty in baseflow discharge has been found to be greater during the low flow period than during the snowmelt period in snowmelt-dominated watersheds in the Upper Colorado River Basin (Miller et al., 2014) and may impact the results about wetland drainage in this study.

5.2.6. Limitations of BFI for Investigating Wetland Drainage

Determining the timing of substantial baseflow is complex as it is a function of different types of hydrologic processes (e.g., snowpack or precipitation) as well as different dimensions

(e.g., timings or magnitudes), and because of the high interannual variability associated with climate and hydrological variables in snowmelt-dominated watersheds (Bales et al., 2006; Li et al., 2017). The primary result of this paper, the relative importance of wetland drainage, relies heavily on the methodology used to determine the timing of substantial baseflow and requires great scrutiny when interpreting results and drawing conclusions. Using just BFI alone to estimate when wetland drainage becomes a substantial component of streamflow is probably not a robust enough method to truly capture wetland drainage processes. Furthermore, BFI data can be sensitive to summer precipitation or the way baseflow discharge is estimated in the CMB model, emphasizing a shortcoming of using threshold BFI values to assess wetland drainage. The threshold BFI values used in this study are considered surrogates for determining the timing of when wetland drainage becomes a substantial component of streamflow and highlights the need to directly measure wetland drainage from the SAW.

5.3. Statistical Evaluation

Many hydroclimate variables considered in this study had poor correlation to t_{sub}, suggesting that t_{sub} is more influenced by other variables not evaluated here or that the relationship between hydroclimate and t_{sub} is more complex than previously thought. Correlation results may be confounded by the small sample size (16 years), because the correlation coefficient can be sensitive to outliers, or because the correlation coefficient does not capture non-linear processes well. Low correlation coefficients signal the need for caution when interpreting the meaning and potential implications of the relationships between hydroclimate variables and t_{sub}.

Furthermore, there may be a deficit in the types of data used in the statistical analysis. Additional meteorological, hydrogeological, watershed, and wetland variables, such as spatial and temporal heterogeneity of snowpack and snowmelt, hydraulic properties (storage, porosity, or hydraulic conductivity) of volcanic bedrock or of peat soils, degree of fracturing, or watershed slope or aspect could be used to better account for other physical processes that may influence wetland drainage. A deeper understanding of flow paths is necessary to understand how water travels through the SAW and the lower portion of the SBB. Also, different statistical approaches could be used, such as multi-variate regression, to provide a more robust analysis of the effects of multiple variables on t_{sub}.

5.4. The Influence of Groundwater on Wetland Drainage

Water table data were recorded during the summer of 2021 in two wells in the SAW: one located near the head of the wetland (USA), and one located near the toe of the wetland (LSA; Figure 2.1). The section of the SAW closest to the stream (near LSA) is likely where the water table is the lowest as the water table in USA is at a higher elevation and because the ground surface at USA is topographically higher than the ground surface at LSA (Figure 2.1). Because the SAW and surface flow are directed southeastward, subsurface hydraulic gradients likely flow towards the southeast section of the SAW and drain to the stream (Figure 2.1, yellow arrows).

Water table data show that during the late summer, USA dried while LSA did not, suggesting that groundwater is a major source of water for supporting the SAW and becomes more evident following snowmelt (Figure C.1). During this time, daily stream discharge never fell below 0.003 m^3/s and water was observed seeping from the toe of the wetland into the stream, generating flow. The pattern of general decline in the SAW water table suggests a loss of

wetland subsurface storage and by the continuous transmission of snowmelt-derived groundwater through peat to the stream. Water released from storage in the SAW is probably too small to maintain baseflow on its own, but may support evapotranspiration (Glenn and Woo, 1997). The groundwater system in the SBB is replenished each year by infiltration of snowmelt but successive dry years could reduce the amount of groundwater recharge, reducing the volume of water stored in the subsurface available for supporting the wetland and baseflow.

Observations from the summer of 2021 shows that the stream reaches upstream of the SAW dried in early August, while the stream reaches adjacent to and downstream of the SAW did not dry and were supported by seepage (Figure 2.2c). Stream drying above the wetland represents a shift towards wetland dominance in the stream because all baseflow is derived from the SAW and no contributions come from upstream of the SAW. Therefore, when reaches of stream upstream of the SAW dry, wetland drainage plays its greatest role in streamflow as it is the sole source of stream water. Importantly, t_{sub} in 2021 (t_{30} to t_{45}: 4 July to 23 July) occurred before stream drying was observed (early August), showing that wetland drainage can potentially play an important role in maintaining streamflow even before drying is observed.

5.5. Conceptual Understanding

In summary, wetland drainage plays an important role in maintaining streamflow in the SBB, but the relative strength of drainage varies each year and is dependent upon the timing and magnitude of hydroclimatic factors and how water is transported through the subsurface to the stream (e.g., movement of precipitation or snowpack to streamflow or recharge). Results from the study period show that in wet years the timing of substantial baseflow occurs later in the year, meaning that wetland drainage plays a smaller role in maintaining streamflow in wet years

compared to dry years. The timing of substantial baseflow can also be affected by large summer precipitation events (2020) or by variables rate of snowmelt (2021).

Maximum snow accumulation (peak SWE) may represent the size of the snowpack and how much water is available to the watershed from snow, but it appears that the timing and relative rate of snowmelt (SAG and peak stream discharge date) exert a greater influence on wetland drainage, highlighting that the transformation of water in snow storage to streamflow is a key control on wetland drainage in the SBB. In one dry year (2018), maximum snowpack accumulation was low and peak stream discharge and SAG occurred earlier than average, suggesting that these processes may occur earlier in dry years, resulting in less water being available for streamflow. Neither the total amount of precipitation that falls in a certain period (water year or seasonal) nor the cumulative amount of flow that crosses the stream gauge appear to have any influence on wetland drainage, implying that wetland drainage is controlled more the timing of water inputs rather than the total amount. Summer precipitation may have a greater influence on wetland drainage than precipitation in other seasons because of the lack of water inputs during summer.

Disentangling the effects of snowmelt period hydrological processes or post-snowmelt low flow period hydrological processes on wetland drainage can be difficult and is dependent upon the relative strengths of the signals of each process. Large summer precipitation events may delay the timing of when wetland drainage becomes a substantial portion of streamflow (late July 2020), suggesting that hydrological processes that occur during low flow can overprint processes that occur during snowmelt. In a dry year (2021), maximum snowpack accumulation occurred earlier and was lower than average, yet summer precipitation was relatively large, and the timing of substantial baseflow occurred near the mean dates, showing that the small and early maximum

snowpack accumulation did not have as strong an impact on the role of wetland drainage. Conversely, even though 2019 (wet) had low summer precipitation, maximum snowpack accumulation and snowmelt occurred later than average, delaying the start of the low flow period. This highlights that large winter snowpacks may offset the lack of water inputs in the summer and delay wetland drainage (i.e., snowmelt signal overprinted a weak summer precipitation signal in the stream). The difference in the strengths of processes during the high flow (snowmelt) and low flow periods further highlights how interannual variability in hydroclimate can affect wetland drainage.

Since there is considerable interannual variability in the timing and magnitude of hydroclimatic processes, the timing of substantial baseflow will occur at different times in each year, thus, wetland drainage does not have the same relative contribution in maintaining streamflow each year. The importance of wetland drainage in the SBB lies along a spectrum and wet or dry years may have a characteristic response of the relative role of wetland drainage (being relatively larger in dry years and relatively smaller in wet years), but because the timing of substantial baseflow is a function of many hydroclimatic factors, the role of wetland drainage will not be the same in every year as wetland drainage is not controlled by a single factor.

CHAPTER 6 – CONCLUSION

The purpose of this study was to investigate the role and relative importance of wetland drainage from a mountain fen in the Senator Beck Basin (SBB) in the San Juan Mountains in southwestern Colorado. The SBB was selected to conduct this investigation because of its high elevation, snowmelt-dominated hydrologic regime, and because it is a headwater tributary to the Colorado River, a major river in the southwestern United States. The SBB was also selected because it contains a single fen and stream, creating a relatively simple hydrogeologic setting under which to explore the effects of wetland drainage on streamflow. Learning about wetland drainage in the SBB furthers the understanding of how hydroclimate variability may affect mountain fens in the future.

In the SBB, wetland drainage always plays an important role in maintaining streamflow because baseflow discharge is constant year-round, yet the relative importance of wetland drainage varies each year due to the high interannual variability in the timing and magnitude of different hydroclimatic processes. In a dry year (2018), the early timing of substantial baseflow shows that wetland drainage became a substantial component of streamflow earlier in the year, placing a relatively larger importance on wetland drainage to maintain streamflow in the dry year. Conversely, in a wet year (2019), the late timing of substantial baseflow shows that wetland drainage became a substantial component of streamflow later in the year, placing a relatively smaller importance on wetland drainage to maintain streamflow in the wet year. In a given year, a larger importance on wetland drainage to maintain streamflow equates to a greater reliance on groundwater to support streamflow because groundwater provides a constant source of water, thus buffering streamflow. The presence of groundwater in the SBB and its importance for

streamflow is consistent with recent research that has also found that groundwater in mountain environments can be important (Hayashi, 2020; Somers and McKenzie, 2020).

Changes to the timing, amount, and phase of water inputs to mountain watersheds will affect watershed and wetland water budgets, potentially altering baseflow regimes. Decreases to winter snowpacks and changes to snowmelt regimes may reduce the amount of water available for infiltration, thus reducing recharge and the volume of water stored in the subsurface available for supporting wetlands and baseflow. With smaller maximum snowpack accumulations and earlier and shorter snowmelt periods, mountain watersheds may become more reliant on temporary reservoirs like wetlands to buffer streamflow.

Changes in climate may affect wetlands more than any other ecosystem (Mitsch and Gosselink, 2007), but it is not known how wetland drainage will be affected by future climate-driven hydrological changes, partially because wetland response to change is difficult to predict and its effects will not be even across all wetlands (Burkett and Kusler, 2000; Lee et al., 2015; Mercer, 2018). Not much is known about future impacts of climate-driven hydrological changes on groundwater recharge in mountain watersheds (Drexler et al., 2013), but mountain fens may be potentially more resilient to the effects of hydrological changes than other landscape units, if the groundwater supply that they are connected to is sufficiently large enough to support them (Winter, 2000; Mitsch and Gosselink, 2007; Tague and Grant, 2009; Drexler et al., 2013; Austin and Cooper, 2015; Somers et al., 2019). Oftentimes, individual wetlands require their own protection and management solutions to preserve wetland water quality and quantity (Winter et al., 2001).

Earlier occurrences of the timing of substantial baseflow may lead to an increased reliance on wetland drainage and snowmelt-derived groundwater to provide streamflow. This

long-term reliance on groundwater may lead to depletion of the groundwater system, reducing baseflow discharge. There is no direct evidence of the size of the groundwater system in the SBB, but observations of perennial saturation and wetland drainage in several years suggest that it is large enough to continue supporting the SAW and streamflow in the future.

CHAPTER 7 – RECOMMENDATIONS

There are many avenues of work that can be taken to continue research on wetland drainage in the SBB. The relatively long-term hydrologic datasets available to this study (both CSAS and SNOTEL data) were of great importance and provide a plethora of opportunities for future research into groundwater and wetland processes in the SBB. In the future, additional areas of research could include: (1) characterizing surface and subsurface flow to create a more detailed conceptual understanding of water movement through the SAW as well as through the entire watershed, and (2) constructing a water budget for the SAW to determine the timing and magnitude of water inputs and outputs. Lastly, it would be interesting to apply and adapt the timing of substantial baseflow methodology used in this study to other high-elevation, snowmelt-dominated, headwater watersheds with fens that support streamflow to determine the influence of wetland drainage on streamflow in those watersheds.

7.1. Exploring SBB Groundwater

More robust monitoring of the stream would give better insight into changes in streamflow and could be related to fluxes from wetland drainage. Differential stream gauging stations could be used to estimate changes in stream discharge (gaining versus losing conditions) along certain reaches or sub-reaches of stream and could be focused along areas of observed seepage (Rosenberry and LaBaugh, 2008).

Hydrograph separations using more than two components can be conducted in smaller watersheds as it is easier to define and measure additional endmembers and because stream channel and meteorological conditions are more spatiotemporally variable in larger watersheds

(Uhlenbrook et al., 2002; Miller et al., 2014). For example, Miller et al., (2020), used the CMB model and graphical methods to quantify the contributions from three components of streamflow (surface water runoff, shallow subsurface flow, and deeper subsurface flow). This work was conducted in watersheds similar to the SBB as they exist at similar elevations, have similar areas, and have snowmelt-dominated hydrologic regimes, suggesting that a similar approach could be applied in the SBB. Additionally, using hourly stream discharge and SC in the CMB model may provide even greater insight to baseflow processes in the SBB.

7.2. Characterizing the Swamp Angel Wetland

Further study should seek to provide more insight into the physical characteristics and processes that govern water movement in the SAW. An obvious next step is to directly measure wetland drainage from the SAW or to estimate the fluxes of surface water and groundwater outflow using a water budget equation (Kitlasten and Fogg, 2015; Streich and Westbrook, 2020). Estimating the water budget of the SAW would require a hydrogeologic characterization and the gathering of hydrogeologic parameters, such as hydraulic conductivity, porosity, bulk density, and storage properties. Installing a dense network of monitoring wells in the SAW could be used to relate water table response to snowmelt and precipitation events (Bourgault et al., 2017; Mercer, 2018). Hydraulic gradients could be constructed to determine the magnitude and direction of flow within the SAW. Water table measurements could also be used to estimate evapotranspiration rates from the wetland. Wetlands also have significant influence on hydrochemistry, which allows the use of hydrochemical data, such as stable isotopes, to determine water sources or fluxes to and from the SAW (Nielson, 2008).

7.3. Wetland Drainage in Other Mountain Watersheds

The relative importance of wetland drainage is easy to define, yet its absolute importance is harder to determine. Still, the importance of wetland drainage in the SBB may be significant for other high-elevation, snowmelt-dominated, headwater watersheds with wetlands that provide a significant contribution to streamflow. Chimner et al., (2010) report that there are about 2000 fens in the San Juan Mountains and these wetlands potentially may have an important influence on streamflow in their respective watersheds, if they have a drainage mechanism and similar hydrogeologic and topographic characteristics (e.g., size, connection to groundwater system, elevation, slopes) to the SAW. Direct contributions from wetlands to streamflow has been observed in high-elevation, snowmelt-dominated, headwater watersheds in the northern Rocky Mountains, Alberta, Canada (Streich and Westbrook, 2020; Hathaway et al., 2022); central Rocky Mountains, Wyoming, United States (Miller et al., 2020); and Cordillera Blanca, Andes Mountains, Peru (Glas et al., 2018), suggesting that wetland drainage may be a common phenomenon in other mountainous regions.

To quantify the potential strength of wetland drainage in other regions, a similar approach to this study could be taken. Determining the importance of wetland drainage would require understanding precipitation, snowpack, streamflow, and baseflow characteristics of the study watershed, but should also include a characterization of the watershed geology and of the wetland that supplies streamflow. A better constraint of the timing of substantial baseflow should be employed to determine precisely when wetland drainage becomes important in the stream.

REFERENCES

Austin, G., and Cooper, D.J., 2015, Persistence of high elevation fens in the Southern Rocky Mountains, on Grand Mesa, Colorado, U.S.A.: Wetlands Ecology and Management, v. 24, p. 317–334, doi:10.1007/s11273-015-9458-7.

Baars, D., 1992, The American Alps: The San Juan Mountains of Southwest Colorado: Albuquerque, New Mexico, University of New Mexico Press, 204 p.

Bales, R.C., Molotch, N.P., Painter, T.H., Dettinger, M.D., Rice, R., and Dozier, J., 2006, Mountain hydrology of the western United States: Water Resources Research, v. 42, doi:10.1029/2005WR004387.

Barnett, T.P., Adam, J.C., and Lettenmaier, D.P., 2005, Potential impacts of a warming climate on water availability in snow-dominated regions: Nature, v. 438, p. 303–309, doi:10.1038/nature04141.

Barnhart, T.B., Molotch, N.P., Livneh, B., Harpold, A.A., Knowles, J.F., and Schneider, D., 2016, Snowmelt rate dictates streamflow: Geophysical Research Letters, v. 43, p. 8006–8016, doi:10.1002/2016GL069690.

Bedford, B.L., and Godwin, K.S., 2003, Fens of the United States: Distribution, characteristics, and scientific connection versus legal isolation: Wetlands, v. 23, p. 608–629, doi:10.1672/0277-5212(2003)023[0608:FOTUSD]2.0.CO;2.

Bishop, K., Seibert, J., Köhler, S., and Laudon, H., 2004, Resolving the Double Paradox of rapidly mobilized old water with highly variable responses in runoff chemistry: Hydrological Processes, v. 18, p. 185–189, doi:10.1002/hyp.5209.

Blair, R., 1996, Origin of Landscapes, *in* Blair, R., Casey, T.A., Romme, W.H., and Ellis, R.N. eds., The Western San Juan Mountains: Their Geology, Ecology, and Human History, Niwot, Colorado, University Press of Colorado, p. 3–17.

Blanken, P.D., 2014, The effect of winter drought on evaporation from a high-elevation wetland: Journal of Geophysical Research: Biogeosciences, v. 119, p. 1354–1369, doi:10.1002/2014JG002648.

Bloomfield, J.P., Allen, D.J., and Griffiths, K.J., 2009, Examining geological controls on baseflow index (BFI) using regression analysis: An illustration from the Thames Basin, UK: Journal of Hydrology, v. 373, p. 164–176, doi:10.1016/j.jhydrol.2009.04.025.

Bourgault, M., Larocque, M., and Garneau, M., 2017, Quantification of peatland water storage capacity using the water table fluctuation method: Hydrological Processes, v. 31, p. 1184–1195, doi:10.1002/hyp.11116.

Bove, D., Hon, K., Budding, K., Slack, J., Snee, L., and Yeoman, R., 2001, Geochronology and Geology of Late Oligocene Through Miocene Volcanism and Mineralization in the Western San Juan Mountains, Colorado: United States Geological Survey USGS Professional Paper 1642.

Branfireun, B.A., and Roulet, N.T., 1998, The baseflow and storm flow hydrology of a Precambrian shield headwater peatland: Hydrological Processes, v. 12, p. 57–72, doi:10.1002/(SICI)1099-1085(199801)12:1<57::AID-HYP560>3.0.CO;2-U.

Burbank, W., and Luedke, R., 1964, Geology of the Ironton Quadrangle, Colorado: United States Geological Survey, scale 1:24,000.

Burkett, V., and Kusler, J., 2000, Climate Change: Potential Impacts And Interactions In Wetlands of the United States: JAWRA Journal of the American Water Resources Association, v. 36, p. 313–320, doi:10.1111/j.1752-1688.2000.tb04270.x.

Caine, J.S., 2003, Characterizing Groundwater Hydrology in High Gradient Terrains Underlain by Complex Geology: Focus on the San Juan Mountains of Southwestern Colorado: Durango, Colorado, 7-9 May, Geological Society of America, 55th Annual Rocky Mountain Meeting https://gsa.confex.com/gsa/2003RM/webprogram/Paper53306.html.

Caine, J.S., and Wilson, A.B., 2011, The Hydrogeology of the San Juan Mountains, *in* Blair, R., and Bracksieck, G. eds., The Eastern San Juan Mountains: Their Geology, Ecology, and Human History, Boulder, Colorado, University Press of Colorado, p. 75–98.

Caine, N., 1989, Hydrograph Separation in a Small Alpine Basin Based on Inorganic Solute Concentrations: Journal of Hydrology, v. 112, p. 89–101.

Caissie, D., Pollock, T.L., and Cunjak, R.A., 1996, Variation in stream water chemistry and hydrograph separation in a small drainage basin: Journal of Hydrology, v. 178, p. 137–157, doi:10.1016/0022-1694(95)02806-4.

Carrara, P., 2011, Deglacial and Post-Glacial Treeline Fluctuation in the Northern San Juan Mountains, Colorado: United States Geological Survey Professional Paper Professional Paper 1782.

Cayan, D.R., Dettinger, M.D., Kammerdiener, S.A., Caprio, J.M., and Peterson, D.H., 2001, Changes in the Onset of Spring in the Western United States: Bulletin of the American Meteorological Society, v. 82, p. 399–415, doi:10.1175/1520-0477(2001)082<0399:CITOOS>2.3.CO;2.

Center for Snow and Avalanche Studies, 2012, Metadata: Senator Beck Stream Gauge: https://snowstudies.org/wp-content/uploads/2022/02/SBSG-Master-Metadata.pdf (accessed March 2025).

Center for Snow and Avalanche Studies, 2020, Metadata: Swamp Angel Study Plot: https://snowstudies.org/wp-content/uploads/2022/02/SASP-Master-Metadata.pdf (accessed March 2025).

Chapin, T.P., Todd, A.S., and Zeigler, M.P., 2014, Robust, low-cost data loggers for stream temperature, flow intermittency, and relative conductivity monitoring: Water Resources Research, v. 50, p. 6542–6548, doi:10.1002/2013WR015158.

Chimner, R.A., Lemly, J.M., and Cooper, D.J., 2010, Mountain Fen Distribution, Types and Restoration Priorities, San Juan Mountains, Colorado, USA: Wetlands, v. 30, p. 763–771, doi:10.1007/s13157-010-0039-5.

Clow, D.W., 2010, Changes in the Timing of Snowmelt and Streamflow in Colorado: A Response to Recent Warming: Journal of Climate, v. 23, p. 2293–2306, doi:10.1175/2009JCLI2951.1.

Clow, D.W., Schrott, L., Webb, R., Campbell, D.H., Torizzo, A., and Dornblaser, M., 2003, Ground Water Occurrence and Contributions to Streamflow in an Alpine Catchment, Colorado Front Range: Groundwater, v. 41, p. 937–950, doi:10.1111/j.1745-6584.2003.tb02436.x.

Cohen, M.J. et al., 2016, Do geographically isolated wetlands influence landscape functions? Proceedings of the National Academy of Sciences, v. 113, p. 1978–1986, doi:10.1073/pnas.1512650113.

Colbeck, S.C., 1976, An analysis of water flow in dry snow: Water Resources Research, v. 12, p. 523–527, doi:10.1029/WR012i003p00523.

Cooper, D.J., 1996, Water and soil chemistry, floristics, and phytosociology of the extreme rich High Creek fen, in South Park, Colorado, U.S.A.: Canadian Journal of Botany, v. 74, p. 1801–1811, doi:10.1139/b96-217.

Cooper, D.J., and Andrus, R.E., 1994, Patterns of vegetation and water chemistry in peatlands of the west-central Wind River Range, Wyoming, U.S.A.: Canadian Journal of Botany, v. 72, p. 1586–1597, doi:10.1139/b94-196.

Cooper, D.J., Chimner, R.A., and Merritt, D.M., 2012, Chapter 22: Western Mountain Wetlands, *in* Batzer, D.P., Baldwin, A.H., and Baldwin, A. eds., Wetland Habitats of North America: Ecology and Conservation Concerns, University of California Press.

Cooper, D.J., and MacDonald, L.H., 2000, Restoring the Vegetation of Mined Peatlands in the Southern Rocky Mountains of Colorado, U.S.A.: Restoration Ecology, v. 8, p. 103–111, doi:10.1046/j.1526-100x.2000.80016.x.

Cooper, D.J., MacDonald, L.H., Wenger, S.K., and Woods, S.W., 1998, Hydrologic restoration of a fen in Rocky Mountain National Park, Colorado, USA: Wetlands, v. 18, p. 335–345, doi:10.1007/BF03161529.

Covino, T.P., and McGlynn, B.L., 2007, Stream gains and losses across a mountain-to-valley transition: Impacts on watershed hydrology and stream water chemistry: Water Resources Research, v. 43, p. 2006WR005544, doi:10.1029/2006WR005544.

Crockett, A.C., Ronayne, M.J., and Cooper, D.J., 2015, Relationships between vegetation type, peat hydraulic conductivity, and water table dynamics in mountain fens: Ecohydrology, v. 9, p. 1028–1038, doi:10.1002/eco.1706.

Doskocil, L.G., Fassnacht, S., and Derry, J., 2021, Estimating Double Peak Streamflow Behavior in the Uncompahgre River Basin, *in* Proceedings, AGU Hydrology Days 2021: Fort Collins, Colorado, Colorado Water Center, v. 38, p. 28–29.

Drexler, J.Z., Knifong, D., Tuil, J., Flint, L.E., and Flint, A.L., 2013, Fens as whole-ecosystem gauges of groundwater recharge under climate change: Journal of Hydrology, v. 481, p. 22–34, doi:10.1016/j.jhydrol.2012.11.056.

Duncan, C.R., 2020, Patterns of Dust-Enhanced Absorbed Energy and Shifts in Melt Timing for Snow of Southwestern Colorado: Colorado State University, 62 p.

Earman, S., Campbell, A.R., Phillips, F.M., and Newman, B.D., 2006, Isotopic exchange between snow and atmospheric water vapor: Estimation of the snowmelt component of groundwater recharge in the southwestern United States: Journal of Geophysical Research: Atmospheres, v. 111, doi:10.1029/2005JD006470.

Environmental Systems Research Institute, 2022, ArcGIS Pro:, version 3.03, https://www.esri.com/en-us/arcgis/products/arcgis-pro/overview.

Fassnacht, S.R., 2006, Upper versus lower Colorado River sub-basin streamflow: characteristics, runoff estimation and model simulation: Hydrological Processes, v. 20, p. 2187–2205, doi:10.1002/hyp.6202.

Fassnacht, S.R., Deitemeyer, D.C., and Venable, N.B.H., 2014, Capitalizing on the daily time step of snow telemetry data to model the snowmelt components of the hydrograph for small watersheds: Hydrological Processes, v. 28, p. 4654–4668, doi:10.1002/hyp.10260.

Fassnacht, S.R., Duncan, C.R., Pfohl, A.K.D., Webb, R.W., Derry, J.E., Sanford, W.E., Reimanis, D.C., and Doskocil, L.G., 2022, Drivers of Dust-Enhanced Snowpack Melt-Out and Streamflow Timing: Hydrology, v. 9, doi:10.3390/hydrology9030047.

Fassnacht, S.R., Patterson, G.G., Venable, N.B.H., Cherry, M.L., Pfohl, A.K.D., Sanow, J.E., and Tedesche, M.E., 2020, How Do We Define Climate Change? Considering the Temporal Resolution of Niveo-Meteorological Data: Hydrology, v. 7, p. 38, doi:10.3390/hydrology7030038.

Fassnacht, S.R., Venable, N.B.H., Khishigbayar, J., and Cherry, M.L., 2013, The probability of precipitation as snow derived from daily air temperature for high elevation areas of Colorado, United States, *in* Gothenburg, Sweden, IAHS Press, v. 360, p. 65–70.

Fetchenhier, S., 1996, Ore Deposits and Minerals, *in* Blair, R., Casey, T.A., Romme, W.H., and Ellis, R.N. eds., The Western San Juan Mountains: Their Geology, Ecology, and Human History, Niwot, Colorado, University Press of Colorado, p. 80–96.

Flint, A.L., Flint, L.E., Hevesi, J.A., and Blainey, J.B., 2004, Fundamental concepts of recharge in the desert southwest: A regional modeling perspective, *in* Hogan, J.F., Phillips, F.M., and Scanlon, B.R. eds., Groundwater Recharge in a Desert Environment: The Southwestern United States, Washington, D.C., USA, American Geophysical Union, Water Science and Application, v. 9, p. 159–184, doi:10.1029/009WSA10.

Flynn, H., Fassnacht, S.R., MacDonald, M.S., and Pfohl, A.K.D., 2024, Baseflow from Snow and Rain in Mountain Watersheds: Water, v. 16, p. 1665, doi:10.3390/w16121665.

Flynn, H., McDonald, M., and Fassnacht, S., 2021, Assessing Baseflow in Snow-Dominated Watersheds, *in* Proceedings, AGU Hydrology Days 2021: Fort Collins, Colorado, Colorado Water Center, v. 38, p. 12–13.

Genereux, D., 1998, Quantifying uncertainty in tracer-based hydrograph separations: Water Resources Research, v. 34, p. 915–919, doi:10.1029/98WR00010.

Glas, R., Lautz, L., McKenzie, J., Mark, B., Baraer, M., Chavez, D., and Maharaj, L., 2018, A review of the current state of knowledge of proglacial hydrogeology in the Cordillera Blanca, Peru: WIREs Water, v. 5, doi:10.1002/wat2.1299.

Glenn, M.S., and Woo, M., 1997, Spring and summer hydrology of a valley-bottom wetland, Ellesmere Island, Northwest Territories, Canada: Wetlands, v. 17, p. 321–329, doi:10.1007/BF03161420.

Godsey, S.E., Kirchner, J.W., and Tague, C.L., 2014, Effects of changes in winter snowpacks on summer low flows: case studies in the Sierra Nevada, California, USA: Hydrological Processes, v. 28, p. 5048–5064, doi:10.1002/hyp.9943.

Gonzales, M.L. et al., 2020, What do we know about Peruvian peatlands? Center for International Forestry Research (CIFOR), doi:10.17528/cifor/007848.

Hall, F.R., 1968, Base-Flow Recessions—A Review: Water Resources Research, v. 4, p. 973–983, doi:10.1029/WR004i005p00973.

Hammond, J.C., Harpold, A.A., Weiss, S., and Kampf, S.K., 2019, Partitioning snowmelt and rainfall in the critical zone: effects of climate type and soil properties: Hydrology and Earth System Sciences, v. 23, p. 3553–3570, doi:10.5194/hess-23-3553-2019.

Harbert, B.L., and Cooper, D.J., 2017, Environmental drivers of subalpine and alpine fen vegetation in the Southern Rocky Mountains, Colorado, USA: Plant Ecology, v. 218, p. 885–898, doi:10.1007/s11258-017-0737-7.

Harpold, A., Brooks, P., Rajagopal, S., Heidbuchel, I., Jardine, A., and Stielstra, C., 2012, Changes in snowpack accumulation and ablation in the intermountain west: Water Resources Research, v. 48, doi:10.1029/2012WR011949.

Hathaway, J.M., Westbrook, C.J., Rooney, R.C., Petrone, R.M., and Langs, L.E., 2022, Quantifying relative contributions of source waters from a subalpine wetland to downstream water bodies: Hydrological Processes, v. 36, doi:10.1002/hyp.14679.

Hayashi, M., 2020, Alpine Hydrogeology: The Critical Role of Groundwater in Sourcing the Headwaters of the World: Groundwater, v. 58, p. 498–510, doi:10.1111/gwat.12965.

Hooper, R.P., and Shoemaker, C.A., 1986, A Comparison of Chemical and Isotopic Hydrograph Separation: Water Resources Research, v. 22, p. 1444–1454, doi:10.1029/WR022i010p01444.

Jenicek, M., and Ledvinka, O., 2020, Importance of snowmelt contribution to seasonal runoff and summer low flows in Czechia: Hydrology and Earth System Sciences, v. 24, p. 3475–3491, doi:10.5194/hess-24-3475-2020.

Johnson, B.G., Jiménez-Moreno, G., Eppes, M.C., Diemer, J.A., and Stone, J.R., 2013, A multiproxy record of postglacial climate variability from a shallowing, 12-m deep sub-alpine bog in the southeastern San Juan Mountains of Colorado, USA: The Holocene, v. 23, p. 1028–1038, doi:10.1177/0959683613479682.

Keen, R.A., 1996, Weather and Climate, *in* Blair, R., Casey, T.A., Romme, W.H., and Ellis, R.N. eds., The Western San Juan Mountains: Their Geology, Ecology, and Human History, Niwot, Colorado, University Press of Colorado, p. 113–126.

Kirchner, J.W., 2003, A double paradox in catchment hydrology and geochemistry: Hydrological Processes, v. 17, p. 871–874, doi:10.1002/hyp.5108.

Kitlasten, W., and Fogg, G.E., 2015, Hydrogeology of a groundwater sustained montane peatland: Grass Lake, California: Wetlands Ecology and Management, v. 23, p. 827–843, doi:10.1007/s11273-015-9422-6.

Landry, C.C., Buck, K.A., Raleigh, M.S., and Clark, M.P., 2014, Mountain system monitoring at Senator Beck Basin, San Juan Mountains, Colorado: A new integrative data source to develop and evaluate models of snow and hydrologic processes: Water Resources Research, v. 50, p. 1773–1788, doi:10.1002/2013WR013711.

Laudon, H., and Slaymaker, O., 1997, Hydrograph separation using stable isotopes, silica and electrical conductivity: an alpine example: Journal of Hydrology, v. 201, p. 82–101, doi:10.1016/S0022-1694(97)00030-9.

Lee, S.-Y., Ryan, M.E., Hamlet, A.F., Palen, W.J., Lawler, J.J., and Halabisky, M., 2015, Projecting the Hydrologic Impacts of Climate Change on Montane Wetlands (C. J. Richardson, Ed.): PLOS ONE, v. 10, doi:10.1371/journal.pone.0136385.

Letts, M.G., Roulet, N.T., Comer, N.T., Skarupa, M.R., and Verseghy, D.L., 2000, Parametrization of peatland hydraulic properties for the Canadian land surface scheme: Atmosphere-Ocean, v. 38, p. 141–160, doi:10.1080/07055900.2000.9649643.

Li, D., Wrzesien, M.L., Durand, M., Adam, J., and Lettenmaier, D.P., 2017, How much runoff originates as snow in the western United States, and how will that change in the future? Geophysical Research Letters, v. 44, p. 6163–6172, doi:10.1002/2017GL073551.

Lipman, P., Steven, T., Luedke, R., and Burbank, W., 1973, Revised Volcanic History of the San Juan, Uncompahgre, Silverton, and Lake City Calderas in the Western San Juan Mountains, Colorado: United States Geological Survey Journal of Research, v. 1, p. 627–642.

Liu, F., Williams, M.W., and Caine, N., 2004, Source waters and flow paths in an alpine catchment, Colorado Front Range, United States: Water Resources Research, v. 40, doi:10.1029/2004WR003076.

Malone, D., and Lemly, J., 2019, Ecological Systems of Colorado: Wetland / Riparian: https://cnhp.colostate.edu/wp-content/uploads/download/documents/temp/EcologialSystem_365208.pdf (accessed March 2025).

Matsubayashi, U., Velasquez, G.T., and Takagi, F., 1993, Hydrograph separation and flow analysis by specific electrical conductance of water: Journal of Hydrology, v. 152, p. 179–199, doi:10.1016/0022-1694(93)90145-Y.

McLaughlin, D.L., Kaplan, D.A., and Cohen, M.J., 2014, A significant nexus: Geographically isolated wetlands influence landscape hydrology: Water Resources Research, v. 50, p. 7153–7166, doi:10.1002/2013WR015002.

Mercer, J.J., 2018, Insights Intro Mountain Wetland Resilience to Climate Change: An Evaluation of the Hydrological Processes Contributing to the Hydrodynamics of Alpine Wetlands in the Canadian Rocky Mountains: University of Saskatchewan, 89 p.

Messerli, B., Viviroli, D., and Weingartner, R., 2004, Mountains of the World: Vulnerable Water Towers for the 21st Century: AMBIO: A Journal of the Human Environment, v. 33, p. 29, doi:10.1007/0044-7447-33.sp13.29.

Meyer, J.L., Kaplan, L.A., Newbold, D., Strayer, D.L., Woltemade, C.J., Zedler, J.B., Beilfuss, R., and Carpenter, Q., 2007, The Scientific Imperative for Defending Small Streams and Wetlands: American Rivers and the Sierra Club.

Microsoft Corporation. 2025. Microsoft Excel, version 2502, https://office.microsoft.com/excel.

Miller, M.P., Johnson, H.M., Susong, D.D., and Wolock, D.M., 2015, A new approach for continuous estimation of baseflow using discrete water quality data: Method description and comparison with baseflow estimates from two existing approaches: Journal of Hydrology, v. 522, p. 203–210, doi:10.1016/j.jhydrol.2014.12.039.

Miller, M.P., Susong, D.D., Shope, C.L., Heilweil, V.M., and Stolp, B.J., 2014, Continuous estimation of baseflow in snowmelt-dominated streams and rivers in the Upper Colorado River Basin: A chemical hydrograph separation approach: Water Resources Research, v. 50, p. 6986–6999, doi:10.1002/2013WR014939.

Miller, R., Bradford, W., and Peters, N., 1988, Specific Conductance; Theoretical Considerations and Application to Analytical Quality Control: United States Geological Survey U.S. Geological Survey Water-Supply Paper 2311, doi:10.3133/wsp2311.

Miller, S.A., Lyon, S.W., and Miller, S.N., 2020, Quantifying contributions of snowmelt water to streamflow using graphical and chemical hydrograph separation: Hydrological Processes, v. 34, p. 5606–5623, doi:10.1002/hyp.13981.

Mitsch, W.J., Bernal, B., and Hernandez, M.E., 2015, Ecosystem services of wetlands: International Journal of Biodiversity Science, Ecosystem Services & Management, v. 11, p. 1–4, doi:10.1080/21513732.2015.1006250.

Mitsch, W.J., and Gosselink, J., 2007, Wetlands: John Wiley & Sons, 600 p.

Nielson, A., 2008, Hydrology and Hydrochemistry of Alpine Wetland: Green Lakes Valley, Colorado Front Range, USA: University of Colorado, Boulder, 128 p.

NRCS, 2014, Chapter 6 - Data Management, *in* National Engineering Handbook: Part 622 Snow Survey and Water Supply Forecasting, Natural Resources Conservation Service, 24 p.,

https://directives.nrcs.usda.gov/sites/default/files2/1720456725/Chapter%206%20-%20Data%20Management.pdf.

Pepin, N. et al., 2015, Elevation-dependent warming in mountain regions of the world: Nature Climate Change, v. 5, p. 424–430, doi:10.1038/nclimate2563.

Pfohl, A.K.D., 2016, Examining Trends in Snowmelt Contribution to Streamflow in the Southern Rocky Mountains of Colorado: Colorado State University, 55 p.

Pfohl, A.K.D., and Fassnacht, S.R., 2023, Evaluating Methods of Streamflow Timing to Approximate Snowmelt Contribution in High-Elevation Mountain Watersheds: Hydrology, v. 10, p. 75, doi:10.3390/hydrology10040075.

Pilgrim, D.H., Huff, D.D., and Steele, T.D., 1979, Use of specific conductance and contact time relations for separating flow components in storm runoff: Water Resources Research, v. 15, p. 329–339, doi:10.1029/WR015i002p00329.

Pinder, G.F., and Jones, J.F., 1969, Determination of the ground-water component of peak discharge from the chemistry of total runoff: Water Resources Research, v. 5, p. 438–445, doi:10.1029/WR005i002p00438.

Price, K., 2011, Effects of watershed topography, soils, land use, and climate on baseflow hydrology in humid regions: A review: Progress in Physical Geography: Earth and Environment, v. 35, p. 465–492, doi:10.1177/0309133311402714.

R Core Team. 2025. R: A language and environment for statistical computing, version 4.2.3, https://www.r-project.org/.

Reeve, A.S., Siegel, D.I., and Glaser, P.H., 2000, Simulating vertical flow in large peatlands: Journal of Hydrology, v. 227, p. 207–217, doi:10.1016/S0022-1694(99)00183-3.

Rondeau, R., Bidwell, M., Neely, B., Rangwala, I., Yung, L., and Wyborn, C., 2020, Seeps, Springs and Wetlands: San Juan Basin, Colorado: North Central Climate Adaptation Science Center.

Rosenberry, D., and LaBaugh, J., 2008, Field Techniques For Estimating Water Fluxes Between Surface Water and Ground Water: United States Geological Survey Techniques and Methods Techniques and Methods 4-D2.

Roulet, N.T., 1990, Hydrology of a headwater basin wetland: Groundwater discharge and wetland maintenance: Hydrological Processes, v. 4, p. 387–400, doi:10.1002/hyp.3360040408.

Rumsey, C.A., Miller, M.P., and Sexstone, G.A., 2020, Relating hydroclimatic change to streamflow, baseflow, and hydrologic partitioning in the Upper Rio Grande Basin, 1980 to 2015: Journal of Hydrology, v. 584, p. 124715, doi:10.1016/j.jhydrol.2020.124715.

Rumsey, C.A., Miller, M.P., Susong, D.D., Tillman, F.D., and Anning, D.W., 2015, Regional scale estimates of baseflow and factors influencing baseflow in the Upper Colorado River Basin: Journal of Hydrology: Regional Studies, v. 4, p. 91–107, doi:10.1016/j.ejrh.2015.04.008.

Serreze, M.C., Clark, M.P., Armstrong, R.L., McGinnis, D.A., and Pulwarty, R.S., 1999, Characteristics of the western United States snowpack from snowpack telemetry (SNOTEL) data: Water Resources Research, v. 35, p. 2145–2160, doi:10.1029/1999WR900090.

Sklash, M.G., and Farvolden, R.N., 1979, The Role of Groundwater in Storm Runoff (W. Back & D. Stephenson, Eds.): Journal of Hydrology, v. 43, p. 45–65.

Somers, L.D., and McKenzie, J.M., 2020, A review of groundwater in high mountain environments: WIREs Water, v. 7, doi:10.1002/wat2.1475.

Somers, L.D., McKenzie, J.M., Mark, B.G., Lagos, P., Ng, G.C., Wickert, A.D., Yarleque, C., Baraër, M., and Silva, Y., 2019, Groundwater Buffers Decreasing Glacier Melt in an Andean Watershed—But Not Forever: Geophysical Research Letters, v. 46, p. 13016–13026, doi:10.1029/2019GL084730.

Spence, C., 2007, On the relation between dynamic storage and runoff: A discussion on thresholds, efficiency, and function: Water Resources Research, v. 43, doi:10.1029/2006WR005645.

Spence, C., Guan, X.J., and Phillips, R., 2011, The Hydrological Functions of a Boreal Wetland: Wetlands, v. 31, p. 75–85, doi:10.1007/s13157-010-0123-x.

Steven, T., and Lipman, P., 1976, Calderas of the San Juan Volcanic Field, Southwestern Colorado: United States Geological Survey Professional Paper USGS Professional Paper 958.

Stewart, I.T., Cayan, D.R., and Dettinger, M.D., 2004, Changes in Snowmelt Runoff Timing in Western North America under a `Business as Usual' Climate Change Scenario: Climatic Change, v. 62, p. 217–232, doi:10.1023/B:CLIM.0000013702.22656.e8.

Stewart, I.T., Cayan, D.R., and Dettinger, M.D., 2005, Changes toward Earlier Streamflow Timing across Western North America: Journal of Climate, v. 18, p. 1136–1155, doi:10.1175/JCLI3321.1.

Stewart, M., Cimino, J., and Ross, M., 2007, Calibration of Base Flow Separation Methods with Streamflow Conductivity: Groundwater, v. 45, p. 17–27, doi:10.1111/j.1745-6584.2006.00263.x.

Stottlemyer, R., 2001, Processes regulating watershed chemical export during snowmelt, Fraser Experimental Forest, Colorado: Journal of Hydrology, v. 245, p. 177–195, doi:10.1016/S0022-1694(01)00352-3.

Streich, S.C., and Westbrook, C.J., 2020, Hydrological Function of a Mountain Fen at Low Elevation Under Dry Conditions: Hydrological Processes, v. 34, p. 244–257, doi:10.1002/hyp.13579.

Sueker, J.K., Ryan, J.N., Kendall, C., and Jarrett, R.D., 2000, Determination of hydrologic pathways during snowmelt for alpine/subalpine basins, Rocky Mountain National Park, Colorado: Water Resources Research, v. 36, p. 63–75, doi:10.1029/1999WR900296.

Tague, C., and Grant, G.E., 2009, Groundwater dynamics mediate low-flow response to global warming in snow-dominated alpine regions: Water Resources Research, v. 45, doi:10.1029/2008WR007179.

Toney, J.L., and Anderson, R.S., 2006, A postglacial palaeoecological record from the San Juan Mountains of Colorado USA: fire, climate and vegetation history: The Holocene, v. 16, p. 505–517, doi:10.1191/0959683606hl946rp.

Trujillo, E., and Molotch, N.P., 2014, Snowpack regimes of the Western United States: Water Resources Research, v. 50, p. 5611–5623, doi:10.1002/2013WR014753.

Uhlenbrook, S., 2012, Hydrological Measurements: https://ocw.tudelft.nl/course-lectures/hydrological-measurements-isothopes-and-hydrographic-separation/ (accessed March 2025).

Uhlenbrook, S., Frey, M., Leibundgut, C., and Maloszewski, P., 2002, Hydrograph separations in a mesoscale mountainous basin at event and seasonal timescales: Water Resources Research, v. 38, doi:10.1029/2001WR000938.

Viviroli, D., Kummu, M., Meybeck, M., Kallio, M., and Wada, Y., 2020, Increasing dependence of lowland populations on mountain water resources: Nature Sustainability, v. 3, p. 917–928, doi:10.1038/s41893-020-0559-9.

Wahl, K., and Wahl, T., 1988, Effects of Regional Ground-Water Level Declines on Streamflow in the Oklahoma Panhandle, *in* Proceedings, Symposium on Water-Use Data for Water Resources Management, Bethesda, Maryland, American Water Resources Association, p. 239–249.

Wels, C., Cornett, R.J., and Lazerte, B.D., 1991, Hydrograph separation: A comparison of geochemical and isotopic tracers: Journal of Hydrology, v. 122, p. 253–274, doi:10.1016/0022-1694(91)90181-G.

Whitfield, P.H., 2013, Is ‘Centre of Volume’ a robust indicator of changes in snowmelt timing? Hydrological Processes, v. 27, p. 2691–2698, doi:10.1002/hyp.9817.

Wigley, T.M.L., and Jones, P.D., 1985, Influences of precipitation changes and direct CO2 effects on streamflow: Nature, v. 314, p. 149–152.

Williams, M.W., and Melack, J.M., 1991, Precipitation chemistry in and ionic loading to an Alpine Basin, Sierra Nevada: Water Resources Research, v. 27, p. 1563–1574, doi:10.1029/90WR02773.

Winograd, I.J., Riggs, A.C., and Coplen, T.B., 1998, The relative contributions of summer and cool-season precipitation to groundwater recharge, Spring Mountains, Nevada, USA: Hydrogeology Journal, v. 6, p. 77–93, doi:10.1007/s100400050135.

Winter, T.C., 2000, The Vulnerability of Wetlands to Climate Change: A Hydrologic Landscape Perspective: Journal of the American Water Resources Association, v. 36, p. 305–311, doi:10.1111/j.1752-1688.2000.tb04269.x.

Winter, T.C., Harvey, J., Franke, O., and Alley, W., 1998, Groundwater and Surface Water: A Single Resource: United States Geological Survey Circular U.S. Geological Survey Circular 1139.

Winter, T.C., Rosenberry, D.O., Buso, D.C., and Merk, D.A., 2001, Water source to four U.S. wetlands: Implications for wetland management: Wetlands, v. 21, p. 462–473, doi:10.1672/0277-5212(2001)021[0462:WSTFUS]2.0.CO;2.

Woods, S.W., MacDonald, L.H., and Westbrook, C.J., 2006, Hydrologic interactions between an alluvial fan and a slope wetland in the central Rocky Mountains, USA: Wetlands, v. 26, p. 230–243, doi:10.1672/0277-5212(2006)26[230:HIBAAF]2.0.CO;2.

Wu, Y., Zhang, G., and Rousseau, A.N., 2020, Quantitative assessment on basin-scale hydrological services of wetlands: Science China Earth Sciences, v. 63, p. 279–291, doi:10.1007/s11430-018-9372-9.

Yager, D., and Bove, D., 2002, Generalized Geologic Map of Part of the Upper Animas River Watershed and Vicinity, Silverton, Colorado: United States Geological Survey, 1:48,000, doi:10.3133/mf2377.

Zhang, R., Li, Q., Chow, T.L., Li, S., and Danielescu, S., 2013, Baseflow separation in a small watershed in New Brunswick, Canada, using a recursive digital filter calibrated with the conductivity mass balance method: Hydrological Processes, v. 27, p. 2659–2665, doi:10.1002/hyp.9417.

Table A.1. Summary of precipitation, snowpack accumulation, and ablation characteristics in the period of record. A description of variables is in Table 3.1. Column 4 represents the date of first snow accumulation which was used to define the winter and summer precipitation groups.

Year	Cum. Precip. (mm)	Wettest Month (mm)	First Accum. (date)	Peak SWE (date)	SAG (date)	Peak SWE (mm)	Winter Precip. (mm)	Resid. Precip. (mm)	Summer Precip. (mm)
2006	1214	Mar (211)	27-Oct	8-Apr	28-May	620	691	57	468
2007	1233	Oct (180)	9-Oct	9-May	12-Jun	602	785	54	369
2008	1238	Jan (197)	15-Oct	14-Apr	19-Jun	874	848	130	269
2009	1220	Dec (205)	15-Oct	19-Apr	28-May	699	757	80	344
2010	1127	Mar (151)	13-Oct	8-Apr	1-Jun	615	664	140	338
2011	1397	Apr (214)	15-Oct	22-May	24-Jun	856	1078	41	310
2012	897	Feb (142)	20-Oct	22-Mar	18-May	452	481	94	243
2013	1045	Sep (148)	6-Oct	26-Apr	24-May	498	588	37	506
2014	1209	Sept (161)	28-Oct	2-May	12-Jun	622	684	90	396
2015	1063	May (201)	12-Oct	26-May	20-Jun	513	756	57	356
2016	1219	Dec (168)	5-Nov	3-May	13-Jun	592	752	96	298
2017	1136	Jan (203)	25-Oct	5-Apr	14-Jun	696	709	152	308
2018	724	Feb (125)	7-Nov	26-Apr	30-May	417	432	40	339
2019	1256	Mar (239)	31-Oct	3-May	6-Jul	925	812	159	154
2020	943	Dec (169)	8-Oct	25-Apr	11-Jun	622	710	76	156
2021	964	Nov / Mar / Jul (125)	19-Oct	2-Apr	12-Jun	536	543	156	380
Mean:	1118	- (177)	19-Oct	23-Apr	9-Jun	634	706	91	327

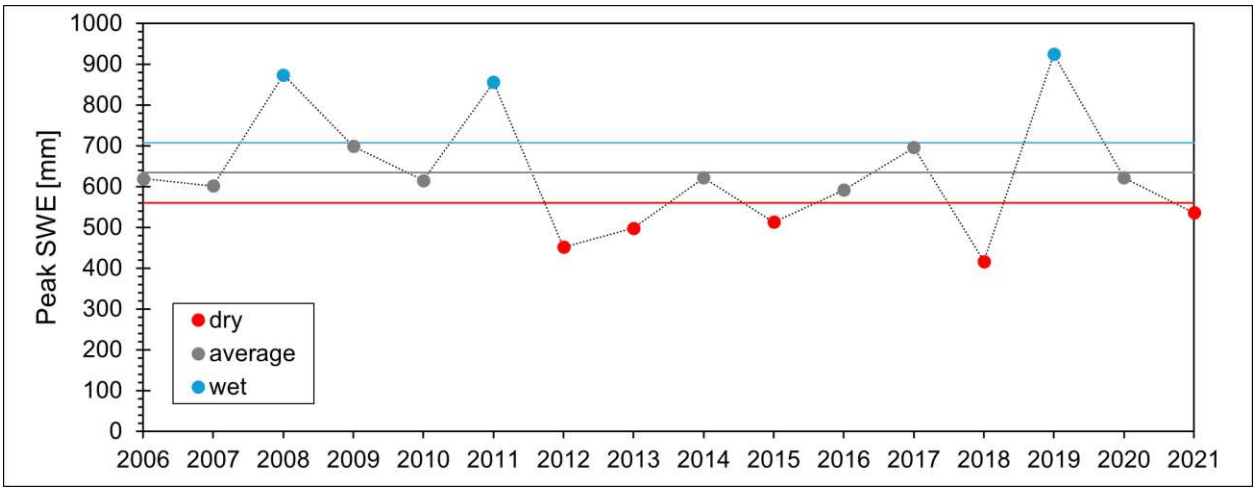

Figure A.1. Hydrologic classification of study years based upon value of peak SWE (mm). Study years were either classified as "Dry", "Average", or "Wet" based upon mean peak SWE ± the standard deviation multiplied by 0.5. Mean peak SWE was 634 mm with a standard deviation of ±147 mm (0.5SD = 74 mm), creating a lower limit of 560 mm and an upper limit of 708 mm. "Dry" years were considered as those with peak SWE values < 560 mm; "Average" years were considered as those with peak SWE values between 560 mm and 708 mm; and, "Wet" years were considered as those with peak SWE values > 708 mm.

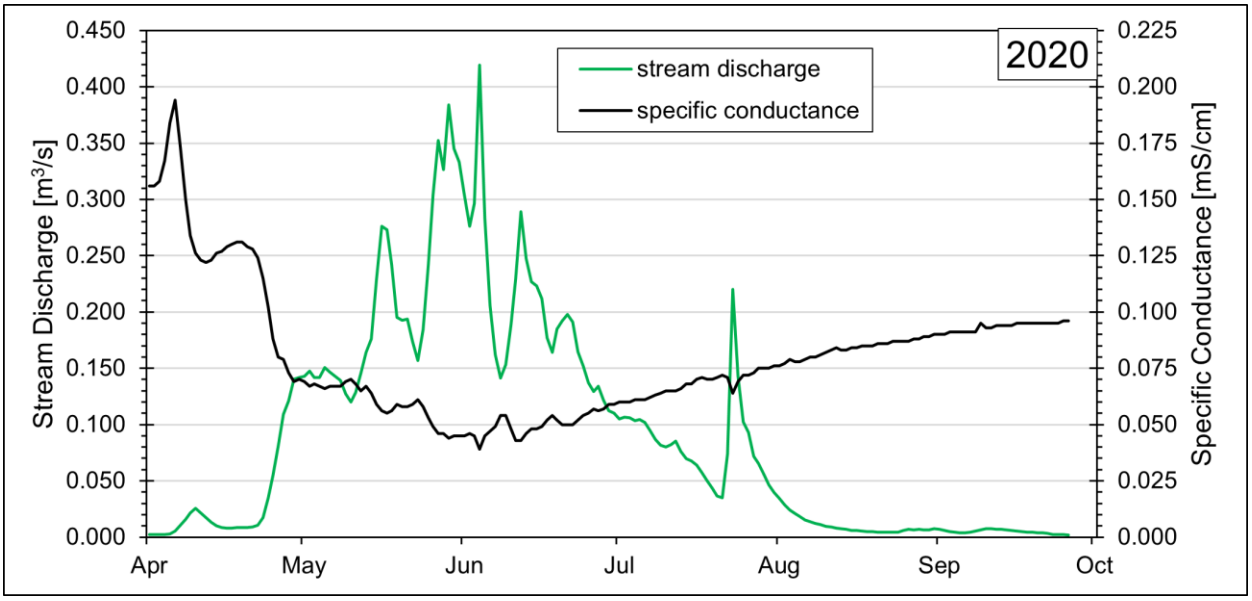

Figure A.2. Hydrograph of 2020 showing the naturally inverse relationship between stream discharge in m^3/s (green) and specific conductance in mS/cm (black). This year was selected as it shows the inverse relationship during snowmelt (May to late June) as well as during large precipitation events (late July to early August).

Table A.2. Summary of specific conductance characteristics from the period of record. A description of variables is in Table 3.1.

Year	Min. Stream Discharge (m^3/s)	Max. Stream Discharge (m^3/s)	Mean Meas. Period SC (mS/cm)	Min. SC (mS/cm)	Max. SC (mS/cm)	SC_{RO} (date)	SC_{RO} (mS/cm)	SC_{BF} (mS/cm)	Peak Baseflow Discharge (m^3/s)	Peak Baseflow Discharge (date)	Period of Peak Baseflow
2006	0.002	0.346	0.090	0.048	0.133	19-Jun	0.031	0.130	0.151	6-Oct	Low Flow
2007	0.005	0.332	0.095	0.058	0.131	18-May	0.031	0.128	0.184	22-Sep	Low Flow
2008	0.002	0.432	0.091	0.050	0.122	18-Jun	0.031	0.119	0.140	21-May	Snowmelt
2009	0.001	0.410	0.094	0.051	0.128	17-May	0.031	0.123	0.174	26-Jun	Snowmelt
2010	0.001	0.509	0.109	0.054	0.176	27-May	0.031	0.173	0.192	1-Jul	Low Flow
2011	0.003	0.479	0.090	0.048	0.118	15-Jun	0.031	0.118	0.137	29-Jun	Snowmelt
2012	0.001	0.293	0.091	*0.031*	0.132	21-May	0.031	0.131	0.049	23-Apr	Snowmelt
2013	0.001	0.381	0.104	0.039	0.182	30-Apr	0.031	0.160	0.102	13-Sep	Low Flow
2014	0.006	0.481	0.099	0.056	0.150	3-Jun	0.031	0.139	0.209	8-Sep	Low Flow
2015	0.004	0.485	0.096	0.045	0.147	2-Jun	0.031	0.132	0.148	10-Jun	Snowmelt
2016	0.005	0.568	0.101	0.057	0.126	5-Jun	0.031	0.125	0.201	7-Jun	Snowmelt
2017	0.000	0.526	0.084	0.034	0.118	11-Jul	0.031	0.117	0.124	1-Jun	Snowmelt
2018	0.001	0.301	0.101	0.041	0.154	5-Jun	0.031	0.151	0.065	9-May	Snowmelt
2019	0.005	0.599	0.036	0.036	0.156	27-Jun	0.031	0.153	0.093	15-Jun	Snowmelt
2020	0.002	0.419	0.080	0.039	0.194	6-Jun	0.031	0.175	0.050	25-Jul	Low Flow
2021	0.003	0.442	0.090	0.048	0.171	6-Jun	0.031	0.162	0.072	8-Jun	Snowmelt
Mean:	0.003	0.438	0.091	0.046	0.146	4-Jun	0.031	0.140	0.131	4-Jul	-

0.031 mS/cm was used as the SC_{RO} value in the CMB for all years, but the minimum values for each year and the date on which SC_{RO} occurred are displayed here for comparison. SC_{BF} has no associated date as those values were linearly interpolated.

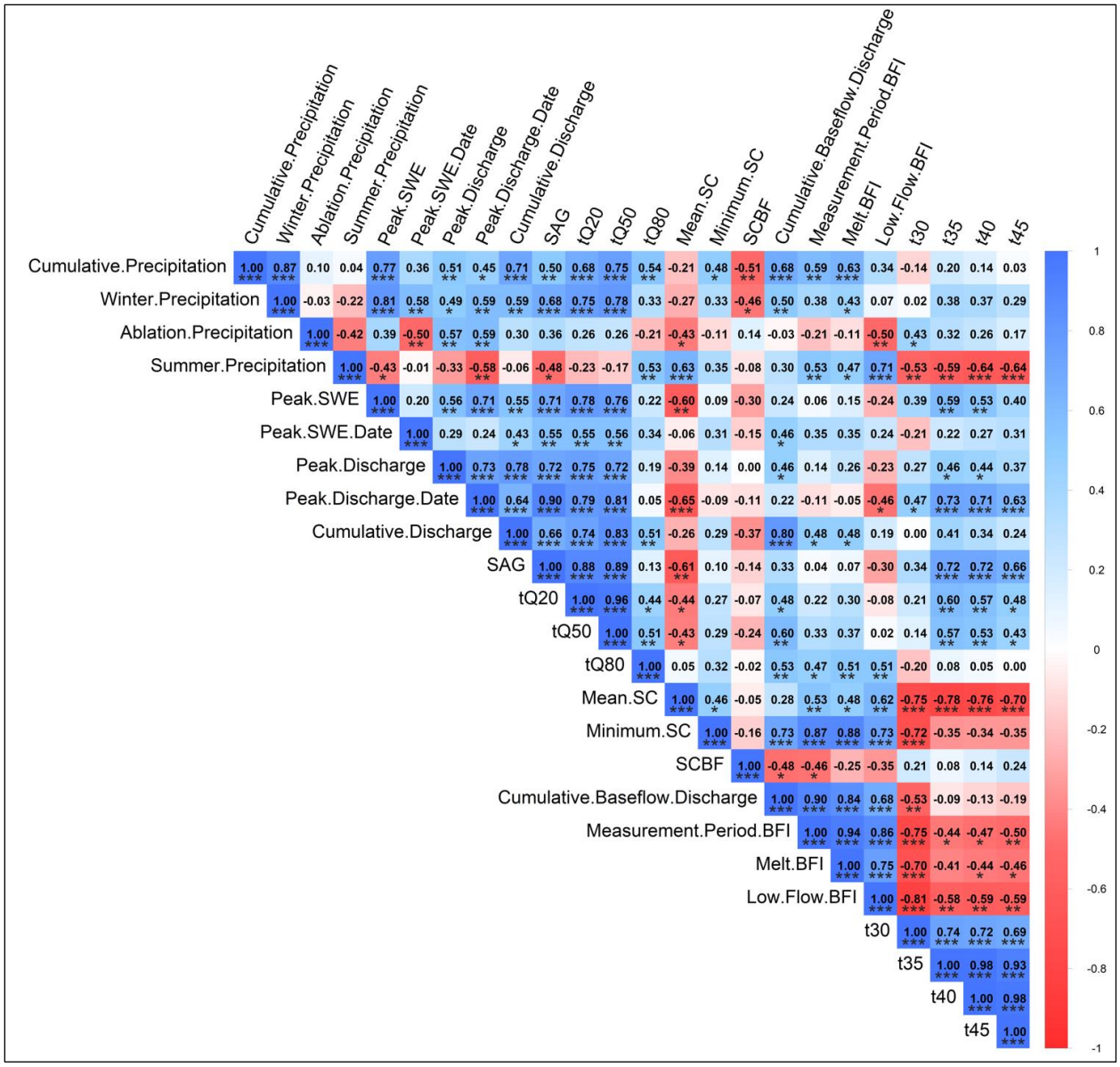

Figure A.3. Correlation matrix (Pearson's r) between various hydroclimate and timing of substantial baseflow variables. Shades of red and blue indicate negative and positive correlations, respectively. The asterisks indicate significant correlations with p-values (p) less than α values of 0.10 (*), 0.05 (**), and 0.01 (***). A description of the variables used in the correlation matrix is in Table 3.1. Because the correlation matrix is symmetric, only the upper half is displayed.

Table A.3. Summary of cumulative stream discharge, cumulative baseflow discharge, and BFI values for the period of record. A description of variables is in Table 3.1.

		Measurement Period			Snowmelt Period			Low Flow Period			Standard Period		
Year	**Classif.**	**Cum. Stream Discharge (mm)**	**Cum. Baseflow Discharge (mm)**	**BFI (%)**	**Cum. Stream Discharge (mm)**	**Cum. Baseflow Discharge (mm)**	**BFI (%)**	**Cum. Stream Discharge (mm)**	**Cum. Baseflow Discharge (mm)**	**BFI (%)**	**Cum. Stream Discharge (mm)**	**Cum. Baseflow Discharge (mm)**	**BFI (%)**
2006	Avg	609	254	42	372	109	29	121	96	79	541	205	38
2007	Avg	652	328	50	395	159	40	130	102	79	571	266	47
2008	Wet	710	289	41	431	129	30	137	73	53	698	228	33
2009	Avg	535	225	42	330	115	35	103	61	59	520	213	41
2010	Avg	649	277	43	394	164	42	128	73	57	624	262	42
2011	Wet	703	283	40	430	133	31	140	78	55	679	263	39
2012	Dry	438	105	24	267	30	11	85	38	45	405	87	21
2013	Dry	576	196	34	353	96	27	115	74	64	517	157	30
2014	Avg	888	422	48	536	203	38	177	134	76	795	357	45
2015	Dry	766	333	43	450	145	32	152	86	57	700	281	40
2016	Avg	816	411	50	495	184	37	160	121	76	768	367	48
2017	Avg	813	249	31	494	99	20	158	53	34	794	232	29
2018	Dry	388	104	27	240	35	14	77	40	52	368	85	23
2019	Wet	846	193	23	518	86	17	166	45	27	842	191	23
2020	Avg	486	90	19	296	38	13	95	25	26	485	90	19
2021	Dry	480	151	31	291	64	22	97	41	42	475	148	31
Mean:	-	647	244	37	393	112	27	127	71	55	611	215	34

Table A.4. Summary of the timing of substantial baseflow variables for the period of record. A description of variables is in Table 3.1.

		t_{sub} variable				Difference from Mean Date			
Year	**Classif.**	**t_{30}**	**t_{35}**	**t_{40}**	**t_{45}**	**t_{30}**	**t_{35}**	**t_{40}**	**t_{45}**
2006	Avg	6-Jul	10-Jul	12-Jul	16-Jul	7	-2	-6	-9
2007	Avg	19-May	1-Jul	7-Jul	15-Jul	-41	-11	-11	-10
2008	Wet	13-Jul	23-Jul	29-Jul	1-Aug	14	11	11	7
2009	Avg	25-Jun	25-Jun	25-Jun	26-Jun	-4	-17	-23	-29
2010	Avg	11-Jun	20-Jun	20-Jun	21-Jun	-18	-22	-28	-34
2011	Wet	19-Jun	19-Jul	26-Jul	29-Jul	-10	7	8	4
2012	Dry	27-Jun	28-Jun	1-Jul	6-Jul	-2	-14	-17	-19
2013	Dry	27-Jun	1-Jul	6-Jul	13-Jul	-2	-11	-12	-12
2014	Avg	7-Jun	24-Jul	25-Jul	28-Jul	-22	12	7	3
2015	Dry	2-Jul	13-Jul	21-Jul	6-Aug	3	1	3	12
2016	Avg	6-Jun	2-Jul	12-Jul	21-Jul	-23	-10	-6	-4
2017	Avg	23-Jul	27-Jul	29-Jul	31-Jul	24	15	11	6
2018	Dry	25-Jun	30-Jun	5-Jul	12-Jul	-4	-12	-13	-13
2019	Wet	14-Aug	19-Aug	30-Aug	11-Sep	46	38	43	48
2020	Avg	30-Jul	12-Aug	31-Aug	27-Sep	31	31	44	64
2021	Dry	4-Jul	9-Jul	16-Jul	23-Jul	5	-3	-2	-2
Mean:	-	29-Jun	12-Jul	18-Jul	25-Jul	-	-	-	-

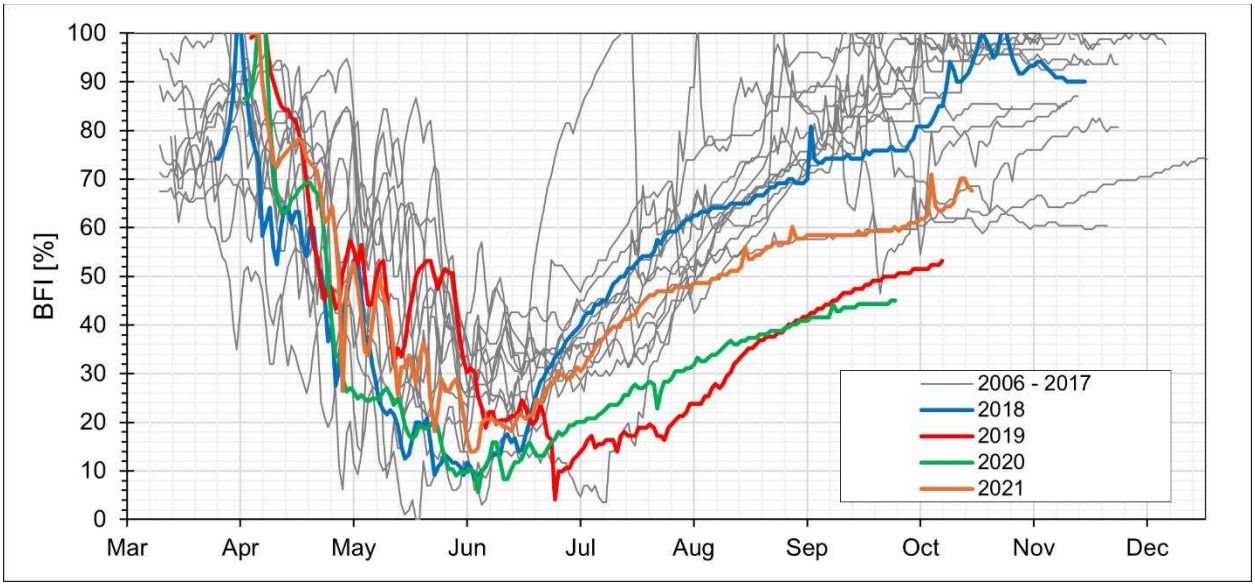

Figure A.4. Daily BFI (%) timeseries for each year in the period of record. Study years outside the study period (2006 – 2017) are in grey while years in the study period (2018 – 2021) are colored: 2018 is blue; 2019 is red; 2020 is green; and 2021 is orange.

Table B.1. Summary of sensor metadata used in this study. Metadata for the data collection stations in the SBB (SASP and SBSG) were available from Landry et al., (2014), Center for Snow and Avalanche Studies (2012), and Center for Snow and Avalanche Studies (2020), while metadata for the SNOTEL station was available from the NRCS website.

Source	Sensor Model + Manufacturer	Data Type (Units)	Accuracy	Notes
SASP	ETI Instrument Systems Noah II All-Weather Precipitation Gauge	Precipitation (mm)	±2.54 mm	Uses alcohol-based antifreeze to measure snow precipitation
	Vaisala PTB101B Barometric Pressure Sensor	Barometric Pressure (mb)	±0.5 mb	–
SNOTEL	*Model and Mfg. Unknown*	SWE (mm)	±2.54 mm	Snow Pillow and Pressure Transducer
SBSG	Druck PDCR 1830-8388 Pressure Sensor	Stream Stage (ft)	±0.1% FS	–
	Campbell Scientific CS547A Conductivity and Temperature Probe	Conductivity (mS/cm)	Combined ±0.1% FS	±10% from 0.005 – 0.44 mS/cm (with standard calibration solutions)
		Temperature (°C)	±0.4°C	–

FS = Full Scale Range

Table B.2. Summary of measurement period characteristics in the period of record. A description of variables is in Table 3.1. Nineteen days of missing data in 2019 were estimated using regression between stream discharge and SC (Figure B.1).

Year	Measurement Period (days)	Measurement Period Start (date)	Measurement Period End (date)	Missing Data at SBSG (days)	No. Days with BFI >100% (days)
2006	209	4-Apr	30-Oct	-	2
2007	248	14-Mar	17-Nov	-	2
2008	253	15-Mar	23-Nov	-	1
2009	262	3-Mar	20-Nov	-	2
2010	264	6-Mar	25-Nov	-	2
2011	245	14-Mar	14-Nov	-	3
2012	242	11-Mar	8-Nov	-	2
2013	289	11-Mar	25-Dec	-	3
2014	257	16-Mar	28-Nov	-	3
2015	258	15-Mar	28-Nov	-	3
2016	282	4-Mar	11-Dec	-	3
2017	239	22-Mar	16-Nov	-	1
2018	238	26-Mar	19-Nov	-	2
2019	189	5-Apr	11-Oct	19	2
2020	178	3-Apr	28-Sep	-	2
2021	197	6-Apr	20-Oct	-	0
Mean:	241	20-Mar	17-Nov	-	2

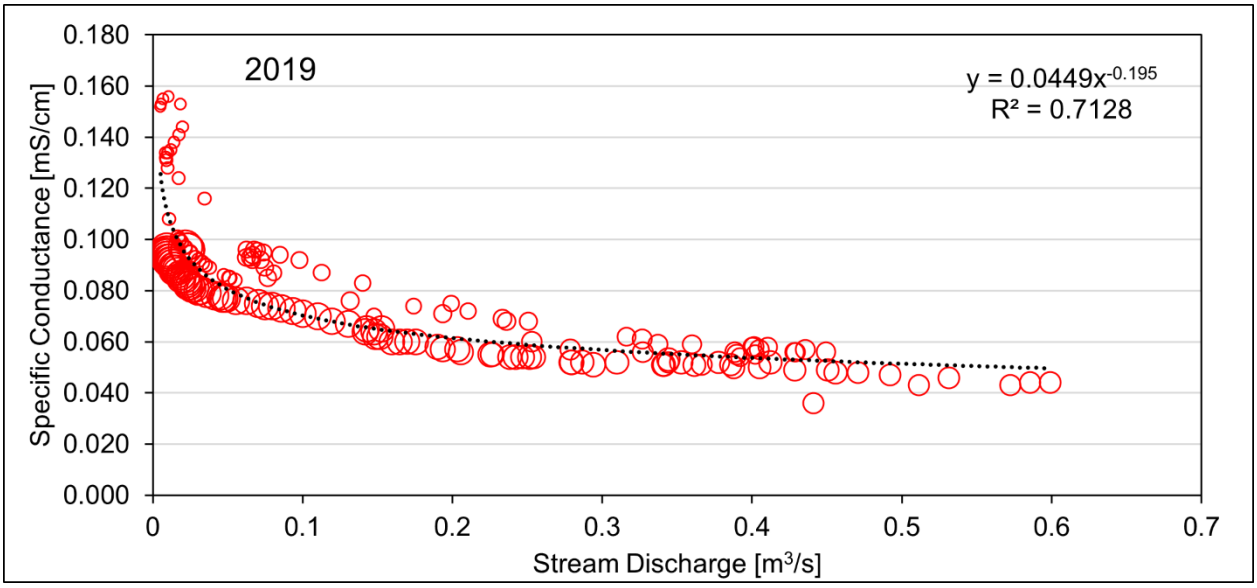

Figure B.1. Daily discontinuous stream discharge and continuous SC for 2019. Increasing bubble size indicates increasing day of year, where smaller bubbles represent values from the beginning of the measurement period and larger bubbles represent values from the end of the measurement period. Data were fitted with a power law equation ($R^2 = 0.71$) to estimate stream discharge during the period of missing data (21 April to 10 May).

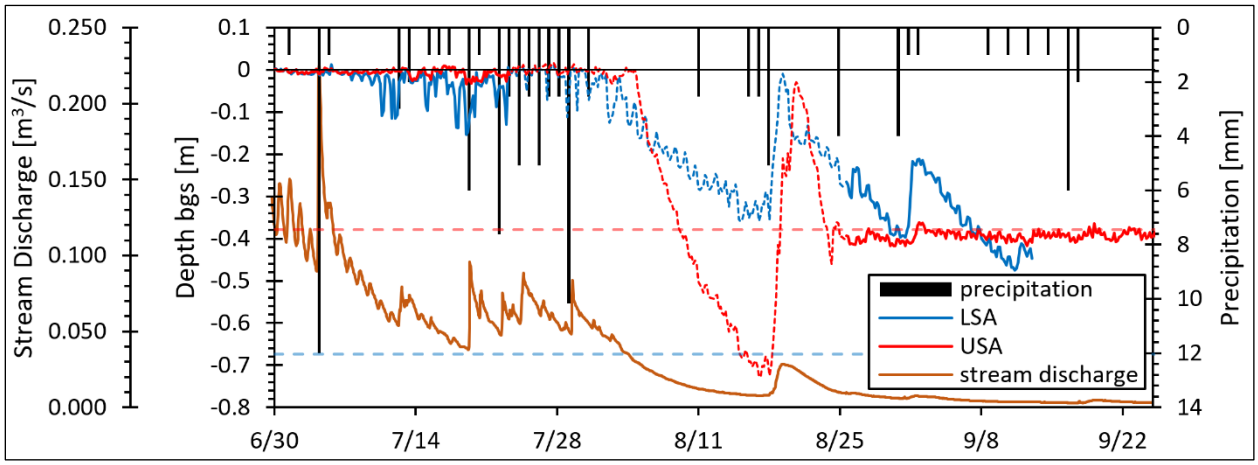

Figure C.1. Water level in meters (relative to local ground surface) for the Upper Swamp Angel well (USA, red) and Lower Swamp Angel well (LSA, blue). Positive values (above 0 m) indicate that the water table was above the surface while negative values (below 0 m) indicate that the water table was below the surface. The solid segments of the water level curves (any period outside of 23 July to 25 August) were corrected using measured barometric pressure data while the dashed segments were corrected using interpolated barometric pressure data (Figure C.2). The horizontal dashed lines represent the sensor depth (depth at which pressure was measured) in each well (USA: -38 cm (red) and LSA: -67 cm (blue)). Precipitation in mm (black bars) and stream discharge in m^3/s (orange) were included to provide context to fluctuations in water level. Water level data were recorded every 4 hours while precipitation and stream discharge data were recorded every hour.

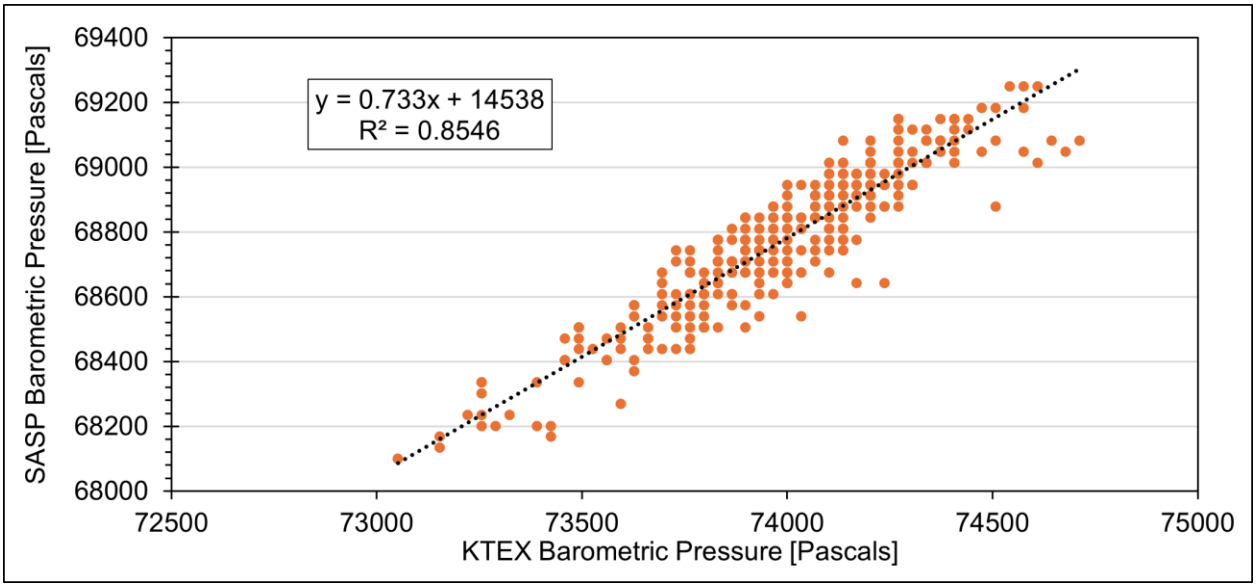

Figure C.2. Linear model used for interpolating barometric pressure data in Pa at SASP. Discontinuous barometric pressure data from SASP were plotted over continuous barometric pressure data from Telluride Regional Airport (KTEX) and produced a linear relationship (R^2 = 0.85). The regression equation was used to reconstruct the missing barometric pressure data at SASP.

Table C.1. Summary of sensor metadata from wells in the SAW and from stream monitoring stations.

Station	What	Variables Measured (Units) [Accuracy]	Install Date	Uninstall Date	Logging Interval	Construction Specifications
Lower Swamp Angel Well	Solinst Levelogger LTC5	- Water Level (m) [±0.05% FS] - Water Temperature (°C) [±0.05 °C] - Electrical conductivity (mS/cm) [>±2%]	30-Jun	25-Sep	4 hours	- Depth from ground surface to bottom of well 76.4 cm - Depth from ground surface to measurement point 67.4 cm
Upper Swamp Angel Well	Solinst Levelogger LT	- Water Level (m) [±0.05% FS] - Water Temperature (°C) [±0.05 °C]	3-Jun	25-Sep	4 hours	- Depth to bottom was 47.6 cm below the ground - Depth to measurement point was 37.9 cm below the ground
Upper Stream Monitoring Station	STICs 4968 and 4995	- Water Temperature (°C) [±0.53 °C] - Time of drying (t)	29-Jun	25-Sep	4 hours	- STICs installed ~5 m downstream of camera due to split in stream
	Time-lapse Camera	- Stream Imagery - Time of drying (t)	2-Jun	25-Sep	0.5 hours	- Images mostly captured from 07:00 to 17:00, and mostly during the day
Lower Stream Monitoring Station	STICs 4993 and 4978	- Water Temperature (°C) [±0.53 °C] - Time of drying (t)	29-Jun	31-Oct	4 hours	- STICs installed ~1 m upstream of camera
	Time-lapse Camera	- Stream Imagery - Time of drying (t)	3-Jun	10-Oct	0.5 hours	- Images mostly captured from 08:30 to 11:30, and mostly during the day

FS = Full Scale Range; STIC stands for Stream Temperature, Intermittency, and Conductivity logger (Chapin et al., (2014)).

GLOSSARY

Baseflow	Water discharged to the stream from subsurface or delayed sources, which may follow shallow subsurface or deeper subsurface flow paths. Baseflow is the dominant source of streamflow during low flow in the SBB.
Component	Distinct parts of streamflow that have discrete flow paths, sources, and chemical signatures.
Cumulative Flow Volumes	Total cumulative stream or baseflow discharge for the respective period (measurement period or standard period).
Difference in time between peak SWE and SAG	How long the snowpack takes to completely ablate.
Endmember	The term for stream component when used in the Conductivity Mass Balance model.
Fen	A type of groundwater-fed wetland, characterized by the presence of peat (a high-organic matter soil), saturated conditions in the growing season, and low-growing vegetation.
Flow Path	Pathways in the landscape through which water is transmitted to a stream. Each flow path has a unique length, travel time, velocity, and chemical signature.
Hydroclimate	A generalized term for climate-driven hydrological processes that occur in the SBB. Includes: precipitation (rain or snow), snowpack accumulation, snowpack peak, snowmelt, streamflow, and baseflow.
Hydrograph Separation Techniques	Methods used to estimate the magnitudes of different stream water components.
Measurement Period	The annual data collection period at the SBSG. The measurement period usually begins in March and ends in November, lasting an average of 240 days. All datasets derived from SBSG, such as stream and baseflow discharge, are limited to the measurement period length.

Post-snowmelt Low Flow Period	A period of low streamflow, dominated by baseflow discharge. Defined as the period between tQ80 and the end of the measurement period, usually starting in July continuing into late autumn. Also referred to as the low flow period.
Residual Precipitation	The summation of precipitation between the day after peak SWE and SAG.
Snow-All-Gone (SAG)	The first date of 0 mm of SWE. Denotes the complete disappearance of snowpack and the end of the snowmelt period (not the end of snowmelt contributions to streamflow).
Snowmelt Period	A period of high streamflow, dominated by surface water runoff. Defined as the period between tQ20 and tQ80, usually occurring between May and July.
Snowmelt-dominated Watershed	Watersheds with an identifiable snowmelt pulse or where peak stream discharge is an order of magnitude greater than low flow conditions.
Specific Conductance	A measure of the ability to conduct an electric current. Commonly used in chemical hydrograph separations.
Standard Period	An annually consistent period created for interannual comparison of discharge data, ranging between 6 April and 28 September.
Summer Precipitation	The summation of precipitation between the day after SAG and the day before the first date of snow accumulation (SWE > 0) of the following winter season.
Surface Water Runoff	Water that travels across the land surface to reach the stream, sourced primarily from melting snow the spring and rainfall in the summer.
Snow Water Equivalent (SWE)	The liquid amount of water contained within the snowpack.
Study Period	The period between 2018 and 2021. This 4-yr period was selected as the focus of this study because of the high observed variability in hydroclimate.

Timing of Substantial Baseflow (t_{sub})	The point in time (after snowmelt) at which baseflow discharge becomes a "substantial" component of streamflow. t_{sub} is comprehensively represented by t_{30}, t_{35}, t_{40}, and t_{45}, which represent the day at which baseflow index equals 30%, 35%, 40%, and 45%, respectively.
tQ20	The timing of the 20th percentile of cumulative discharge. Represents the start of snowmelt contributions to streamflow.
tQ50	The timing of the 50th percentile of cumulative discharge. Represents the center of volume of snowmelt.
tQ80	The timing of the 80th percentile of cumulative discharge. Represents the end of snowmelt contributions to streamflow.
Water Year	A 365-day year that begins on 1 October and ends on 30 September of the following year.
Wetland Drainage	Water released from wetlands to streams. In the SBB, wetland drainage was conceptualized as a component of baseflow and is composed of groundwater transmitted through the Swamp Angel Wetland. When the upper reaches of stream are known to dry, baseflow is entirely composed of wetland drainage.
Winter Precipitation	The summation of precipitation between the first date of snow accumulation (SWE > 0) and the date of peak SWE.

LIST OF ABBREVIATIONS

BFI	Baseflow Index
CMB	Conductivity Mass Balance method
CSAS	Center for Snow and Avalanche Studies
KTEX	Telluride Regional Airport
LSA	Lower Swamp Angel Well
LSMS	Lower Stream Monitoring Station
NRCS	Natural Resources Conservation Service
Q_{BF}	Baseflow Discharge Component
Q_{RO}	Surface Water Runoff Component
Q_S	Total Stream Discharge
SAG	Snow-All-Gone
SASP	Swamp Angel Study Plot
SAW	Swamp Angel Wetland
SBB	Senator Beck Basin
SBSG	Senator Beck Stream Gauge
SBSP	Senator Beck Study Plot
SC_{BF}	Baseflow Discharge Endmember
SC_{RO}	Surface Water Runoff Endmember
SC_S	Total Specific Conductance of Stream
SNOTEL	Red Mountain Pass Snow Telemetry Station
STIC	Stream Temperature, Intermittency, and Conductivity logger

SWE	Snow Water Equivalent
tQ20	The Timing of the 20th Percentile of Cumulative Discharge
tQ50	The Timing of the 50th Percentile of Cumulative Discharge
tQ80	The Timing of the 80th Percentile of Cumulative Discharge
t_{sub}	Timing of Substantial Baseflow
USA	Upper Swamp Angel Well
USMS	Upper Stream Monitoring Station